

The Tri-Cities Ozone Precursor Study (T-COPS)

Final Report

December 12, 2017

Prepared by
Laboratory for Atmospheric Research
Department of Civil & Environmental Engineering
Washington State University

Preface

The Laboratory for Atmospheric Research at Washington State University submits this Final Report as part of a contract project from the Washington Department of Ecology to conduct the Tri-Cities Ozone Precursor Study (T-COPS). We acknowledge Jill Schulte at the Washington Department of Ecology for contributions to this report on the mobile monitoring analysis. We would also like to thank the Benton Clean Air Agency staff for generously providing a site for MACL, assistance in satellite site selection, and hosting WSU staff during the field experiment.

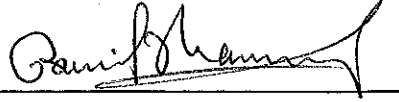
Contacts:

Tom Jobson
Laboratory for Atmospheric Research
Department of Civil & Environmental Engineering
Washington State University

Graham VanderSchelden
Laboratory for Atmospheric Research
Department of Civil & Environmental Engineering
Washington State University

Approval Page

Washington Department
of Ecology
Air Quality Program



Ranil Dhammapala

Phone: 360-407-6807

Email: ranil.dhammapala@ecy.wa.gov

12/13/2017.
Date

Executive Summary:

Air quality managers have been paying close attention to ozone levels in the Tri-Cities for the past 5 years after it was noticed that AIRPACT, a daily predictive air quality forecast model operated by Washington State University (WSU), consistently showed elevated ozone in the Tri-Cities area. It has been determined from ozone monitoring that began in 2013 that elevated ozone occurs in the summer months on hot days > 85 °F with light NNE winds (< 6 mph). The Tri-Cities region of Washington is comprised of the cities of Richland, Kennewick, and Pasco. The Metropolitan Statistical Area covering these three cities has a combined population of 283,830 (WA Office of Financial Management, 2017). This area has seen significant population growth over the past decade with the city of Pasco growing by 20% from 2010 to 2017.

The Washington State Department of Ecology commissioned the Tri-Cities Ozone Precursor Study (T-COPS), a field study that collected data from July 27 to August 18, 2016 to investigate the causes of high ozone in the Tri-Cities. Fixed-site measurements of ozone and ozone precursors were made by WSU at the Benton Clean Air Agency (BCAA) in Kennewick, and at a location in Horn Rapids to the north-west of Richland. Fixed site measurements were also made in Burbank by the Washington State Department of Ecology and the RJ Lee Group Inc. Mobile measurements using an instrument van were also conducted by the RJ Lee Group.

Five ozone events were noted during T-COPS where 1-hr ozone mixing ratios were greater than 70 ppbv at either the BCAA site or the Burbank site. Two of these events occurred when the area was impacted by wildfire smoke (the Range 12 Fire near Yakima) which may have brought ozone and ozone precursors into the area. During these events ozone mixing ratios were similar between BCAA, Horn Rapids and Burbank. For the other 3 events, ozone at BCAA and Burbank was significantly larger (15 to 20 ppbv) than the Horn Rapids site, implying the main area of ozone production is localized to the immediate urban area of the Tri-Cities. This is consistent with mobile monitoring that showed low levels of ozone and ozone precursors at the northern boundaries of the study area. It is unlikely that long range transport of ozone and ozone precursors plays a substantial role in explaining elevated ozone levels in the Tri-Cities, with the possible exception of wildfire events. Ozone levels during the day at BCAA and Burbank were very similar, with typical afternoon mixing ratios of 55 ppbv, about 15 ppbv greater than the regional background.

Based on the emission inventory and observations of CO and NO_x, traffic emissions are a major source of NO_x in the Tri-Cities. Isoprene emitted from vegetation, and the aldehydes, formaldehyde and acetaldehyde, which have both primary and secondary sources, were the most significant VOC precursors measured. It is estimated that vehicle emissions of CO, aromatics, alkenes and alkanes would collectively comprise a hydroxyl radical reactivity comparable to isoprene. Thus traffic emissions of hydrocarbons and CO have a similar importance as ozone precursors as isoprene at the BCAA site.

Large point or area sources of NO_x and VOCs likely make some contribution toward ozone formation, as do some agrochemicals. However there is no evidence to suggest these are solely responsible for elevated ozone in the airshed.

While ozone precursor concentrations are relatively low compared to large urban areas, the study results suggest that conditions in the airshed produce ozone efficiently. From indicator ratio analyses we conclude that ozone formation chemistry is not strongly limited by the availability of any one precursor. This suggests that either VOC or NO_x emission reductions could reduce ozone in the airshed. However a detailed modeling study is required to quantify the airshed sensitivity to NO_x and VOC reductions, and identify the most effective control measures given the photochemical conditions that exist in the Tri-Cities.

The prevalence of hot days with calm winds produce stagnant conditions that reduce dispersion of urban emissions in the airshed and result in the accumulation of ozone. When such days are forecast, air quality managers could implement ozone precursor reduction strategies from the preceding day onward.

List of Abbreviations:

AIRPACT	Air Indicator Report for Public Awareness and Community Tracking - Version 5. The WSU Air Quality Forecasting Model
BCAA	Benton Clean Air Agency
CH ₃ CHO	Acetaldehyde
CH ₃ CN	Acetonitrile
CH ₃ OOH	Methylhydroperoxide
CO	Carbon Monoxide
CO ₂	Carbon Dioxide
DoE	Washington Department of Ecology
EI	Emissions Inventory
FEM	Federal Equivalent Method
FRM	Federal Reference Method
H ₂ O	Water
HCHO	Formaldehyde
HNO ₃	Nitric Acid
HO	Hydroxyl Radical
HO ₂	Hydroperoxy radical
MACL	WSU Mobile Atmospheric Chemistry Laboratory
MOVES	Motor Vehicle Emissions Simulator
NO	Nitric Oxide
NO ₂	Nitrogen Dioxide
NO _x	Nitrogen oxides (the sum of NO and NO ₂)
NO _y	Total oxidized nitrogen

NO _z	Oxidized nitrogen less NO _x (NO _y - NO _x)
O ₂	Oxygen
O ₃	Ozone
ppbv	Parts per Billion by Volume
ppmv	Parts per Million by Volume
pptv	Parts per Trillion by Volume
PST	Pacific Standard Time
PTR-MS	Proton Transfer Reaction Mass Spectrometer
QA	Quality Assurance
QC	Quality Control
RH	Relative Humidity
SO ₂	Sulfur Dioxide
T-COPS	Tri-Cities Ozone Precursor Study
VOCs	Volatile Organic Compounds
WS OFM	Washington State Office of Financial Management
WS DoE	Washington State Department of Ecology
WSU	Washington State University

Table of Contents:

1. Introduction10

2. Project Objectives and Tasks19

3. Report Format21

4. Study Methodology22

4.1. Site Descriptions23

 4.1.1. Benton Clean Air Agency23

 4.1.2. Horn Rapids Satellite Site24

 4.1.3. Burbank Satellite Site25

 4.1.4. Mesa Satellite Site27

5. Instrument Descriptions28

5.1 Site Measurement Schedule28

5.2 BCAA Site Instruments28

 5.2.1. Gas Phase Instrumentation Inlet29

 5.2.2. AQD NO_x/NO_y Analyzer30

 5.2.3. Proton Transfer Reaction Mass Spectrometer (PTR-MS).....30

 5.2.4. Teledyne CO Monitor31

 5.2.5. Teledyne NO_x Monitor32

 5.2.6. Teledyne O₃ Monitor33

 5.2.7. Teledyne SO₂ Monitor33

 5.2.8. LICOR CO₂/H₂O Monitor33

 5.2.9. WXT Surface Meteorology Measurements33

5.3. Horn Rapids Satellite Site Instruments34

5.3.1. TECO 42C NO _x	34
5.3.2. TECO 48 O ₃	34
5.3.3. Dasibi 1008 O ₃	34
5.3.4. Meteorological Measurements	35
5.4. Department of Ecology Burbank Instrumentation	35
5.4.1. Teledyne API 300EU CO monitor	35
5.4.2. Teledyne API 200 EU NO _x Monitor	36
5.4.3. 2B Technologies 202 O ₃ Monitor	36
5.5 RJ Lee Van and Trailer	36
5.5.1. RJ Lee Mobile Laboratory (Van)	36
5.5.2. RJ Lee Stationary Laboratory (Trailer)	36
5.5.3. 2B Technologies O ₃ Monitor	37
5.5.4. TECO 42 NO _x Monitor	37
5.5.5. LICOR Li-840 A CO ₂ /H ₂ O Monitor	37
5.5.6. PTR-QMS	37
5.5.7. PTR-TOF	38
6. Data	39
6.1.Fixed Site Data Quality and Completeness.....	39
6.2. Study Overview - Weather Conditions	41
6.3. Temperature	43
6.4. Wind Speed	44
6.5. Wind Direction	46
6.6. Pollutant Time Series BCAA	50

6.7. Pollutant Time Series Horn Rapids	55
6.8. Pollutant Time Series Burbank	56
6.9. Measurements at Burbank in the Summer of 2017	57
7. Chemical and Meteorological Drivers of Ozone.....	62
7.1. Tri- Cities Regional Ozone	62
7.2. Influence of Wildfire	69
7.3. Ozone Precursor Emissions Inventory.....	72
7.4. Time of Day Trends in Vehicle Traffic Pollutants	79
7.5 Spatial Distribution of NO _x	84
7.6. Ozone Episodes: Analysis of mid-August Stagnation Period.....	89
7.7 Analysis of VOC and NO _x Limitation.....	96
7.8 VOC Reactivity.....	100
7.9. Results of Mobile Monitoring for O ₃ , NO _x , and VOCs	106
7.10 Comparisons to AIRPACT-5	111
8. Summary and Conclusions	115
9. References.....	118
10. Appendix	122

1. Introduction

Ground level ozone is a criteria air pollutant regulated by the US Environmental Protection Agency under the Clean Air Act. Ozone is a regulated pollutant because of its adverse health effects on the respiratory system as documented in both short term and long term health effects studies (US EPA ISA 2013). In 2015 the National Ambient Air Quality Standard (NAAQS) for ozone was set at 70 ppbv. The standard for ozone has been revised several times in the past 20 years. It was set at 80 ppbv in 1997, changed to 75 ppbv in 2008, and then revised again in 2015 to the current 70 ppbv standard. NAAQS compliance is determined based on a metric known as the design value (DV), which is calculated according to a defined form and averaging time for each pollutant. The ozone NAAQS is attained if the 3 year average of the annual 4th highest Maximum Daily 8-hour average (MDA8) remains below 70 ppbv, the so called design value (40 C.F.R § 50.4, 2015).

Ozone is monitored in or around most urban areas throughout the US, and ozone levels are mostly elevated in summer months. Many metropolitan urban areas are classified by the EPA as nonattainment for ozone. Currently, there are no areas in the Pacific Northwest designated nonattainment for ozone. In the State of Washington ozone is continuously monitored at 14 locations as shown in Figure 1.1. The figure shows the preliminary 2016 ozone design values and most sites have design values much less than 70 ppbv, the exceptions being Kennewick and the Mud Mountain Dam site downwind of Seattle-Tacoma.

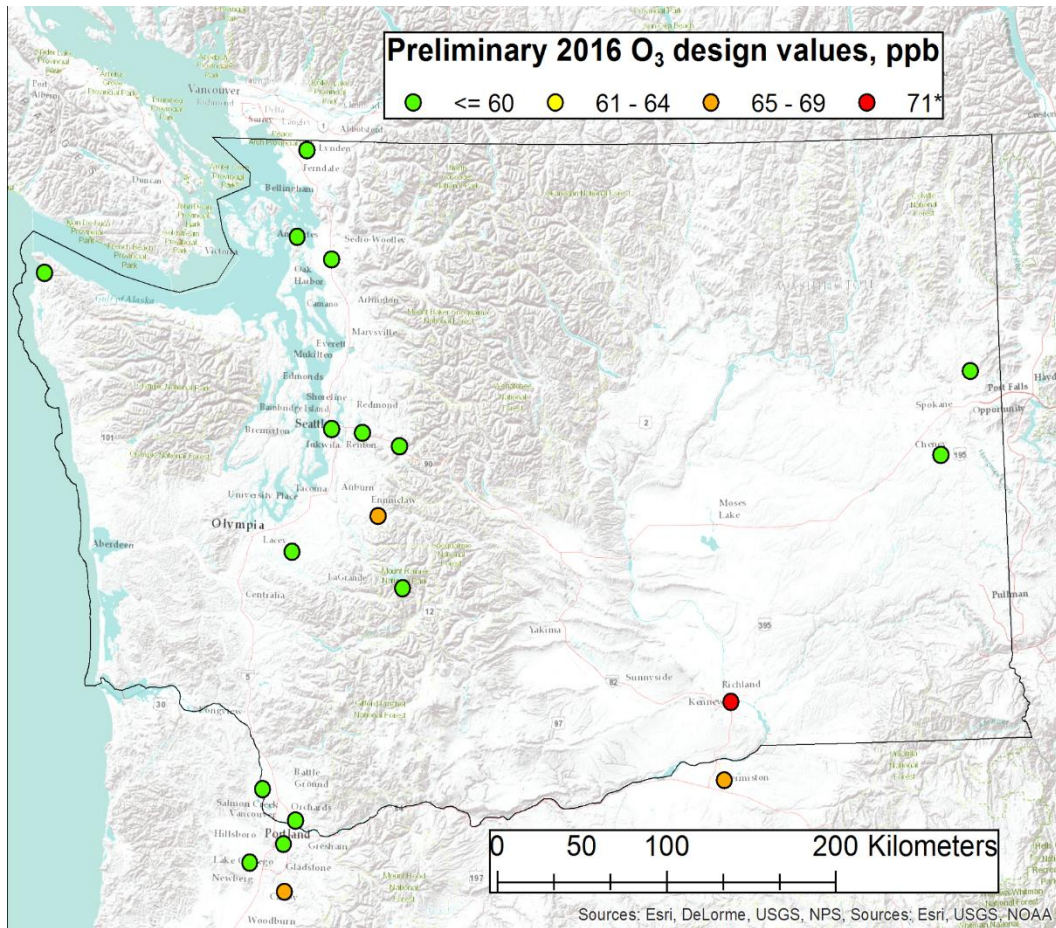


Figure 1.1. Ozone monitoring sites and the 2016 DVs in and around Washington State.

This project is motivated by recent observations of elevated ozone in Kennewick, WA. Air quality managers in Washington have been paying close attention to ozone levels in the Kennewick area since Washington State University's daily predictive 4km photochemical grid model (<http://lar.wsu.edu/airpact>) consistently showed a previously unknown ozone hotspot in the Tri-Cities area. In August 2013, the Washington State Department Ecology (Ecology) set up a temporary ozone monitor at West Metaline Avenue in Kennewick, to verify the model predictions. Data collected through the rest of the ozone season confirmed the presence of elevated ozone levels in the area, leading to another round of temporary monitoring conducted the following summer. When that too confirmed elevated ozone readings, the decision was made to install a permanent, federal equivalent method (FEM) ozone monitor in May 2015, at the office of Benton Clean Air Agency (BCAA) and submit the data to EPA.

Though the ozone DV in Kennewick cannot be calculated because the official Department of Ecology monitor has not been operational for at least 3 years, recent levels have been higher than those downwind of the Seattle-Tacoma area as measured by the monitor at Mud Mountain Dam in Enumclaw. Table 1.1 shows fourth highest daily maximum values for ozone at Kennewick in

comparison to Mud Mountain, and the cities of Spokane (Greenbluff site) and Hermiston, OR. Spokane and Hermiston are the nearest cities to Kennewick with ozone monitoring. In 2015, Kennewick exceeded the current NAAQS ozone standard 4 times, while the Mud Mountain Dam site exceeded it 5 times.

Table 1.1 Fourth highest daily maximum ozone value in ppbv.

Year	Mud Mountain Dam	Spokane	Kennewick	Hermiston
2014	67	60	-	64
2015	74	63	75	70
2016	61	56	68	63

Investigative mobile monitoring for ozone in the Tri-Cities area was conducted on two days in the summer of 2013, followed by 5 days in 2015. Data indicated elevated ozone was also present around the city of Burbank, WA, ~ 10 miles to the east of Kennewick. A fixed ozone monitor was placed in Mesa, about 25 miles north of the Tri Cities in the summer of 2015 but elevated levels of ozone were not observed there. Kennewick ozone levels were also higher than those observed downwind of Spokane (the largest urban area in eastern Washington) and Hermiston, OR (about 30 miles south of the Tri-Cities). The observational evidence suggested that the Tri-Cities urban area produced photochemical ozone pollution in summer. Ozone builds up in the Tri-Cities on hot days (>85°F), under mild to moderate (mostly < 6 mph) north-northeast winds, as shown by the ozone pollution rose in Figure 1.2. In the figure, only hours with O₃ > 60 ppbv are shown, indicative of elevated levels compared to regional background levels. Ozone levels over 80 ppbv were often observed.

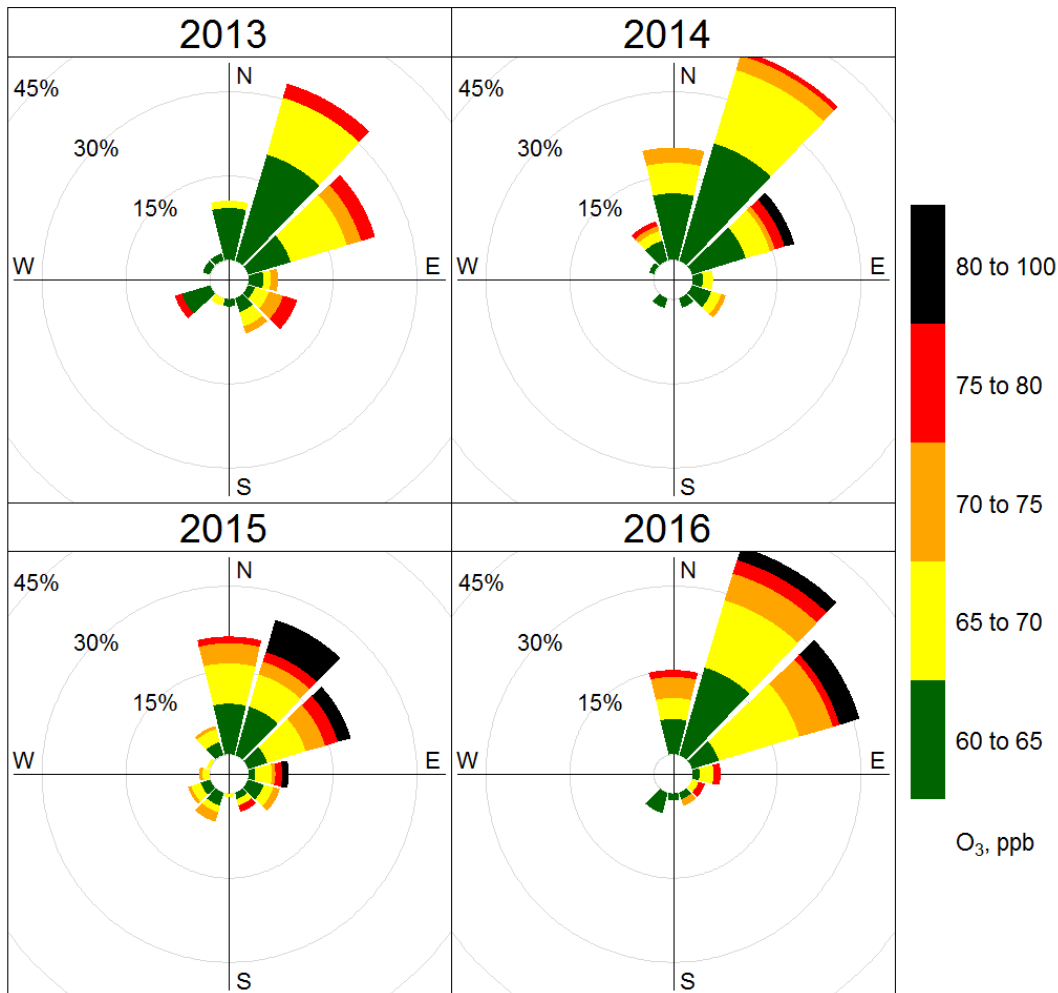


Figure 1.2. Comparison of ozone pollution roses measured in Kennewick for the past four summers. The 2013 and 2014 data are from the Metaline site. The 2015 and 2016 data are from the BCAA site.

Ozone is a secondary pollutant, formed as a by-product of photochemical oxidation of hydrocarbons in the presence of nitric oxide (NO). Photochemical ozone formation in urban areas is a reasonably well understood chemical process (National Research Council, 1991). The photochemical reactions are initiated by solar ultraviolet (UV) radiation. Summertime, with longer daylight hours and higher UV light levels, is typically the time of year when elevated ozone is observed in urban areas. In urban areas, sources of hydrocarbons and NO_x (NO + NO₂) include fossil fuel combustion, notably gasoline motor vehicle emissions, and commercial and industrial activities. Ozone can accumulate in the urban airshed when meteorological conditions and topography limit dispersion. In summertime, stagnant conditions from high pressure systems that result in clear skies, elevated temperatures, and low surface wind speeds are favorable to ozone formation and accumulation.

Ozone is formed from the photolysis of nitrogen dioxide (NO₂) followed by the immediate 3-body reaction of the oxygen atom with O₂:



where M represents another molecule (such as N₂, O₂, Ar). Ozone also rapidly reacts with NO to reform NO₂.



During the daytime, NO₂, NO, and O₃ are in chemical equilibrium, and changes in light levels through the day and the abundance of NO from surface emission sources change the relative amounts of NO₂ and O₃. In urban areas with high NO concentrations, O₃ may not be very abundant due to its reaction with NO to form NO₂. Ozone can accumulate during the day from the rapid oxidation of NO to NO₂ by peroxy radicals such as hydroperoxy radical (HO₂) and organic peroxy radicals (RO₂). Both are formed in the hydroxyl radical (HO) initiated oxidation of hydrocarbons.



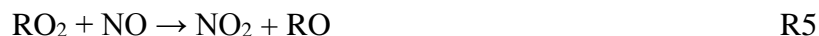
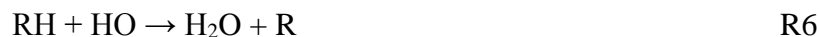
Ozone production chemistry is thus initiated by HO radical oxidation of hydrocarbons in the presence of NO. The ozone production rate (P_{O₃}) is determined by the sum of the R4 and R5 reaction rates:

$$P_{\text{O}_3} = k_4[\text{HO}_2][\text{NO}] + k_5[\text{RO}_2][\text{NO}] \quad (1)$$

where k_4 and k_5 are the respective rate constants for reactions R4 and R5.

The abundance of the HO radical is a strong function of UV light levels. In urban areas HO radical is formed principally from the photolysis of ozone with contributions from photolysis of other precursors such as aldehydes (i.e. formaldehyde) and nitrous acid (Mao et al., 2010; Ren et al., 2013). The oxidation of hydrocarbons occurs as a sequence of rapid successive reactions. In the sequence of reactions both HO and NO are regenerated and thus behave as catalysts. In the case of NO, it is oxidized to NO₂ by reactions R4 and R5, and is then rapidly regenerated by the photolysis reaction R1, which results in an ozone molecule from R2. An NO molecule may be oxidized and recycled to NO multiple times before being lost from the cycle in the formation of an oxidation product. A single NO molecule may thus produce many ozone molecules. This re-cycling efficiency of NO is an important description of the ozone production process. Ozone production rates have been shown to be non-linear functions of the NO concentration (Lin et al., 1988).

The oxidation of hydrocarbons by HO occurs in a sequence of reactions that re-form HO. The recycling efficiency of HO is also important for understanding ozone formation (Tonnesen and Dennis, 2000). An example reaction mechanism is shown below for the oxidation of a generic hydrocarbon denoted *RH*. A common initial reaction is for the HO radical to remove an H-atom from the hydrocarbon, to produce a very reactive alkyl radical, and this step initiates a radical chain reaction sequence involving oxygen (O₂) and NO:





The final step in the sequence is reaction R4, which regenerates the HO radical lost in reaction R6. Thus an HO molecule may initiate the oxidation of many hydrocarbons. In this example the *RH* photoproduct is the aldehyde $\text{R}'\text{CHO}$ in reaction R9. Two NO_2 molecules were also formed in the reaction sequence which rapidly photolyze in the daytime to produce ozone. In this illustrative example the oxidation sequence for one hydrocarbon produced 2 ozone molecules. A schematic of the relevant reactions important to ozone formation is shown in Figure 1.3.

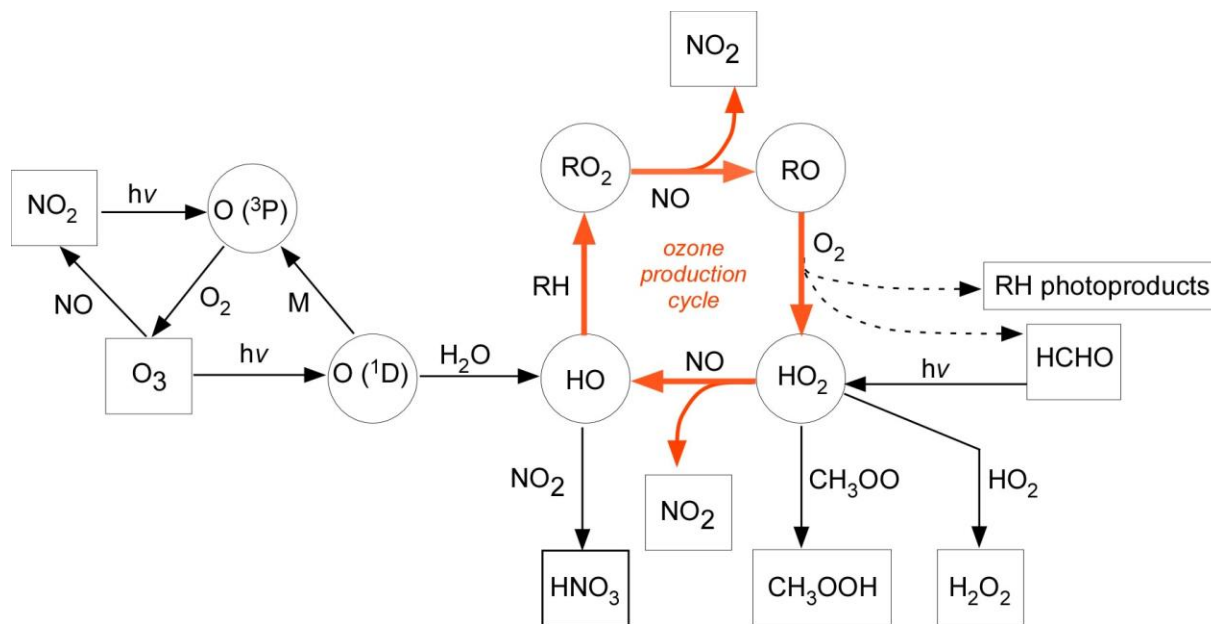


Figure 1.3. Block diagram schematic of major chemical species and reactions involved in ozone production as discussed above. Chemical species within circles are short lived reactive species, while species in boxes are long lived species. The symbol $h\nu$ represents a photolysis reaction.

The reaction rate of hydrocarbons with the HO radical depends on the nature of the hydrocarbon; some compounds are very reactive with the HO radical (i.e. isoprene) while other are less reactive (i.e. acetone). Hydrocarbons that are both high in abundance and have a rapid reaction with HO radical are the most important ozone precursors. The reactivity with HO radical is described by the reaction rate coefficient (k) and these rate coefficients are reasonably well known for the suite of organic compounds commonly found in urban areas. The rate of removal of hydrocarbon compound RH_i by HO radical is given by:

$$d[\text{RH}_i] / dt = k_i [\text{RH}_i][\text{HO}] \quad (2)$$

The product of the organic compound abundance $[\text{RH}_i]$ and its HO rate coefficient k_i is referred to as the HO radical loss frequency (units of s^{-1}) and is a useful metric for quantifying the relative importance of hydrocarbon compounds as ozone precursors. Values of k can range orders of magnitude, from the very reactive compound isoprene ($k = 1.10 \times 10^{-10} \text{ cm}^3 \text{ molecule}^{-1} \text{ s}^{-1}$) to the

relatively unreactive methane ($k = 6.3 \times 10^{-15} \text{ cm}^3 \text{ molecule}^{-1} \text{ s}^{-1}$). Detailed knowledge of the types of organic compounds in urban air is important for understanding ozone formation chemistry. During T-COPS selected hydrocarbons were continuously measured.

There are several important reactions that consume HO_x radicals ($\text{HO}_x = \text{HO}$ and HO_2) and NO_x ($\text{NO}_x = \text{NO}$ and NO_2) and thus terminate the oxidation cycle that produces ozone. These reactions are known as chain termination reactions. The most important chain termination reaction is the reaction between HO and NO_2 to produce nitric acid (R10).



When NO_2 concentrations are high, the abundance of HO radical is lowered and this can impact ozone production rates by reducing the rate of hydrocarbon oxidation in R6. There is thus a competition for HO radical between NO_2 (R10) and hydrocarbons (R6). Other losses of NO_x can occur in the hydrocarbon oxidation to produce organic nitrates compounds (R11) or peroxyacetyl nitrate type compounds (R12):



Nitric oxide is thus oxidized and lost from the ozone production cycle to form series of products (HNO_3 , RC(O)ONO_2 , RONO_2 , etc.). Collectively, these nitric oxide oxidation products together with NO_x are called NO_y compounds. The difference between measured NO_y and NO_x is called NO_z . NO_z and ozone are by-products of hydrocarbon photo-oxidation and their relative abundance describes the catalytic efficiency of NO, the number of times NO is recycled before being lost to a reaction forming a NO_z compound. NO_y , NO and NO_2 were measured during T-COPS.

Another set of chain termination reactions remove peroxy radicals. The two most important form hydrogen peroxide (R13) and methyl hydroperoxide (R14):



Like NO_z compounds, peroxides are also continuously formed along with ozone. In T-COPS methyl hydroperoxide (CH_3OOH) was measured.

In urban areas the production rate of radicals (HO, HO_2) is central to understanding ozone production rates. The HO radical initiates the oxidation sequence of hydrocarbons that leads to ozone production. The hydrocarbon oxidation rate depends on the HO concentration which depends on the radical production rate. High rates of hydrocarbon oxidation can lead to high rates of ozone production. The radical production rate Q is balanced by the loss rate of radicals through the formation of NO_z compounds and peroxides (Kleinman et al., 1997; Kleinman et al., 2005). The most important sources of radicals in urban areas are the photolysis of ozone, formaldehyde, nitrous acid and glyoxal, with their relative importance varying between cities and changing over the course of the day (Mao et al, 2010). Ozone photolysis (R15) leads to HO production (R16) in the presence of water vapor and is typically the primary radical source during midday when ozone concentrations are high.



Formaldehyde can photolyze (R17) to produce HO₂ radicals (R18 & R19)



The ozone production mechanism is commonly described as either hydrocarbon sensitive or NO_x sensitive. In a hydrocarbon sensitive regime changing the emissions of hydrocarbons (or concentrations) has a larger impact on ozone concentrations than corresponding changes in NO_x. Conversely in a NO_x sensitive regime, changing NO_x emissions (or concentrations) in an airshed has a more pronounced impact on ozone concentrations than similar changes to hydrocarbons. From a regulatory perspective, understanding the airshed's sensitivity to reductions in NO_x or hydrocarbon emissions informs decisions on how best to reduce ozone. It has been shown through analytical arguments and chemical transport models that the proportion of radicals lost to reactions with NO_x (LNO_x) to the total radical production rate (Q) provides a good metric to describe ozone production in terms of NO_x or hydrocarbon sensitive regimes (Sillman, 1995, Kleinman et al., 1997; Kleinman, 2000, Mao et al., 2010). When the loss rate of radicals to NO_x reactions (i.e. R10, R11, R12) exceeds 50% of the total radical production rate, the ozone production chemistry is considered hydrocarbon sensitive, otherwise it is NO_x sensitive (Sillman, 1995, Kleinman et al., 2005, Mao et al., 2010). That is, the primary loss pathway for removing radicals determines the O₃ sensitivity regime. Box modeling analysis has been performed on several metropolitan areas with ozone pollution to determine ozone sensitivity in terms of the LNO_x/Q metric. Houston and Mexico City, display NO_x sensitive chemistry in the afternoon, and hydrocarbon limited chemistry in the morning, while New York City displays hydrocarbon sensitive chemistry throughout the day (Mao et al., 2010). Ren et al. (2013) have shown that in Houston, on days when O₃ exceeded the 70 ppbv standard, O₃ production was VOC sensitive through most of the day. The sensitivity of urban ozone to NO_x and hydrocarbons can also be determined from the measured ratios of certain photoproducts (Sillman et al; 1995, Tonnesen and Dennis, 2000). Such indicator ratios provide a time integrated measure of the evolution of ozone photochemistry over the course of the day.

The relationship between the ozone production rate (P_{O₃}), the radical production rate (Q), the concentration of organic compounds [RH], and nitric oxide [NO] can be simply illustrated from an analysis of the general oxidation reactions described above for the NO_x and hydrocarbon limited regimes. For the situation with low NO_x concentrations such that the loss of radicals is dominated by formation of peroxides (R13) and the ozone chemistry is thus very NO_x sensitive, the ozone production rate is given by:

$$P_{\text{O}_3} = 2k_4[\text{NO}] [Q / k_{13}]^{0.5} \quad (3)$$

In this NO_x sensitive chemistry regime the ozone production rates scales with NO concentration. For the hydrocarbon sensitive regime, where NO_x concentrations are high and loss of radicals is dominated by formation of nitric acid (R10), the ozone production rate is given by:

$$P_{\text{O}_3} = 2Q k_6[\text{RH}] / k_{10}[\text{NO}_2][\text{M}] \quad (4)$$

In this case the ozone production rate is sensitive to the HO loss frequency to hydrocarbons (k₆[RH]) relative to that of NO₂ (k₁₀[NO₂][M]). In both cases ozone formation is sensitive to the radical

production rate Q , but ozone formation is more sensitive to Q in the hydrocarbon sensitive regime. The hydrocarbon sensitive regime can also be thought of as being radical limited. An urban airshed may change whether it is NO_x or hydrocarbon sensitive over the course of the day as the ratio of $[\text{RH}] / [\text{NO}_2]$ varies due to time of day variation in hydrocarbon and NO_x emission rates from anthropogenic and biogenic sources and concentration changes caused by time of day variation in dilution rates. An airshed may also be neither very NO_x limited or hydrocarbon limited and display similar sensitivity to hydrocarbons and NO_x . In this case the airshed ozone chemistry is described as being on the “ridgeline” where ozone production makes the most efficient use of available NO and HO (Tonnesen and Dennis, 2000).

2. Project Objectives and Tasks

The primary motivation of the project is to provide the Washington State Department of Ecology with a data set sufficient to meet two major study objectives: 1) to understand spatial and temporal patterns of main ozone precursors around the Tri-Cities; and 2) evaluate the AIRPACT 5 regional air quality forecast model by comparison against T-COPS observations. To better understand the conditions of ozone formation in the Tri-Cities, the Department of Ecology formulated an ozone field experiment study. Stakeholders consisting of Ecology's regional offices, BCAA, Oregon Department of Environmental Quality (ODEQ) and the Washington State Department of Transportation (WSDOT) discussed project scoping and logistics with researchers from Washington State University (WSU). Gridded emissions inventories were examined and staff familiar with air emissions in the area were consulted. After agreeing on a list of chemical species and monitoring locations, WSU and RJ Lee Group (RJLG) were contracted to conduct field monitoring in July and August, 2016. The field study was called T-COPS.

The objective of T-COPS was the monitoring of ozone, its major precursors, and meteorological conditions within the Tri-Cities metropolitan area for a 3 week period at three fixed site locations. These locations would provide a better understanding of temporal and spatial variation of ozone and its precursors in the Tri-Cities area. Mobile monitoring of ozone and selected precursors was conducted by RJLG. WSU was tasked with the collection of air quality and meteorological data from two field sites to address the major objectives. Detailed analysis and model evaluation of AIRPACT 5 will be conducted separately from this work.

The T-COPS study included the following tasks: 1) Instrument calibration and MACL integration at WSU; 2) field observations; 3) data reduction and validation; 4) data analysis to address project objectives; and 5) reporting of results.

Task 1: The equipment listed in Table 5.1 was integrated into WSU's Mobile Atmospheric Chemistry Laboratory (MACL) in early June 2016 and was deployed to the BCAA site in Kennewick for the T-COPS study on July 25. Instruments were recalibrated again upon set-up at BCAA.

Task 2: MACL field observations were made at the BCAA field site from July 27, 2016 to Aug 19, 2016. WSU also set-up a 10-m meteorological tower and O₃ and NO_x air quality monitoring equipment at the Horn Rapids site. Meteorological and air quality observations were made from July 27 to August 19. On-site activities were carried out by WSU staff with assistance from Washington Department of Ecology and BCAA staff. On-site operations included: 1) inspection of instruments and data from the acquisition systems; 2) periodic performance tests; 3) documentation of instrument, station, and meteorological conditions; 4) preventive maintenance; 5) corrective maintenance; and 6) transmission of data and documentation. On-site operations were supported by Pullman-based WSU staff that stayed in the Tri-Cities for the duration of the field experiment. This support included: 1) daily visits to the BCAA site and periodic visits to the Horn Rapids site to check

on instrument operation; 2) periodic download and examination of field data; 3) replenishment of consumables and supplies; 4) regular contact and operations review with field staff; and 5) site visits as needed for instrument calibration, repair, and maintenance. Task 2 was completed August 19.

Task 3: Data were reduced to engineering units where required and the BCAA and Horn Rapids data checked and validated with in house QA/QC procedures that included inspection of time series for all variables and examination of scatter plots to check for outliers. Field audit data (spans and zeroes) were removed. Data was time averaged into 10-min and 60-min averages for archiving as an Excel spreadsheet and uploaded to DropBox and made available to Ecology staff. Task 3 was completed in November 2016.

Task 4: Data analysis was conducted on the BCAA, Horn Rapids, Burbank, and RJ Lee data sets to address the project objectives. Data analysis was conducted by WSU and Ecology staff. Data analysis was completed in July 2017.

Task 5: WSU has prepared this final report within input from Ecology staff. The report summarizes project operations, data assessment, and data analysis activities. The report was completed in November, 2017.

3. Report Format

This report is organized into 8 major chapters to describe the motivations, context, and methodology of the T-COPS study as well as the results and conclusions.

Chapter 1. Introduces the background and context of ozone levels in the Tri-Cities and other areas in Washington State as well as a description of ozone formation chemistry.

Chapter 2. Details the tasks and objectives of the T-COPS project as put forth in the initial work plan.

Chapter 3. Report format description.

Chapter 4. Describes the T-COPS field sites: Benton Clean Air Agency (BCAA), Horn Rapids, Burbank, and Mesa.

Chapter 5. Discusses the technical details of the instrumentation and other equipment deployed to the study sites.

Chapter 6. Summarizes the data collected during the study including data quality and meteorological observations.

Chapter 7. Presents data analysis of observations, designed to answer the motivating scientific questions for the study including understanding the spatial and temporal variation of ozone, identifying sources of ozone precursors, assessing the main chemical and meteorological drivers of ozone pollution events, and evaluating the performance of the AIRPACT 5 regional forecast model.

Chapter 8. Summarizes the major findings of the study and outlines directions for further research.

4. Study Methodology and Site Descriptions

The three week study was conducted from July 27 to August 19 to best overlap with the expected time period in summer when the Tri-Cities experiences elevated levels of ozone based on previous monitoring by the WA DoE. To measure spatial gradients of ozone and ozone precursors, the study design for T-COPS combined three fixed sites for continuous observations of ozone, ozone precursors, and surface meteorology as well as a mobile instrumented van operated by RJ Lee Group (Pasco, WA) that measured O₃, NO_x, and selected VOCs. The BCAA office location was chosen as the “master” fixed site for the WSU Mobile Atmospheric Chemistry Lab (MACL) instrument suite. More limited observations were made at the Burbank satellite site, operated by the WA DoE, and the Horn Rapids satellite site, operated by WSU. An additional fourth site, the Mesa site, in the town of Mesa, WA, was used to obtain information on ozone levels for a nearby eastern WA location outside of the Tri-Cities airshed. The Mesa site did not operate continuously but was periodically visited using the mobile instrumented van. The locations of the 3 principal fixed sites are shown in Figure 4. Detailed site descriptions are given in section 4.1

Tri-Cities region of Washington which is comprised of the cities of Richland, Kennewick, and Pasco. The city of West Richland, is much smaller, but is located in the same developmental footprint west of Richland. Richland, West Richland, and Kennewick are in Benton County, while Pasco is in Franklin County. The small town of Burbank (population ~ 3,000) where the satellite was located is in Walla Walla County. The cities are located at the confluence of the Columbia, Snake, and Yakima Rivers in Eastern Washington. The cities directly border each other and together comprise a moderate sized urban area with a combined population estimated to be 220,800 as of April 1, 2017 (Washington State Office of Financial Management, Forecasting Division). This area has seen significant population growth over the past decade with the city of Pasco growing by 20% from 2010 to 2017.

The climate of the Tri-Cities region is semi-arid. Mean annual precipitation is 224 mm per year (8.83”) (1981-2010 average, NOAA NWS). July and August are the hottest months. In August the mean daily maximum temperature is 32.2 °C, while the mean daily minimum temperature is 13 °C. Average monthly precipitation is 6.8 mm. Summer days are characterized by clear skies and hot temperatures. The area surrounding the Tri-Cities is primarily irrigated farmland to the east, north and due west. The Hanford Nuclear Reservation borders the Tri-Cities north of Richland. The Tri-Cities are bordered to the south by the Horse Heaven Hills, which are about 350-m above the city’s elevation. Interstate I-82 runs SE-NW on the southern side of the Horse Heaven Hills. A map of the Tri-Cities area with the T-COPS fixed site locations is shown in Figure 4.1.

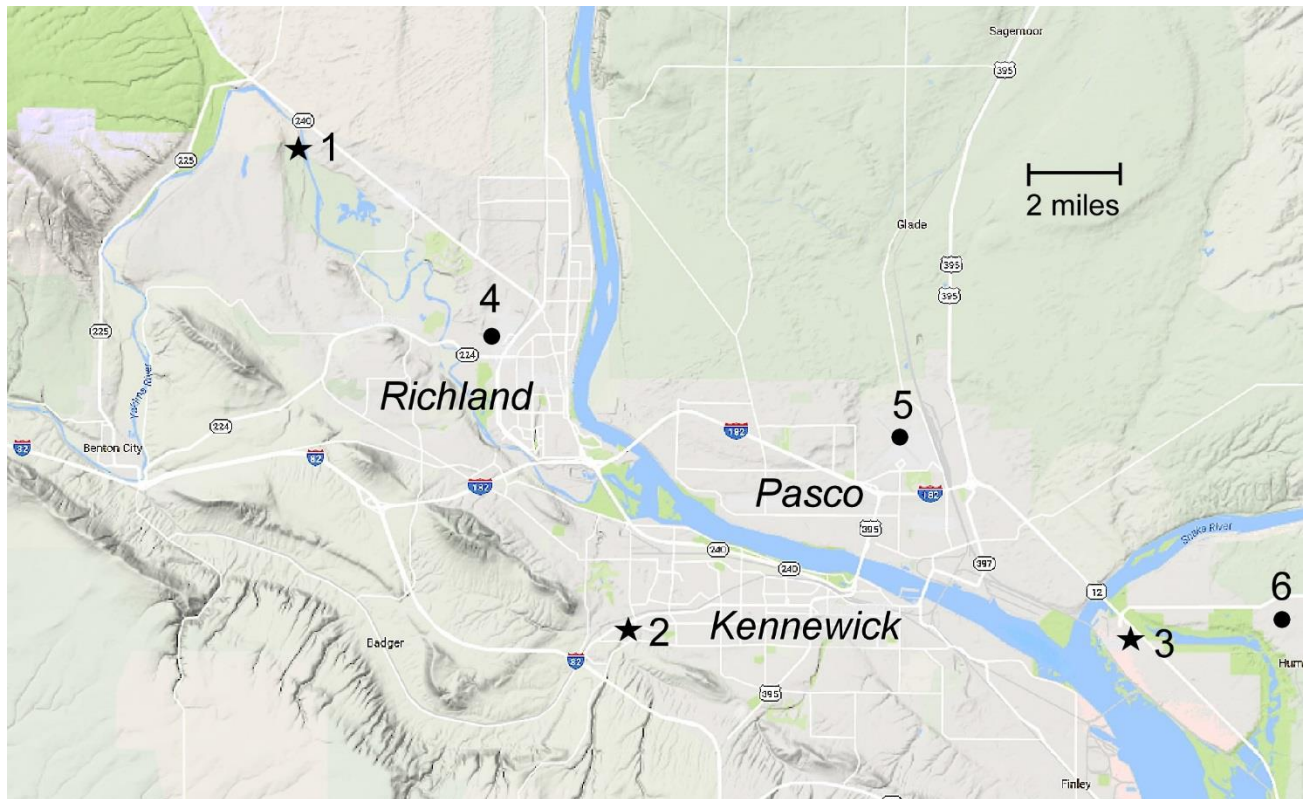


Figure 4.1. Map of the Tri-Cities area with locations of the 3 principal T-COPS air quality measurement sites noted as star symbols: 1 = Horn Rapids (Benton County), 2 = BCAA site (Kennewick, Benton County), 3=Burbank (Walla Walla County). Meteorological data from the Richland and Pasco airports and the LeGro MESO West site was used in the study (circles): site 4 = West Richland Airport (Benton County), site 5 = Tri-Cities Regional Airport (Franklin County), and site 6= the LeGro MESO West site. The Horse Heaven Hills, running NW – SE, defines the southern edge of the urban area. Interstate highway I-182, and state highway 240 and 395 connect the three cities of Richland, Kennewick and Pasco.

4.1. Site Descriptions

4.1.1. Benton Clean Air Agency

The Benton Clean Air Agency (BCAA) office location at 526 Clodfelter Road, Kennewick was the site for the WSU Mobile Atmospheric Chemistry Lab (MACL). Site elevation was 160-m ASL (525 feet). The MACL is a 20 foot long shelter designed for air quality observations. The MACL air quality instrumentation is described in Chapter 5. The shelter was parked in paved lot behind the BCAA office. The location is a mixed commercial and residential area near the southwestern side of Kennewick. Figure 4.2 shows a photograph of MACL at the BCAA site looking towards the east. The trailer was located about 100-m west of Clodfelter Road, a street with low traffic volume principally serving housing developments to the east of the site. Figure 4.3 shows a satellite view of the immediate area, the MACL shelter is visible in the middle of the view. About 250-m to the north was a more busy urban arterial road, Clearwater Avenue, that serves residences

and businesses and provides an access to interstate highway I-82, about 2.0 km south-west of the site. Roughly 100-m to the west of the site was a small residential area, separated from the BCAA property by a stream (Amon Wasteway). The banks of the stream were vegetated with Russian olive trees and sage brush. To the immediate north of the site was an undeveloped lot, and to the immediate south was a commercial business with a large empty gravel lot. Overall the site had good fetch in all directions and was not immediately impacted by local traffic emissions.



Figure 4.2. Photograph of the MACL equipment shelter at the BCAA location on July 28, 2016 for the T-COPS study. The MACL is equipped with a telescoping mast that provided a support tower for a surface meteorological weather station visible at the top of the mast as well as inlets for air sampling.



Figure 4.3. Satellite view of the immediate area surrounding the BCAA site illustrating proximity to residential neighborhoods and commercial businesses. North is top of view. The MACL location is given by the star symbol in the middle of the view between the Amon Wasteway canal and Clodfelter Road.

4.1.2. Horn Rapids Satellite Site

Ozone, NO_x , and surface meteorology measurements were made at the Horn Rapids site with equipment provided and operated by WSU. This site was private property. The owner was known to the WSU participants and was asked about participating in the study. The Horn Rapids site was

22 km NNE from the BCAA site. It is located in a relatively new residential area, near the Yakima River and the intersection of state highway 225 and 240, at the edge of a ridge known as Rattle Snake Mountain. To the north of this site is the Hanford Nuclear Reservation. The immediate area is relatively unpopulated and could be described as rural. This site is on the boundary of what could be considered the Tri-Cities airshed. The immediate area is either irrigated farmland or scrub desert. The elevation of the site is 135-m ASL (442 feet). To the immediate west was farmland. The property was located at the base of a grade that rose to ~ 183-m ASL. A 10-m meteorological tower was erected in the southeast corner of the property of the residence. The ozone and NO_x instruments were located inside the house. A roof top inlet was erected to bring in outside air for the instruments. Figure 4.4 shows photos of the meteorological tower and roof top inlet.



Figure 4.4. Left photograph shows the 10-m meteorological tower at the Horn Rapids site. Photo shows view looking south. Right photo shows air sampling inlet mounted on a tripod on the property owner's roof. Teflon tubing conveyed air to instruments located in a room inside the house.

4.1.3. Burbank Satellite Site

Burbank is a small city (~ population 300 people) located in Walla Walla County. The city is built along a strip bordered by the Columbia River to the west, the Snake River to the north, and state highway 12 to the east. The Burbank site was located at a school bus depot on the NW corner of the intersection of West Humorist Road and Jantz Road. The WA DoE deployed an instrumented

trailer to the site to measure CO, NO_x, and O₃. Periodic measurements of VOCs were also made at Burbank by RJLG. Both the RJLG's trailer and mobile van were located at the site. Figure 4.5 shows a photograph of the WA DoE instrumented trailer at the Burbank site. The site is 19 km east of the BCAA site. This was selected as it was in an open area and enclosed by security fencing. School buses were not used or serviced during the study period. Figure 4.6 shows a satellite view of the immediate area. State highway 12 runs in a NW-SE slant about 350-m to the immediate east of the site. The immediate south of the site is residential while to the immediate north was an undeveloped lot. Further to the north and east across highway 12 is the McNary National Wildlife Refuge. Downriver on the Columbia, following Highway 12 to the south is the Boise Cascade Paper mill and other industries, about 12 km SSE from the Burbank site.



Figure 4.5. Burbank trailer with instruments and inlets installed. Inlets were located approximately 4-m above ground level and 1-m above the trailer roof.



Figure 4.6. Satellite view of the Burbank site with Department of Ecology instrumented trailer location given by star symbol at corner of Humorist Road and Jantz Road. Highway 12 ran SE-NW to the east of the site

4.1.4. Mesa Satellite Site

The Mesa site was chosen because it was thought to be uninfluenced by the Tri-Cities and represents an entry point into the airshed under conditions of northerly wind flow. Mesa is a small town (population 495) in Franklin County surrounded by farmland as shown in Figure 4.7. The Mesa site was located about 37 km north east of the Tri-Cities along highway 395 at the Watermaster's Headquarters building. The RJLG van was deployed to the site periodically to measure surface meteorology, NO_x , O_3 , and VOCs.



Figure 4.7. Satellite view of the Mesa site.

5. Instrument Descriptions

5.1. Site Measurement Schedule

Measurements at the BCAA site began on 7/27/2016 at 22:00. This included surface meteorology and all air quality instruments except for the AQD NO_x/NO_y instrument and the PTR-MS. The PTR-MS was brought online on 7/28/2016 at 11:00 and the AQD NO_x/NO_y instrument was brought online on 7/28/2016 at 13:00. Measurements continued uninterrupted (aside from calibrations and performance audits) until 8/19/2016 at 9:00, when the instruments were shut down.

At the Horn Rapids site, surface meteorological measurements began on 7/27/2016 at 17:00 and NO_x and O₃ measurements began on 7/28/2016 at 18:00. Ozone measurements were made with the TECO 48 ozone instrument until 8/3/2016 at 13:00 at which point a Dasibi 1008 O₃ analyzer was used.

At the Burbank site, the WA DoE measured CO, NO_x, and O₃ from 7/27/2016 through 8/19/2016. No surface meteorological measurements were made by at the site. The RJLG trailer was at this site from August 3-4 and August 12-18.

5.2 BCAA Site Instruments

The WSU MACL was located at the BCAA site. The MACL was equipped with various air quality monitoring instruments and a 10 m crank up tower to for a weather station and to support air sampling inlets. A picture of the MACL is shown below in Figure 5.1. The weather station was located 11-m height above the ground. The main air sampling inlet was 6.7-m above the ground. The air inlet for the NO_y measurements was 6.1-m above the ground (grey box mounted to tower visible in Figure 5.1). Table 5.1 lists the MACL equipment operated for the T-COPS study. The Teledyne equipment was purchased new in April 2016.

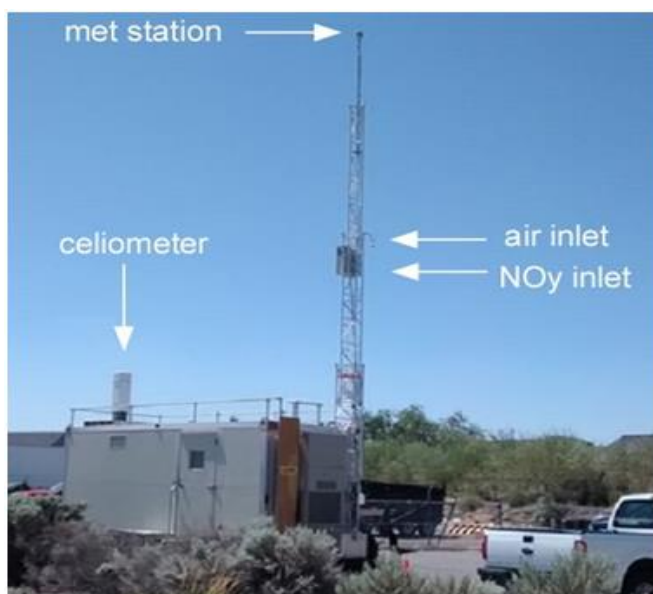


Figure 5.1. The WSU MACL with instrumentation and inlets installed. The white object on the MACL roof is a ceilometer. Ceilometer data was not used in this study.

Table 5.1. Measurements and instrumentation at the BCAA site.

Description	Label	Instrument	Range	Resolution
ozone	O3	Teledyne T400	0 – 500 ppbv	0.1 ppbv
carbon monoxide	CO2	Teledyne T300U	0 – 2,000 ppbv	0.5 ppbv
Nitric oxide	NO	Teledyne T200U	0 – 200 ppbv	0.05 ppbv
Nitrogen dioxide	NO2	Teledyne T200U	0 – 200 ppbv	0.05 ppbv
Sulfur dioxide	SO2	Teledyne T100U	0 – 100 ppbv	0.1 ppbv
Carbon dioxide	CO2	LiCor 840A	0 – 20,000 ppmv	1 ppmv
Water vapor	H2O	LiCor 840A	0 – 60 ‰	0.01‰
Barometric	Pres	Vaisala WXT-510	600 – 1100	0.1 mbar
Air temperature	Temp	Vaisala WXT-510	-52 to 60 °C	0.1 °C
Relative humidity	RH	Vaisala WXT-510	0 – 100% RH	0.1% RH
Wind speed	WinSpd	Vaisala WXT-510	0 – 60 m/s	0.1 m/s
Wind direction	WinDir	Vaisala WXT-510	0- 360 deg	0.1 deg
Nitric oxide	NO	Air Quality Design	0 – 500 ppbv	0.001 ppbv
Nitrogen dioxide	NO2	Air Quality Design	0 – 500 ppbv	0.001 ppbv
Nitrogen oxides	NOy	Air Quality Design	0 – 500 ppbv	0.001 ppbv
Volatile organic	VOC	Ionicon PTR-MS	0 – 500 ppbv	0.001 ppbv

5.2.1 Gas Phase Instrumentation Inlet

Sample air was provided to the individual gas phase instruments through a common 0.5” outer diameter PFA sample line. The sample line was attached to the crank up meteorological tower at a height of approximately 6.7 meters with a PFA funnel attached to the outdoor end to protect the inlet from precipitation. Sample air was drawn through the tube by a diaphragm pump housed in the trailer, which pulled air through the line at a flow rate of approximately 30 liters per minute. All of the instrumentation housed in the MACL (PTR-MS, CO, Teledyne NO_x, O₃, SO₂, CO₂ and H₂O) sub sampled from this flow except for the AQD NO_x/NO_y instrument, which had its own dedicated inlet.

The AQD NO_x/NO_y analyzer’s inlet system was housed in a NEMA enclosure and mounted to the meteorological tower approximately 0.6 m below the main gas phase inlet. The NO_x/NO_y inlet enclosure housed a molybdenum catalyst for converting NO_y compounds to NO as well as a blue

light LED photolysis cell for converting NO₂ to NO. The utility of housing these converters outdoors near where sample air was drawn in was to avoid losses of NO_y compounds such as nitric acid to sample line surfaces between the inlet and the analyzer. The inlet consisted of a 0.25" outer diameter PFA tube that protruded about 1 inch below the inlet box. The PFA tubing within the enclosure was thermostated to 30 °C to prevent losses to inlet surfaces. The inlet flow was split between two channels inside the box, one that passed through the molybdenum catalyst (NO_y, channel 1) and one that passed through the photolysis cell (NO_x, channel 2).

5.2.2 AQD NO_x/NO_y Analyzer

A two channel chemiluminescence NO detector (Air Quality Design) was used to measure NO, NO₂, and NO_y. NO_y was measured continuously on one channel by converting NO_y to NO using a molybdenum oxide reduction catalyst and using the chemiluminescence analyzer to measure NO. NO and NO₂ were measured on the other channel using a blue light converter to photolyze NO₂, yielding NO. The NO₂ converter was cycled on and off every 30 seconds, meaning that the instrument was measuring NO for 30 seconds (while the converter was off) and NO_x for 30 seconds (while the converter was on). The difference between NO_x and NO measurements was reported as NO₂. NO_y is defined as NO_x plus the compounds that result from the oxidation of NO_x. This includes, but is not limited to: HNO₃, HONO, PAN, organic nitrates, NO₃, and N₂O₅. Data were recorded at 1 Hz and NO_y, NO, and NO₂ mixing ratios were reported at 1 minute intervals. Instrument sensitivity was determined using a EPA certified standard 101.4 ppmv ±1% (Scott Marrin) diluted in dry zero air to produce a calibration mixing ratio of 125 ppbv. Calibrations were performed about every 5 days to ensure that instrument sensitivity had not drifted. Calibration of the NO₂ converter efficiency was done using gas phase of titration of NO to NO₂. Instrument zeroes were performed every 30 minutes by titrating NO to NO₂ in "zero volumes" for two minutes. Instrumental backgrounds were determined by interpolating measured zeros.

5.2.3. Proton Transfer Reaction Mass Spectrometer (PTR-MS)

Measurements of VOCs were made using a PTR-MS (Ionicon Analytik, Austria). The PTR-MS measures VOCs by chemical ionization using a proton transfer reaction whereby H₃O⁺ transfers a proton to an organic (R) to create a positively charged organic ion (RH⁺).



Ions were detected using a quadrupole mass spectrometer. The PTR-MS method is described in detail in the literature (Lindinger et al., 1998; de Gouw et al., 2006). This proton transfer reaction is fast for compounds with a proton affinity greater than that of water. Many compounds associated with urban air pollution sources can be measured using the PTR-MS including aromatics (benzene, toluene, xylenes) and aldehydes (formaldehyde, acetaldehyde). The PTR-MS technique is not sensitive to compounds that have proton affinities substantially less than water, notably smaller alkanes (~C₆ and smaller). There are two factors that can complicate the interpretation of PTR-MS measurements. First are isobaric interferences, where multiple compounds share a common molecular weight and thus produce the same RH⁺ ion. An example of this type of interference is

between acetone and propanal. Secondly, the proton transfer reaction takes place in an ion drift tube which has an electrical potential applied to it to increase ion kinetic energy. This extra kinetic energy is designed to break apart clusters that form between reagent ions and water vapor ($\text{H}_3\text{O}^+\cdot\text{H}_2\text{O}$), but a side effect of this additional kinetic energy is that proton transfer reactions with many compounds are dissociative. These dissociation reactions can produce positive interferences. For example, ethylbenzene fragments to produce protonated benzene, and thus benzene measurements made by a PTR-MS operated at high electric field strength in the drift tube are biased high.

For the T-COPS field project, the PTR-MS was operated with a lower electrical field strength to mitigate the problem of dissociative proton transfer reactions. Drift tube conditions are quantified in units of Townsends, which is the ratio of the drift tube electrical potential to the molecular number density of air inside the drift tube (E/N , $1 \text{ Td}=10^{-17} \text{ V cm}^2$). During T-COPS, the drift tube was operated at 80 Td conditions (drift pressure=2.01 mbar, drift temperature=60 °C, drift voltage=320 V). To allow for operation at 80 Td, a sample dehumidifier was employed to limit clustering between reagent ions and ambient water vapor and improve sensitivity to formaldehyde. The dehumidifier worked by pulling the air sample through a -30 °C cold zone and is described in detail by Jobson and McCoskey (2010).

The PTR-MS was calibrated using multicomponent component compressed gas standards (Scott-Marrin and Apel-Reimer Environmental). Formaldehyde calibrations were performed using a permeation tube (Kin-Tek). Calibrations were performed about every three days throughout the study. Sensitivities for the compounds reported were averaged and used for the entire study, as they were consistent over the study period. Instrumental backgrounds were determined by measuring zero air daily for one hour, from 1:00 – 2:00 am. The zero air was produced by passing ambient air through a heated Pt catalyst. The PTR-MS was operated in multiple ion detection (MID) mode during the T-COPS study. Selected ions that were monitored and the associated compounds are given in Table 5.2. The acronym MVK refers to methyl vinyl ketone and MACR to methacrolein, these compounds are isoprene photoproducts. C_2 -alkylbenzenes is the sum of the alkylated monoaromatic compounds p-xylene, o-xylene, m-xylene, ethylbenzene, and benzaldehyde. The C_3 -alkylbenzene and C_4 -alkylbenzene data similarly sum the isomeric alkylated monoaromatics of the same molecular mass. While the signal at m/z 69 is attributed to the compound isoprene, emitted largely from trees, it is known to WSU that other compounds also produce at ion at this mass due to dissociation reactions, notably cycloalkanes emitted in vehicle exhaust (Gueneron et al, 2015). Data collection frequency for this mass list was about 1 minute.

5.2.4. Teledyne CO Monitor

Carbon monoxide was measured using the gas filter correlation technique by a Teledyne T300 U instrument. This instrument is certified as an Automated Reference Method by the EPA. The instrument has a detection limit of less than 20 ppbv and precision of $\pm 0.5\%$. The instrument was calibrated by diluting with dry air an EPA grade compressed gas CO standard (39.9 ppmv $\pm 1\%$, Scott Marin, CA) purchased for this project. The instrument was set to a span range of 2 ppmv and

calibrations were performed at 80 % of full scale range (1.6 ppmv). The CO instrument performance was audited periodically during T-COPS as described in section 5.10.

Table 5.2. Selected ions and corresponding compound association measured by the PTR-MS during T-COPS

m/z	compound	formula	notes
31	formaldehyde	HCHO	
33	methanol	CH ₃ OH	
42	acetonitrile	CH ₃ CN	wild fire tracer
45	acetaldehyde	CH ₃ CHO	
49	methylhydroperoxide	CH ₃ OOH	photoproduct
59	acetone + propanal	C ₃ H ₆ O	
69	isoprene	C ₅ H ₈	biogenic
71	MVK + MACR	C ₄ H ₆	isoprene photoproducts
73	2-butanone + butanal	C ₄ H ₈	
79	benzene	C ₆ H ₆	
93	toluene	C ₇ H ₈	
105	styrene	C ₈ H ₈	
107	C ₂ -alkylbenzenes	C ₈ H ₁₀	
121	C ₃ -alkylbenzenes	C ₉ H ₁₂	
135	C ₄ -alkylbenzenes	C ₁₀ H ₁₄	
137	monoterpenes	C ₁₀ H ₁₅	biogenic

5.2.5. Teledyne NO_x Monitor

In addition to the AQD NO_x/NO_y analyzer, NO_x was also measured by a Teledyne T200U instrument. This instrument is certified as an Automated Reference Method by the EPA for NO₂. This instrument uses the chemiluminescence technique to measure NO. NO₂ was converted to NO using a molybdenum catalyst with the NO_x concentration being measured when the sample flow was diverted through the catalyst. The NO₂ concentration was reported as the difference between the NO_x and the NO₂ concentrations. The instrument had a detection limit of 0.05 ppbv and a precision of 0.5%. The NO_x instrument was calibrated by diluting an EPA certified standard of NO (4.02

ppmv $\pm 1\%$, Scott Marin, CA) with dry zero air. The instrument was set to 200 ppbv range and calibration was performed at 80% of full scale range (160 ppbv). Instrument performance was audited periodically during T-COPS as described in section 5.10.

5.2.6. Teledyne O₃ Monitor

Ozone was measured using the UV absorption technique by a Teledyne T400 analyzer. This instrument is certified as an Automated Equivalent Method by the EPA. The instrument had a detection limit of 0.4 ppbv and a precision of $\pm 0.5\%$. The instrument was calibrated using a secondary O₃ reference generator, a Teledyne T700U dynamic dilution calibrator. The Teledyne O₃ photometer in the T700U had been calibrated and certified on March 30, 2016 by Teledyne against a NIST traceable photometer. The O₃ instrument performance was performance was audited periodically during T-COPS as described in section 5.10.

5.2.7. Teledyne SO₂ Monitor

Sulfur dioxide was measured using ultraviolet fluorescence by a Teledyne T100 U analyzer. This instrument is certified as an Automated Equivalent Method by the EPA. The instrumental detection limit was 0.05 ppbv and the precision was $\pm 0.5\%$. Measurements of SO₂ were not in the original study plan but we added this instrument as it was available as part of the MACL instrument suite. This instrument was factory calibrated and performance audits only included checking zero air backgrounds.

5.2.8. LICOR CO₂/H₂O Monitor

Carbon dioxide and water vapor were measured using non-dispersive infrared absorption by a LI-COR LI-840A analyzer. Factory response factors were used for determination of CO₂ and H₂O concentrations. Instrumental detection limits were 2 ppmv for CO₂ and 0.02 parts per thousand for H₂O. Measurement precision for CO₂ and H₂O were both $\pm 1.5\%$.

5.2.9. WXT Surface Meteorology Measurements

Surface meteorological measurements were made using a Vaisala WXT-510 weather station. The WXT was mounted atop the MACL's 10-m tall crank up tower. The WXT measured relative humidity, atmospheric pressure, air temperature, wind speed, and wind direction. The weather station specifications are shown in the Table 5.3.

Table 5.3. WXT-510 weather station specifications

	Units	Range	Precision	Accuracy
pressure	mbar	600-1100	0.1 mbar	± 1 mbar
temperature	°C	-52 to 60	0.1 °C	± 0.3 °C
relative humidity	%	0 - 100	0.1 %RH	± 3 RH
wind speed	m/s	0- 60 m/s	0.1 m/s	0.3 m/s
wind direction	deg from true North	0 - 360	0.1 deg	± 3 deg

5.3. Horn Rapids Satellite Site Instruments

For chemical measurements at the Horn Rapids site, NO_x and O₃ instruments were housed within a room in the property owner's residence. The air sample inlet was positioned on a tripod near the crown of the roof and a 0.375" outer diameter PFA tube was used to draw air at 5 SLPM to the instruments inside. Instruments sub sampled from this flow. Data were logged as 1 minute averages.

5.3.1. TECO 42C NO_x

The TECO 42C NO_x analyzer uses the chemiluminescence technique to measure NO and NO_x by converting NO₂ to NO using a molybdenum catalyst. This instrument had a detection limit of 0.4 ppbv and precision of ±0.4 ppbv. The TECO 42C NO_x analyzer was calibrated at WSU using the same Teledyne T700U calibrator and span gas used to calibrate the BCAA site Teledyne NO_x analyzer. Data were logged as 1 minute averages using the 10 volt analog outputs from the monitors. Data were logged using a Labjack U12 AD converter and data displayed and logged using Azeotech Daqfactory software running on a lap top computer.

5.3.2. TECO 48 O₃

The TECO 48 O₃ monitor used the UV absorption technique. This instrument reported very noisy data on the 1 minute time basis, so measurements were smoothed to a 30 minute average in the field. Measurements from the TECO 48 O₃ monitor are reported until 8/3/2016 13:00 at which point a Dasibi 1008 O₃ instrument was installed. Both monitors were calibrated against the Teledyne T700U O₃ photometer at WSU before being deployed to the field.

5.3.3. Dasibi 1008 O₃

The Dasibi 1008 O₃ monitor operated using the UV absorption technique. The detection limit of the instrument was 1 ppbv and the precision was ±1 ppbv. This monitor was deployed on 8/3/2016 13:00 and O₃ data reported after this time are from the Dasibi 1008.

5.3.4. Meteorological Measurements

Surface meteorological measurements used an AirMar WX200 weather station at top of a 10-m aluminum tower erected in the backyard, in the southeast corner of the property. At 2-m height temperature and relative humidity were measured using a Campbell Scientific temperate and RH sensor (CS215 probe). The weather station was powered by solar panels, with data logged as 1 minute averages onto a Campbell Scientific data logger. Data were collected from July 27, 14:49 to Aug 19, 11:00.

Table 5.5. Horn Rapids site surface weather station measurement specifications

AirMar WX200	Units	Range	Precision	Accuracy
pressure	mbar	300-1100	0.1 mbar	± 1 mbar
temperature	°C	-40 to 55	0.1 °C	± 1.1 °C
relative humidity	%	10 - 95	0.1 %RH	± 5 RH
wind speed	m/s	0- 40 m/s	0.1 m/s	0.5 m/s
wind direction	deg from true North	0 - 360	0.1 deg	± 5 deg
CS215 probe				
temperature	°C	-40 to 70	0.01 °C	± 0.4 °C
relative humidity	%	0 - 100	0.03 %RH	± 2 RH

5.4. Ecology Burbank Instruments

Instruments at the Burbank site were housed in a temperature-controlled 8' x 12' utility trailer. Instrument inlets were routed out the side of the trailer and through rigid tubing extending vertically approximately 1 meter above the trailer roof. Inlet material was ¼" outer diameter PFA tubing. Each analyzer had a dedicated sample inlet line.

5.4.1. Teledyne API 300U CO Monitor

CO measurements were conducted in the WSDOE trailer using a Teledyne API 300EU monitor. This instrument employs the gas filter correlation technique. The instrument has a detection limit of 20 ppbv and precision of ±0.5%. This instrument is designated as an Automated Reference Method by the EPA. Instrument performance was audited weekly to ensure that the zero was within ± 50 ppbv and that the response was within ± 15%.

5.4.2. Teledyne API 200EU NO_x Monitor

NO_x measurements were conducted using a Teledyne API 200EU monitor. This instrument measured NO_x using the chemiluminescence technique and measured NO₂ by converting NO₂ to NO using a molybdenum catalyst. The instrumental detection limit was 0.05 ppbv and measurement precision of the technique was the greater of 1% of full scale range or 0.1 ppbv. Instrument performance was audited weekly to ensure that the zero was within ± 5 ppbv and the response was within $\pm 15\%$.

5.4.3. 2B Technologies 202 O₃ Monitor

Measurements of O₃ were made using a 2B Technologies 202 FEM O₃ monitor. This instrument used the UV absorption technique. The instrumental detection limit was 3 ppbv and the precision was the greater of ± 1.5 ppbv or $\pm 2\%$ of the reading. The ozone instrument performance was audited weekly at 0, 15, 70, and 100 ppbv. The zero was maintained within ± 5 ppbv and the tolerance for the other ozone levels was $\pm 10\%$.

5.5. RJ Lee Group Van and Trailer

5.5.1. Mobile Laboratory (Van)

The RJLG mobile analytical laboratory was a Mercedes Sprinter van designed for making air quality measurements while in motion and during short stops. The van housed a Time of Flight (TOF) PTR-MS, a LICOR Li-840A CO₂ monitor, a GPS-based weather station, a TECO 42 NO_x analyzer, and a 2B Technologies O₃ analyzer (instruments described below). The O₃ and NO_x analyzers were provided by WSU and were installed into their own rack so that they could be moved between the van and the trailer described below in section 5.5.2. A marine meteorological GPS instrument (New Mountain Innovations, NW 100) was used to monitor meteorological parameters as well as geographical position. Sampling was performed from an inlet on the rooftop of the van, providing a sampling height of approximately 3-m. Sample air was transported to the instruments using a $\frac{3}{8}$ " OD PFA tubing with excess flow provided by a diaphragm pump. Instruments subsampled off of this main line. Table 5.6 shows the sampling locations of the van during the T-COPS field experiment. Typically, the van only made short stops ranging from 10 minutes to 1 hour at the different locations. However when the van was at Mesa sampling was done over several continuous hours. The van was deployed at Mesa on 3 occasions, for a total of 136 hours of sampling over 11 calendar days.

5.5.2. RJ Lee Stationary Laboratory (Trailer)

In addition to the van, which was primarily used for mobile sampling, a trailer was also employed for stationary sampling at Burbank from August 3-4, and then from August 12-18. The trailer was a Forest River toy-hauler, modified to house air quality instrumentation. The trailer housed a quadrupole PTR-MS owned by RJLG, and a LICOR Li-840A CO₂ monitor, a TECO 42 NO_x analyzer, and a 2B Technologies O₃ analyzer owned by WSU. A mast was installed on the outside of the trailer to house the sampling inlet, allowing for a sampling height of approximately 4 m. Sample was transported to the instruments through $\frac{1}{4}$ " OD PFA tubing using a diaphragm pump

to pull excess flow. The instruments sub-sampled off of this main line. Between the van and the trailer, VOC sampling was conducted at Burbank for a total of 228 hours. However some data quality concerns during the 8/12- 8/18 period prompted further work the following summer. This is explained in Section 6.9.

Table 5.6. Sampling locations of the RJ Lee Van during the T-COPs field experiment

Date	Mesa	Agrium	Tree Farm	Orchard	Railroad	CAFO	Wallula	Hanford
8-1	x	x						
8-2	x							
8-3	x							
8-5	x		x	x	x	x	x	
8-6	x							
8-7	x							
8-8	x							
8-9								x
8-10								x
8-11	x		x	x				x
8-12	x							
8-13	x							
8-14	x							
8-16			x	x	x	x	x	

5.5.3. 2B Technologies Ozone monitor

Ozone was measured using a 2B Technologies 205 O₃ monitor. Its detection limit was 2 ppbv and its precision was 2% of reading. The 2B O₃ instrument was installed in a rack with the TECO 42 NO_x and were only used in the RJ Lee van. The instrument was audited weekly after being deployed.

5.5.4 TECO 42 NO_x Monitor

The TECO 42 NO_x instrument used the chemiluminescence technique to measure NO and measured NO_x by converting NO₂ to NO using a molybdenum catalyst. The instrument was audited weekly after being deployed.

5.5.5 LICOR Li-840 A

Carbon dioxide and water vapor were measured using non-dispersive infrared absorption by a LI-COR LI-840A analyzer. Factory response factors were used for determination of CO₂ and H₂O concentrations. Instrumental detection limits were 2 ppmv for CO₂ and 0.02 parts per thousand and precisions for CO₂ and H₂O were both ±1.5%.

5.5.6 PTR-QMS

The Quadrupole PTR-MS (PTR-QMS) is described above in section 5.2.3 and in the literature (Lindinger et al., 1998; de Gouw et al., 2006). The unit operated in the RJ Lee trailer was

functionally the same as the one operated in the WSU MACL. During the study, zero air measurements were made daily by sampling zero air from a compressed air tank. Sensitivity checks were performed twice using the same compressed gas standard as the WSU PTR-MS, before deployment and after measurements were complete, to assure that the PTR-MS was operating properly. These calibrations and zero checks were only used to verify the instrument was operating properly and were not used during the data work up process. The calibrations yielded similar sensitivities before and after the campaign.

Data was translated into mixing ratios using the default method from Ionicon using the PTR-MS Viewer software. Raw instrument response was first adjusted to account for ion transmission using the default transmission curve provided by Ionicon. The response was normalized to the H_3O^+ count rate and divided by the sensitivities determined theoretically from ion kinetics.

5.5.7 PTR-TOF-MS

The PTR-TOF operates via the same principle as the PTR-QMS described in section 5.2.3, except that it identifies ions using a time-of-flight mass spectrometer. The PTR-TOF methodology is presented in the literature by Graus et al. (2010) and the instrument was operated using RJ Lee standard operating procedures. A calibration and zero system (CZS) from Ionicon was used in concert with a multicomponent compressed gas standard to zero and calibrate the PTR-TOF, producing zero air by passing ambient air through a catalyst to remove VOCs. During continuous sampling, analytical blanks were conducted at minimum every 8 hours by sampling zero air. Instrument sensitivity was audited daily by sampling a calibration gas and zero air mixture and multipoint calibrations were also performed to ensure accuracy.

6. Data

6.1. Fixed Site Data Quality and Completeness

Data for each instrument described above in Chapter 5 were assessed for quality. Instrument logs were consulted to remove any data not associated with ambient measurements and any data when instruments or data acquisition systems were not functioning properly. Data was shared with the WA DoE in two separate data files, one data file was averaged to a 60 minute averaging period and the other averaged to 10 minutes. Table 6.1 shows the data completeness for instruments operated by WSU and Ecology at BCAA, Burbank, and Horn Rapids. The data completeness value is the percentage of 10 minute averaging periods populated in the final data archive. The 10 minute averaging period was chosen because it is the shortest common averaging period between instruments at all sites. The data completeness for the Horn Rapids site was reported for the 60 minute averaging period due to issues with noise in the TECO O₃ instrument. Overall, data completeness was quite high, with data completeness greater than 90% for each measurement. Most instruments lost data due to calibrations, performance audits, and zero air background determinations. Additionally, BCAA CO data was lost when the instrument was restarted to replace its sample line filter and it took almost a day for the instrument performance to stabilize again. At the beginning of the campaign, the data acquisition sequence did not handle vector averaging of wind directions at BCAA properly, causing wind direction data to be lost. The MACL data acquisition system crashed once overnight, causing a small loss of meteorological data. Both the SO₂ and AQD NO_x/NO_y instrument lost data due to sampling zero air for an extended period of time.

At Horn Rapids, data was only lost for instrument maintenance. However, data from the TECO 48 ozone monitor was quite noisy, necessitating a 60 minute averaging period to smooth the data. The Dasibi ozone monitor was deployed on 8/3 to the Horn Rapids site to provide a redundant ozone measurement and to verify accuracy of the TECO 48 instrument. The final data archive reported ozone from the TECO 48 until 8/3 and from the Dasibi after 8/3. When compared with the Dasibi monitor, it was determined that the TECO monitor was slightly over reporting ozone. The observations made by the TECO monitor previous to the Dasibi coming online (8/3 and before) were corrected to account for the difference in concentration observed when the two monitors were both operating (8/3 and later). The measurement trends were well correlated on a 60 minute averaging period (r^2 of the correlation between the two was 0.97), but there were a small slope and offset (intercept of the TECO vs. Dasibi correlation =2.3 ppbv and slope=1.07). Ozone, NO_x, and CO measurements in the Ecology trailer ran without incident at Burbank.

Table 6.1. Data Coverage for WSU and Ecology Operated Instruments at BCAA, Horn Rapids, and Burbank

Measurement	Measurements	Instrument	Data Coverage
WSU MACL BCAA (10 minute average)			
Carbon Monoxide	CO	Teledyne T300 U	94.3
Nitrogen Oxides	NO _x	Teledyne T200 U	99.5
Ozone	O ₃	Teledyne T400	99.3
Sulfur Dioxide	SO ₂	Teledyne T100 U	96.3
Carbon Dioxide	CO ₂	LICOR 840a	98.9
Water Vapor	H ₂ O	LICOR 840a	99.3
Meteorological Parameters	Wind Direction	Vaisala WXT-510	91.9
	WS, T, P, RH	Vaisala WXT-510	98.2
Oxides of Nitrogen	NO _x /NO _y	AQD NO _x /NO _y	93.7
Volatile Organic Compounds	VOCs	PTR-MS	92.8
Horn Rapids (60 minute average)			
Surface Meteorology	WD, WS, T, P, RH	AirMar WX200	100
Nitrogen Oxides	NO _x	TECO 42c	99.6
Ozone	O ₃	TECO 48	99.2
Ozone	O ₃	Dasibi	72.8
Ozone	O ₃	TECO & Dasibi	99.4
Burbank (10 minute average)			
Nitrogen Oxides	NO _x	Teledyne 200EU	99.4
Ozone	O ₃	2B Tech. 202	99.7
Carbon Monoxide	CO	Teledyne 300EU	98.6

6.2 Study Overview – Weather Conditions

Conditions during the T-COPS study period from Thursday, July 27 to Friday, August 19 were generally clear and sunny. Figure 6.1 provides a general overview of the study conditions showing time series data of ozone, wind speed, wildfire smoke tracers (acetonitrile and $\text{PM}_{2.5}$), solar radiation, and meteorological conditions as identified at the local airports. Four ozone events are noted in the figure, corresponding to days when hourly ozone exceeded 70 ppbv. Meteorological conditions reported at the West Richland and Tri-Cities Regional airports indicate a cloudy overcast period with some light rain between Aug 8 starting at 17:50 and with skies clearing on Aug 9 at 20:50. Solar radiation data from the LeGro MESO West weather monitoring site indicate a reduction in afternoon solar radiation consistent with cloud cover for this period. In general the solar radiation data show most daylight periods were cloud free.

The T-COPS study period started on the Thursday before the Columbia Cup hydroplane boat race weekend (Saturday, July 30 and Sunday, July 31). This was a clear sky period and the hottest day during T-COPS occurred on Friday, July 29. The highest ozone at BCAA was also measured on this day and this is labelled ozone event #1 in Figure 6.1. For about a 24-hr period starting on Aug 1, 17:20 and ending Aug 2 15:30 smoke conditions were reported at the Tri-Cities Airport. The smoke likely originated from the Range 12 fire that started July 30 at 7 PM on the Department of Defense Yakima Training Center lands, about 40 miles WNW of the Tri Cities. A related back burn set on Rattlesnake Mountain on Sunday, July 31 to keep the fire from spreading onto the Hanford Nuclear Reservation also contributed smoke to the area. This fire was reported as a smoldering fire that was spreading through grass and sagebrush. The impact of the wildfire smoke was evident in the BCAA site data as elevated acetonitrile and CO mixing ratios and elevated $\text{PM}_{2.5}$ concentrations (peaking around $30 \mu\text{g}/\text{m}^3$) as reported from the DoE Metaline site. Acetonitrile is a good biomass burning tracer, as elevated levels have been consistently observed in biomass burning plumes but not urban plumes (de Gouw et al., 2003). Acetonitrile has been used in many other studies to identify forest fire plumes (de Gouw et al., 2003; Karl et al., 2007; Yokelson et al., 2009; Lack et al., 2013) and agricultural burning plumes (Holzinger et al., 2005; Yokelson et al., 2009; Yuan et al., 2010). As the wildfire plume entered the area on July 30 21:00, acetonitrile increased from its background level of about 80 pptv to over 1000 pptv. Between this time and Aug 2 acetonitrile mixing ratios were variable but elevated, averaging 280 ± 140 pptv. On August 2, winds increased to their highest values observed in the study, ~ 8 to 12 m/s at Tri-Cities Airport and ~ 5 m/s at BCAA, resulting in lower $\text{PM}_{2.5}$ and acetonitrile mixing ratios. After this period of windy weather ended on August 3, acetonitrile and $\text{PM}_{2.5}$ slowly increased before returning to typical background levels on August 6. A large spike in acetonitrile and $\text{PM}_{2.5}$ occurred on August 6, around 22:30, lasting for about 1.5 hours. Owing to the very high concentrations observed and its short duration, we concluded this was a more local fire event and unrelated to the Range 12 wild fire.

Given the impact of the wildfire emissions on the chemical measurements, and impact of higher winds and overcast skies from August 8 – August 10 on mitigating photochemical ozone production, the data from these periods were identified for separate consideration from the remaining clear sky data in the subsequent data analysis. These periods are delineated in Figure 6.1. The

wildfire impacted period was assigned as July 30 21:00 to August 6 00:00. Interestingly, two of the ozone events occurred during the wildfire impacted period and these are label events #2 (Monday, August 1) and #3 (Friday, August 5) in Figure 6.1. The windy-overcast period was assigned as Aug 7 00:00 to August 10 00:00. Daily maximum ozone was lowest during the rainy cloudy period, and on windy days of July 31 and August 2. The period from August 10 to August 19 was a clear sky period with light winds, conducive to ozone formation. A day of elevated ozone occurred during this period on Tuesday, August 16, indicated by label #4 in Figure 6.1.

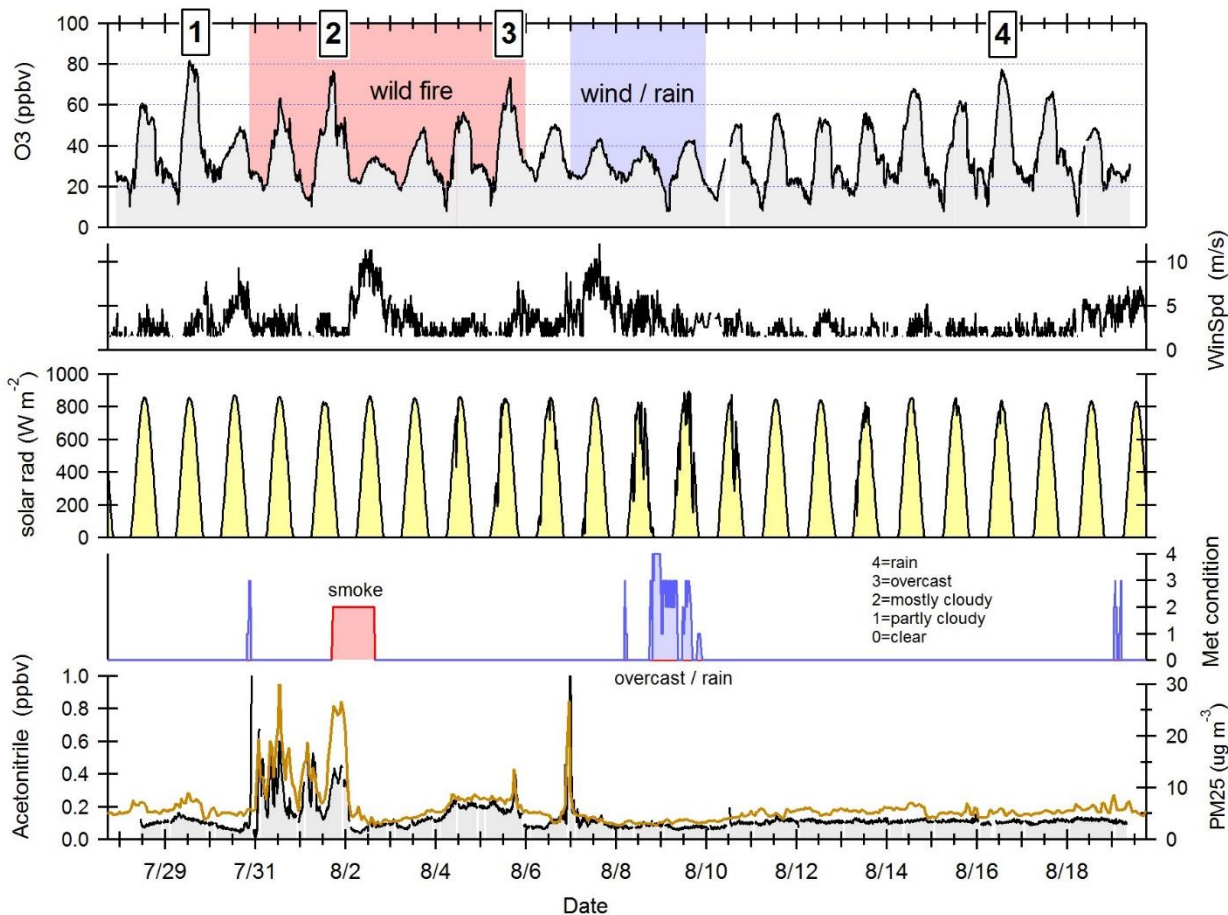


Figure 6.1. Time series of ozone and acetonitrile (brown trace) mixing ratios and wind speed as measured at BCAA, PM_{2.5} measured at the DoE Metaline site, meteorological conditions as reported at the Tri-Cities Regional airport, and solar radiation from the LeGro meteorological site. For most of the study skies were clear. Periods where the Tri-Cities was impacted by wildfire emissions (red shading) and inclement weather (blue shading) are identified. Periods when hourly ozone exceeded 70 ppbv at BCAA are indicated by numeric labels.

6.3 Temperature

The temperature record for the T-COPS study period is shown in Figure 6.2 together with solar radiation data from the LeGro site and surface wind speeds measured at Horn Rapids, BCAA and LeGro. In general highest afternoon temperatures were observed at the Horn Rapids site. The overall hottest day in the Tri-Cities was July 29. The lowest nighttime temperature were often observed at the Pasco airport. The period of windy and rainy weather from August 7 to August 9 was followed by a gradual warming trend (Aug 10 to Aug 12) and several consecutive days (August 14 to August 18) with afternoon temperatures over 35 °C throughout the Tri-Cities. Table 6.1 shows the average, minimum and maximum temperatures observed during the T-COPS study period. Figure 6.3 shows the observed Pasco Airport temperatures during the T-COPS study period in comparison with normal high and low temperatures and record high and low temperatures for the past 17 years (2000 to 2017). The week long period from August 12 to August 18 was consistently warmer by about 3.5 °C than normal daily maximums.

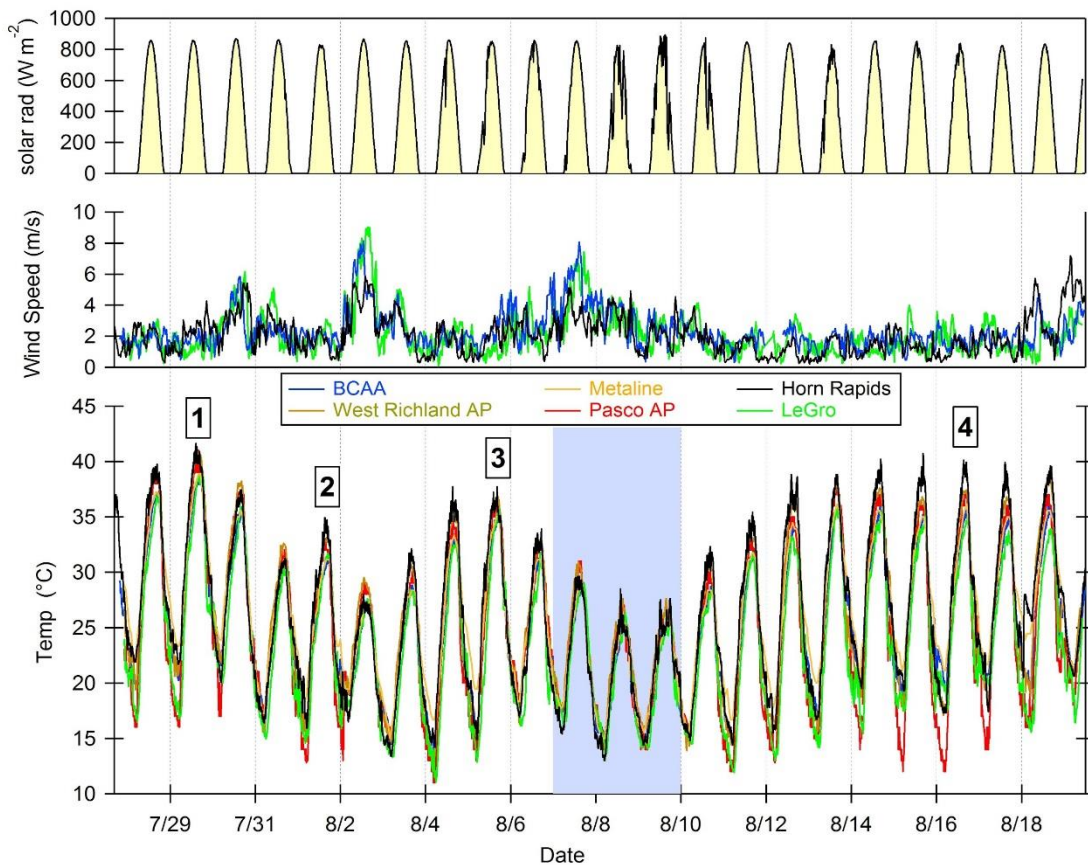


Figure 6.2. Study conditions during T-COPS. Top panel shows solar radiation data from LeGro. Middle panel shows surface wind speeds measured at BCAA (red), Horn rapids (black) and LeGro (green). Bottom panel shows temperature record for the indicated sites. Numeric labels indicate ozone event days. Shading in the bottom panel indicates the period of wind and rainy weather.

Table 6.1. Temperature statistics for the T-COPS study period

	Average (C)	Min (C)	Max (C)
BCAA	25.0	13.5	38.7
Horn Rapids	26.0	13.0	41.6
Metaline	25.9	15.0	38.9
West Richland Airport	25.9	13.0	40.8
Pasco Airport	24.3	11.0	41.1
LeGro	23.4	11.1	39.2

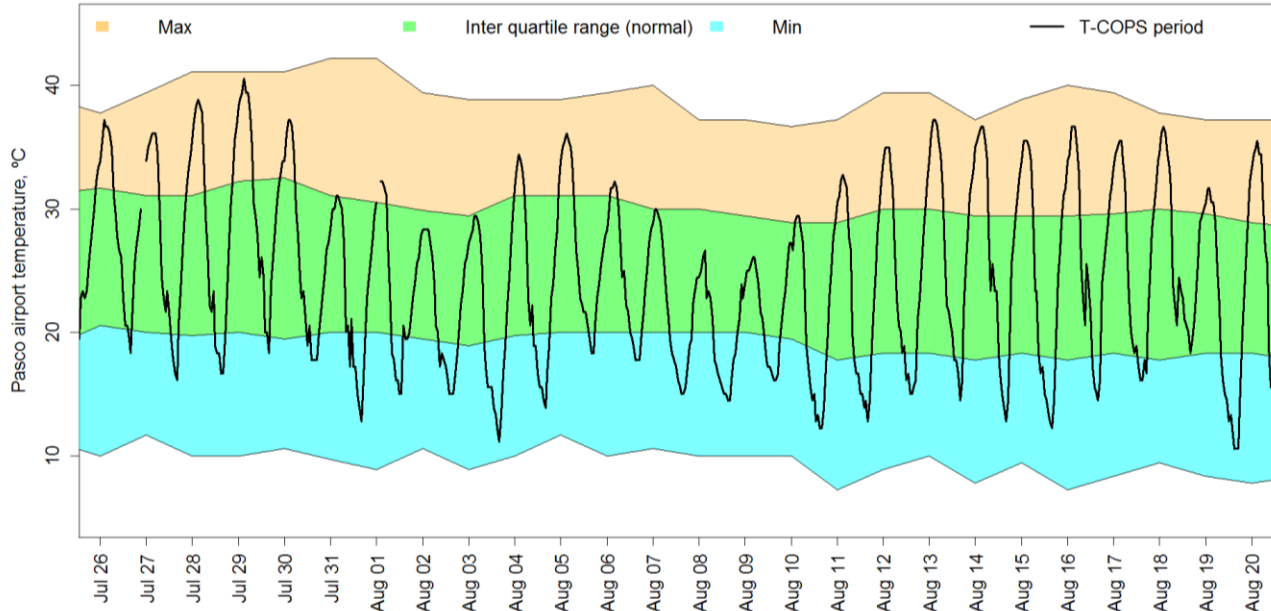


Figure 6.3. Observed hourly temperatures overlaid on daily high (orange shading), low (blue) and interquartile range (normals; green) at the Pasco Airport (KPSC). Historical data from 2000 onward were considered. The period from August 12 to August 18 was warmer than normal but did not set temperature records.

6.4 Wind Speed

Wind speeds for the Horn Rapids, BCAA, LeGro and Metaline sites are displayed in Figure 6.4. Shown are ½ hour averages with the exception of Metaline which is a 1 hr average. The airports do not report values for wind speeds less than 1.5 m/s; these are listed as calm winds and no

wind speed or wind direction values are reported. Calms were 26% of the data from the Pasco airport. During the clear sunny period starting August 11, the BCAA, Horn rapids and Metaline sites displayed a diel (24 period duration) pattern with low wind speeds at night and in the morning and higher afternoon wind speeds.

Wind speed distribution for the BCAA, LeGro and Horn Rapids sites are shown in Figure 6.5. The greater frequency of occurrence of low wind speeds at Horn Rapids is evident. Median wind speeds at BCAA were 2.0 m/s, 1.9 m/s at Horn Rapids, and 1.8 m/s at LeGro. The Horn Rapids site typically had the lowest wind speeds; 59% of the wind speeds were below 2 m/s.

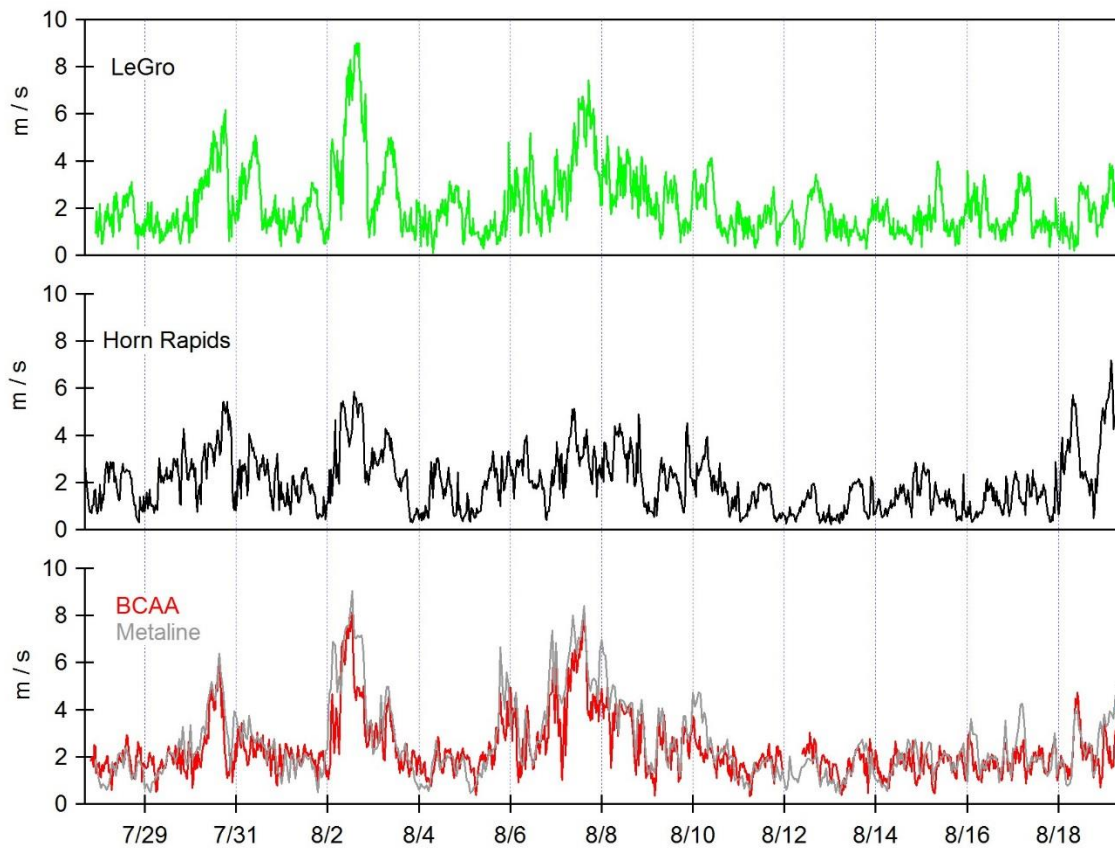


Figure 6.4. Wind speeds measured during the T-COPS study period showing $\frac{1}{2}$ hour average data for LeGro, BCAA and Horn rapids and 1-hr data from Metaline.

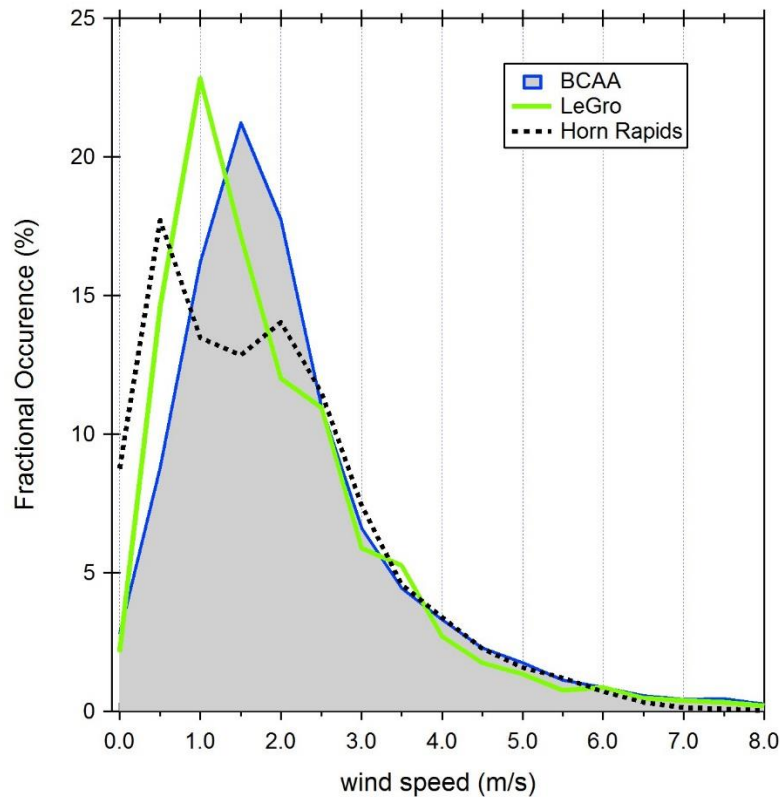


Figure 6.5. Wind speed distribution measured at the BCAA (shaded area) and Horn Rapids (green trace) sites and reported from the LeGro site (black trace) for the T-COPS period. For BCAA and Horn Rapids the 1 minute wind speed data were used. Wind speed bins are 0.5 m s^{-1} .

6.5 Wind Direction

Wind rose plots are shown in Figure 6.6. Wind roses are shown for time of day periods for the Pasco and West Richland Airports, the Horn Rapids site, BCAA, and LeGro (Burbank). At the BCAA site, nocturnal winds were typically from the southern sector and the site is likely impacted by drainage flow along the Coldfelter Creek / Amon Wasteway that runs south to north through the site. This has important consequences for data interpretation for this site. At night the site would receive air from outside the Tri-Cities airshed. Morning winds were typically from the S and SW from all sites; the Pasco airport had a higher fraction of northerly winds in the morning than the other sites. Morning wind speeds were typically in the 3 to 5 m/s range. During the afternoon winds were typically light throughout the Tri-Cities area ($< 3 \text{ m/s}$). In general most sites had a northerly wind component dominating. Wind direction in the area thus shifts from southerly in the morning to northerly in the afternoon. At the BCAA site, afternoon winds were mostly from the NE while at Burbank (LeGro) NW winds predominated. At the Pasco airport afternoon winds from the N and NW dominated. At the Horn Rapids afternoon winds were from the SE, compared to SW winds in the morning. The spatial variation in predominant wind direction suggests that the light winds in the afternoon are affected by local topography and air circulation in the airshed may be complex. The relative locations of the four stationary sites are shown on the map below in Figure 6.7 overlaid with

wind roses constructed from meteorological measurements made during the study period. Hermiston's wind rose is also shown to demonstrate the distinct influence of terrain on airflow.

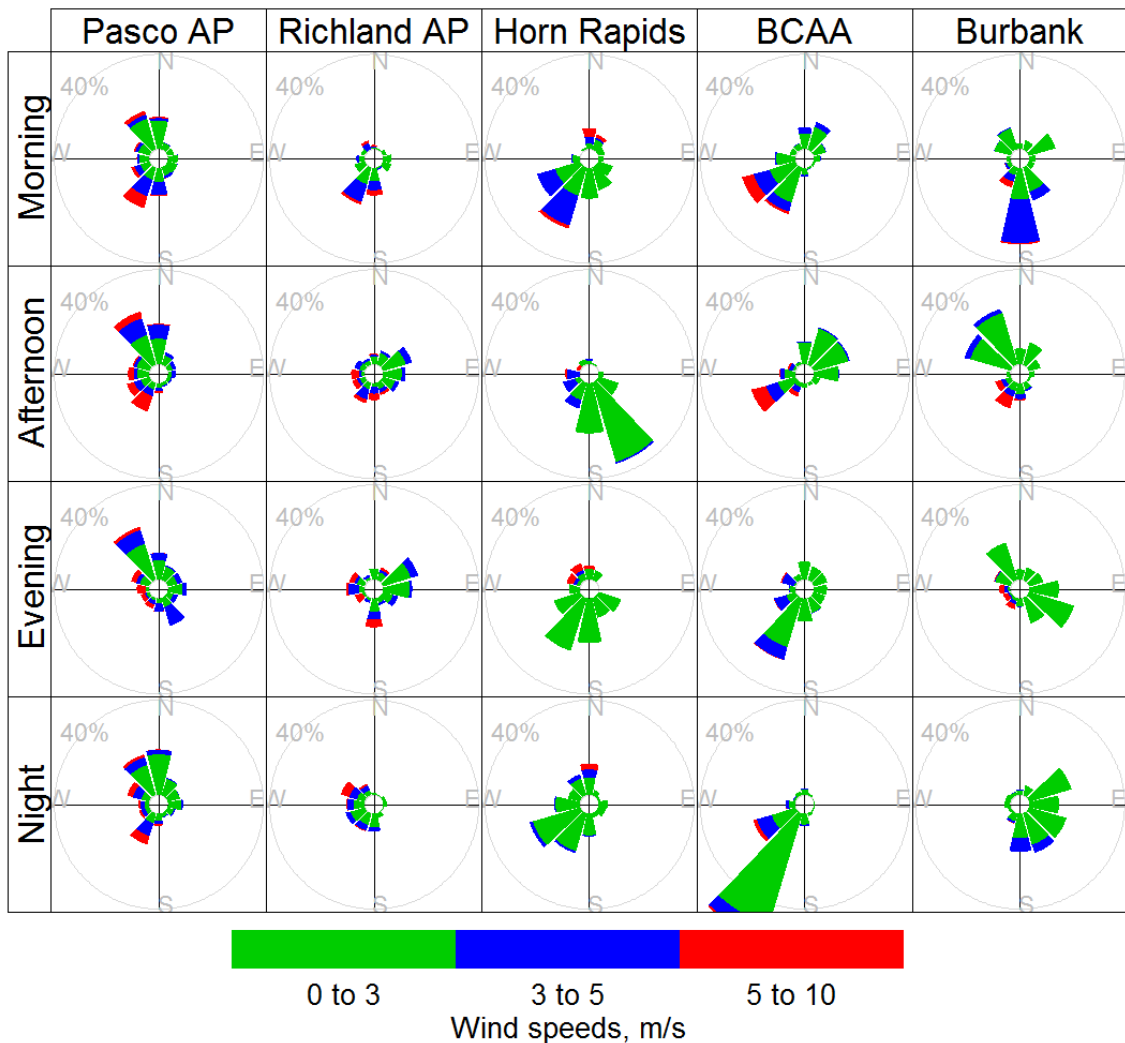


Figure 6.6. Wind rose plots for the T-COPS study period showing differences between the Pasco airport, West Richland airport, the Horn Rapids site, BCAA, and the Burbank site area (LeGro data).

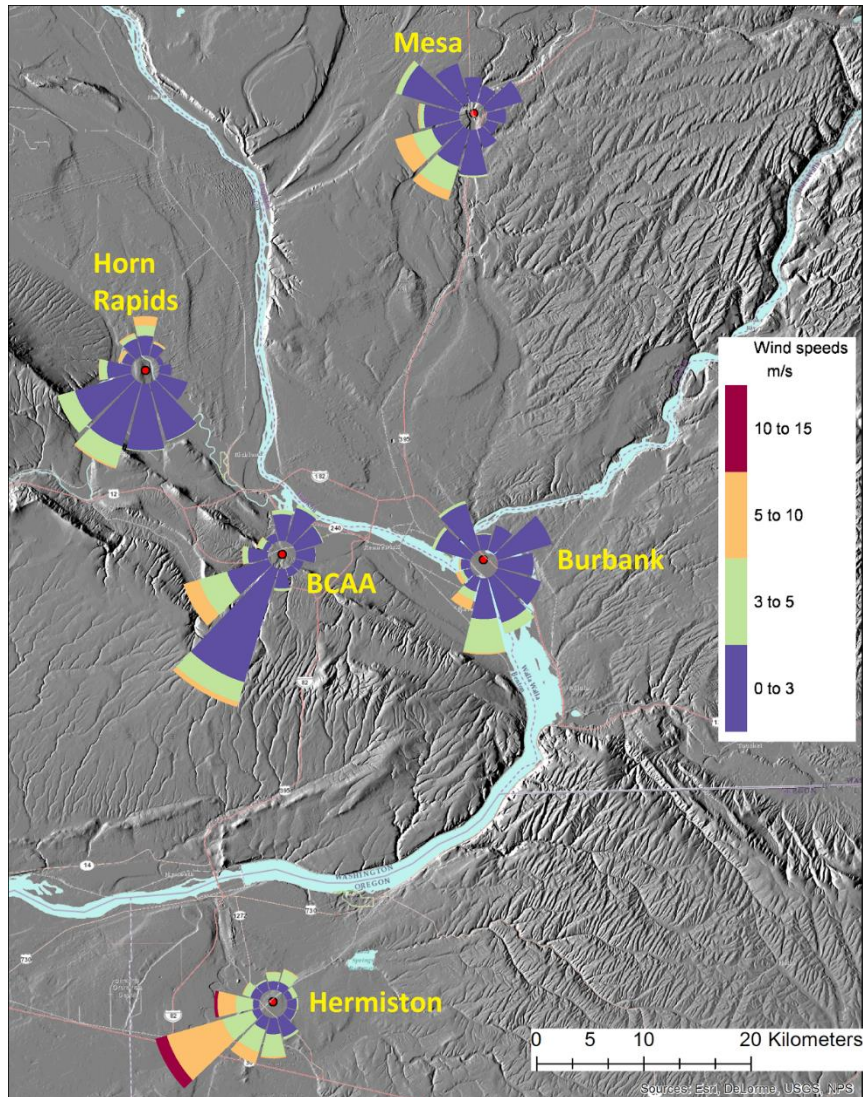


Figure 6.7. Wind roses for selected sites during the T-COPS period overlaid on a terrain map centered on the Tri-Cities.

Though no observations were available to visualize upper air winds and circulation patterns, the Weather Research and Forecasting (WRF) model run at a 4-km horizontal resolution by the University of Washington confirmed light winds aloft between 12 and 14 August (Figure 6.8a). Similarly, the 1.33km WRF model runs for 12- 14 August show that 6-hour back trajectories ending at Pasco at 2PM at various heights do not have a very long fetch (Figure 6.8b-d). This suggests air masses carrying precursors at times most conducive for ozone formation, likely originated in the vicinity. There is little evidence to suggest long range or regional transport of precursors.

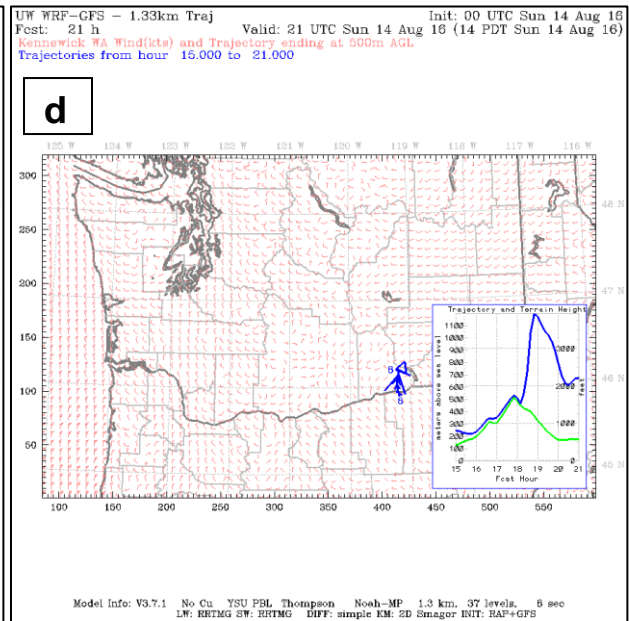
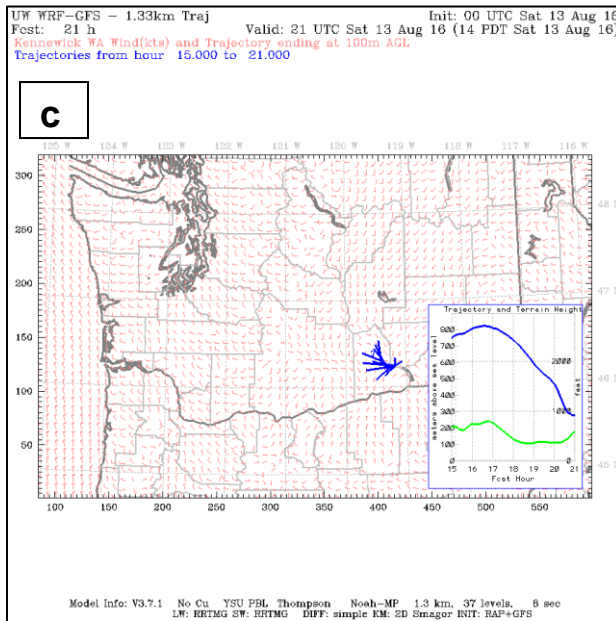
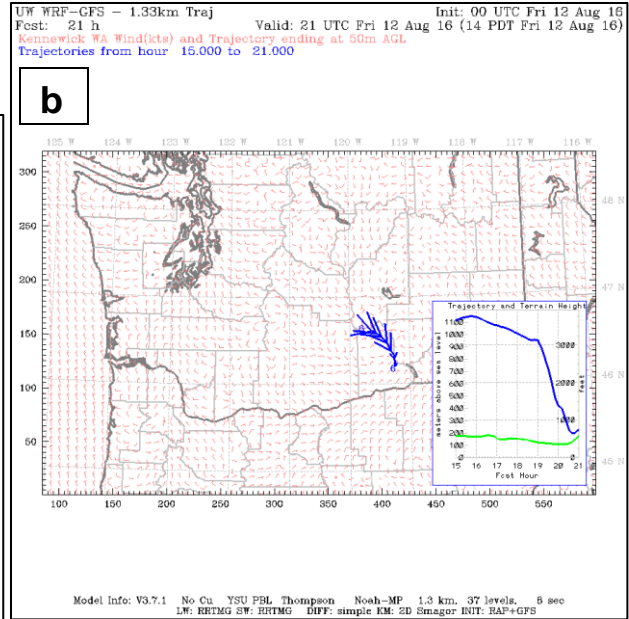
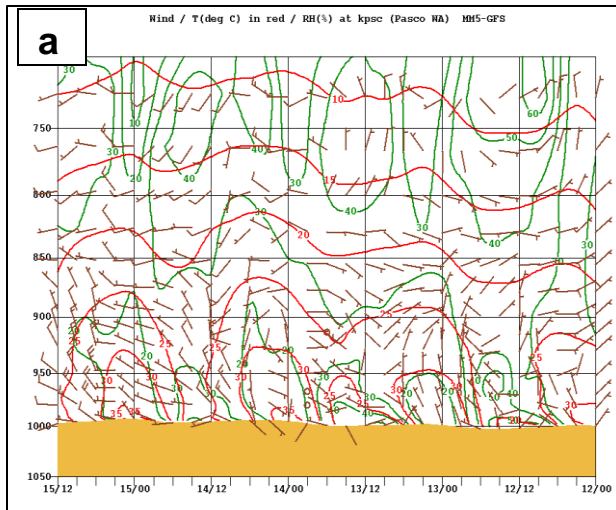


Figure 6.8: Select UW-WRF-model forecast products in the area around the stagnant period. (a) 4km timeheights over Pasco showing temperature (red), RH (green) and wind barbs from the surface through 700mb, from 5PM PDT 11 August to 5AM PDT 15 Aug (read x-axis right to left, times in GMT). (b) 1.33km WRF 6-hr back trajectory into Pasco airport, ending at 2PM PDT 12 August, at 50m above ground level. (c) 1.33km WRF 6-hr back trajectory into Pasco airport, ending at 2PM PDT 13 August, at 100m above ground level. (d) 1.33km WRF 6-hr back trajectory into Pasco airport, ending at 2PM PDT 14 August, at 500m above ground level.

6.6 Pollutant Time Series BCAA

Figures 6.9 to 6.13 show 1-hr average mixing ratios of trace gases measured at BCAA. Figure 6.9 shows O₃, CO, SO₂, CO₂, and H₂O mixing ratios. Figure 6.10 shows NO, NO₂, NO_x, and NO_y mixing ratios. Figure 6.11 shows mixing ratios of aromatic compounds, and figures 6.12 and 6.13 mixing ratios of other organic compounds. Highest NO_x (35.7 ppbv) were observed on the morning of Friday, July 29. Typically NO_x and aromatic VOCs were highest during the morning rush hour period and higher at night compared to the day. Figure 6.11 shows formaldehyde levels typically ranged from 2 to 4 ppbv and were significantly impacted by wild fire. Acetaldehyde and methanol displayed a distinct time of day variation with higher levels at night. Methanol was the most abundant hydrocarbon measured with mixing ratios typically between 3 and 12 ppbv. Interestingly the period with the highest methanol mixing ratios occurred on the evening / morning of August 8 and 9, a period rainy weather, where methanol mixing ratios were over 16 ppbv. After the cloudy and windy period, conditions became stagnant (winds less than ~3 m/s) under sunny skies. During this time, primary pollutant concentrations (NO, CO, aromatic hydrocarbons) displayed a clear diel pattern, with typically high mixing ratios in the mornings and evening and low mixing ratios in the afternoons. Figure 6.13 shows the biogenic hydrocarbons isoprene and monoterpenes. Isoprene levels were highest during the day as expected and were typically less than 0.5 ppbv. Monoterpene mixing ratios were highest at night and generally low (< 0.1 ppbv) with the exception of an event that occurred on the same August 8 / 9 evening as the elevated methanol, where monoterpene mixing ratios were as high as 1 ppbv.

During the stagnation period, oxygenated compounds shown in Figure 6.12 appear to accumulate in the airshed, with each day and night being slightly worse than the previous (see Figure 6.11 between 8/11 and 8/15). MVK and CH₃OOH in Figure 6.13 also behave similarly, as does NO_z (data not shown). RJLG van data from Mesa show a similar trend for acetaldehyde and m/z 59. However other species shown in Figures 6.9 through 6.13 do not exhibit this behavior. We surmise that production of reactive secondary species such as aldehydes are enhanced during this event and carries over into subsequent days.

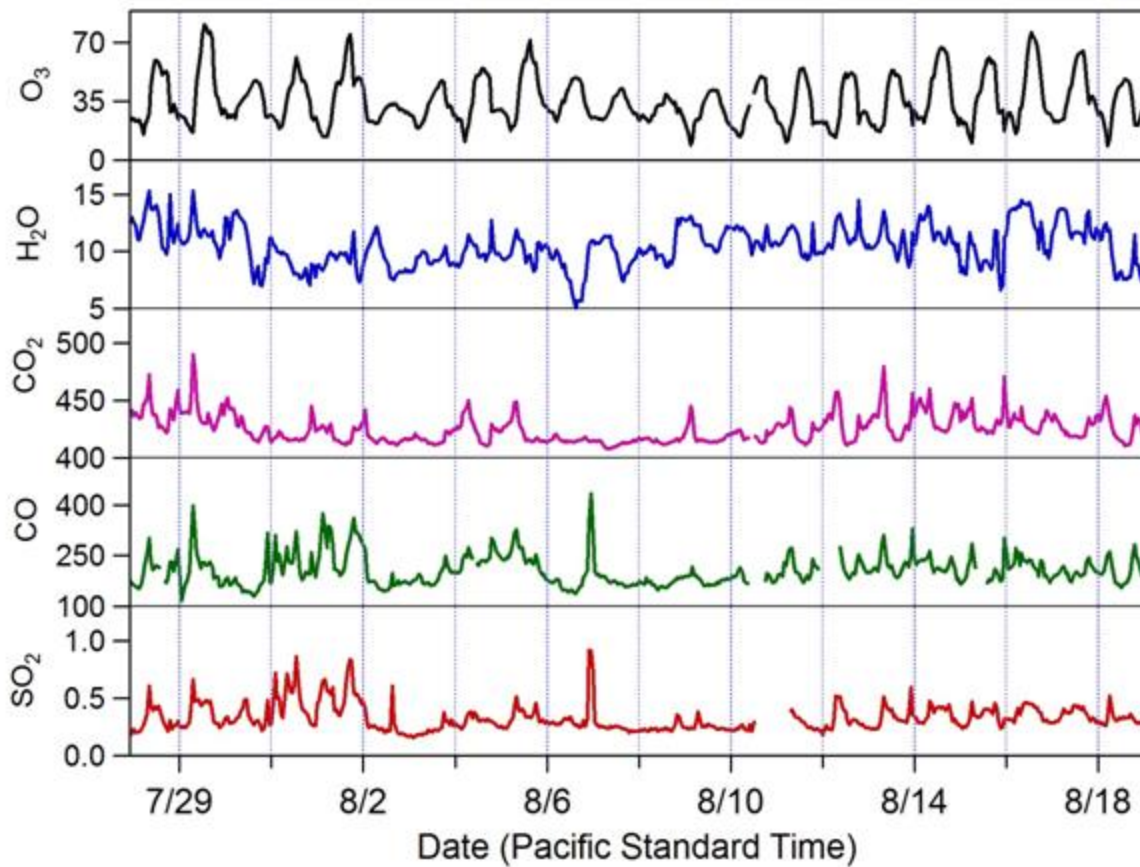


Figure 6.9. Time series of O₃, H₂O, CO₂, CO, and SO₂ at BCAA. Units are parts per billion by volume (ppbv) for O₃, CO, and SO₂, parts per thousand by volume for water vapor; and parts per million by volume (ppmv) for CO₂.

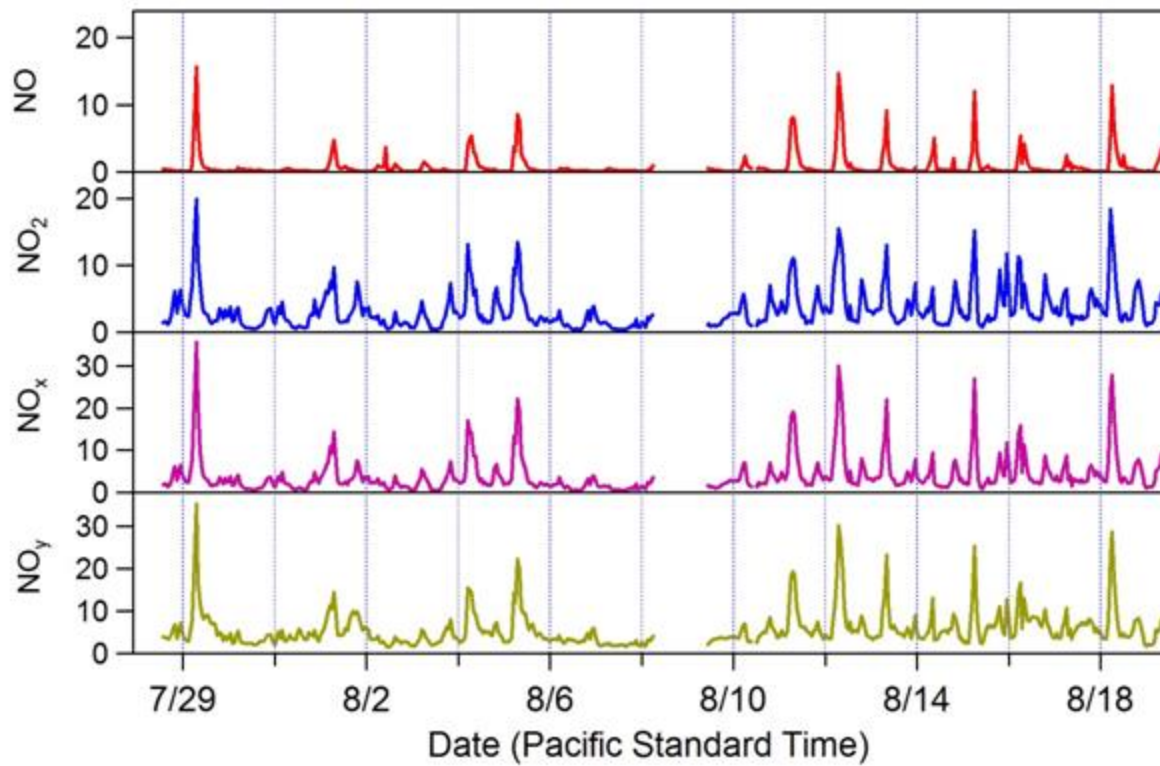


Figure 6.10. Time series of oxides of nitrogen ($\text{NO} + \text{NO}_2 = \text{NO}_x$) and total oxidized nitrogen (NO_y) measured by the AQD instrument at BCAA. Units are ppbv.

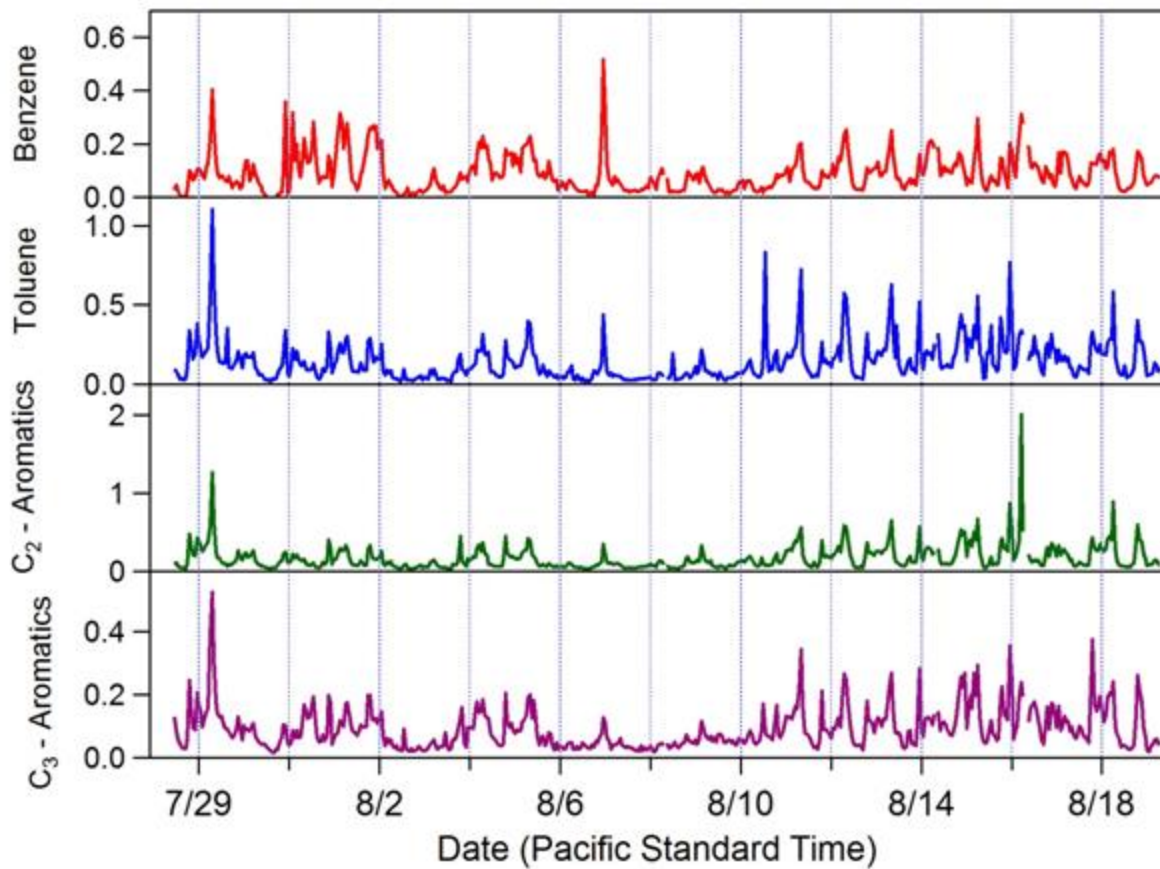


Figure 6.11. Time series of PTR-MS measurements of aromatic hydrocarbons at BCAA. Units are ppbv.

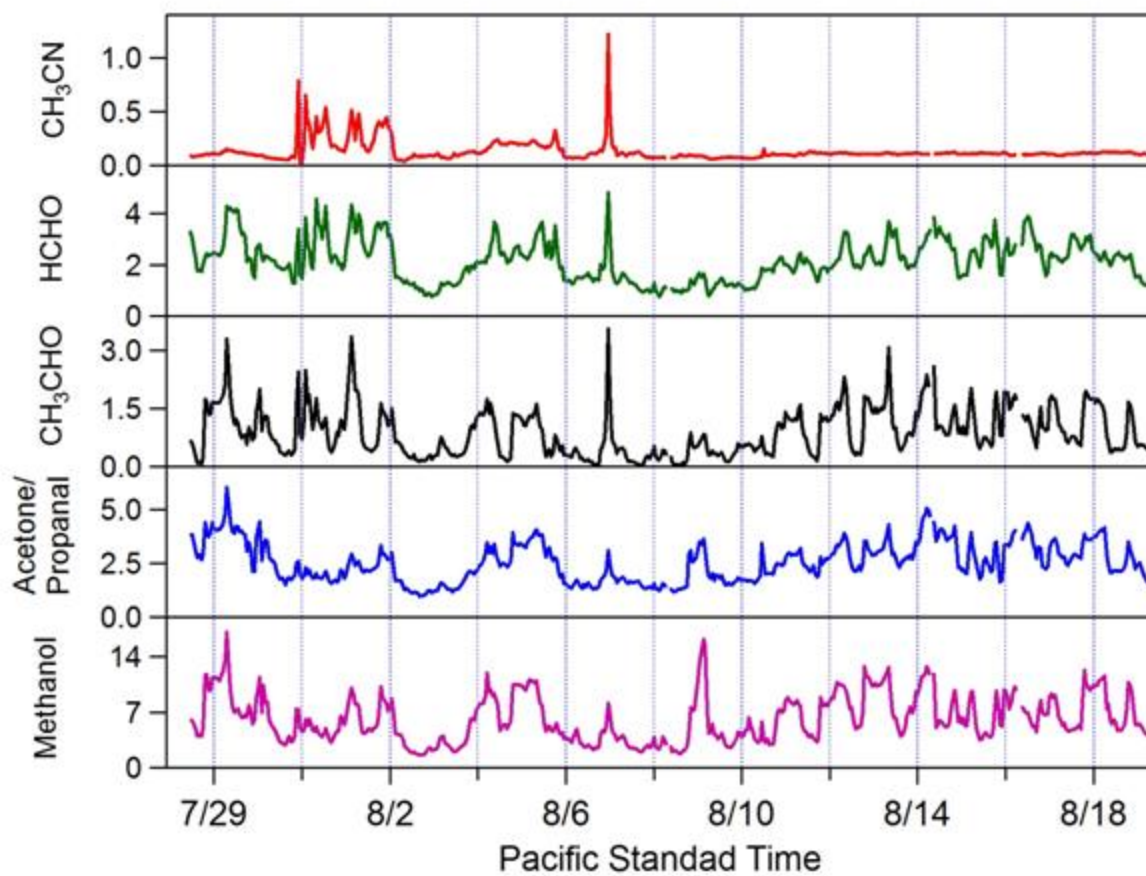


Figure 6.12. Time series of PTR-MS measurements at BCAA of acetonitrile (CH_3CN), formaldehyde (HCHO), acetaldehyde (CH_3CHO), ion mass m/z 59 which corresponds to acetone and propanal, and methanol. Units are ppbv.

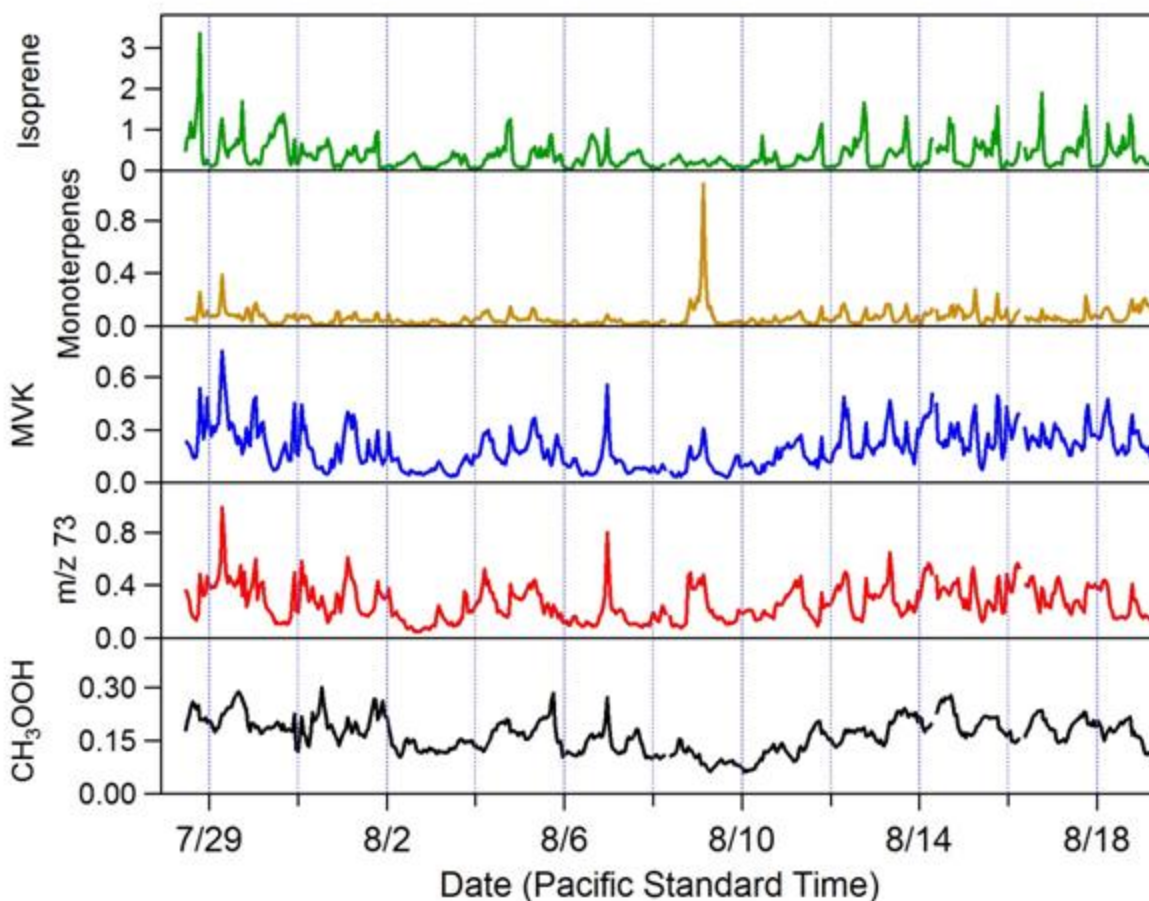


Fig 6.13. Time series of isoprene, monoterpenes, MVK - an isoprene oxidation product that also includes methacrolein, m/z 73 (methyl ethyl ketone and a variety of PTR-MS alkyl fragments), and methylhydroperoxide (CH_3OOH) at BCAA. Units are ppbv. Measurements of isoprene, monoterpenes, MVK, and m/z 73 should be interpreted carefully, as there are many known interferences to the PTR-MS measurements of these compounds.

6.7 Pollutant Time Series Horn Rapids

Figure 6.14 shows the time series of NO_x and ozone measured at Horn Rapids. Trends were somewhat different than BCAA, in that the pronounced influence of urban emissions was not present. Whereas NO concentrations tended to spike at BCAA starting around 6:00 am, coinciding with the beginning of morning rush hour, the NO concentration at Horn Rapids did not show similar behavior. The magnitude of NO enhancement tended to be much smaller than at BCAA and began in the evening when the boundary layer collapsed and lasted until the morning when the boundary layer expanded. This suggests that there were not large local sources of NO_x near the Horn Rapids site. The NO_2 trend at Horn rapids tended to mirror the NO trend with a few notable exceptions. Most interestingly, there were instances during the wildfire period (7/31, 8/1, 8/2) where NO_2 was

enhanced without significant accompanying NO. This suggests that aged smoke plumes may have influenced the site on these days. These air masses appeared to be aged since the majority of NO in them had been oxidized to NO₂ and are likely associated with wildfires due to the abnormally high NO_x concentrations and concurrent acetonitrile enhancement at BCAA. Two of the higher ozone days occurred following these periods of high NO₂ (7/31, 8/1). Overall, ozone concentrations were fairly low at Horn Rapids, tending not to exceed 60 ppbv except for a few key days (7/29, 8/1, 8/5).

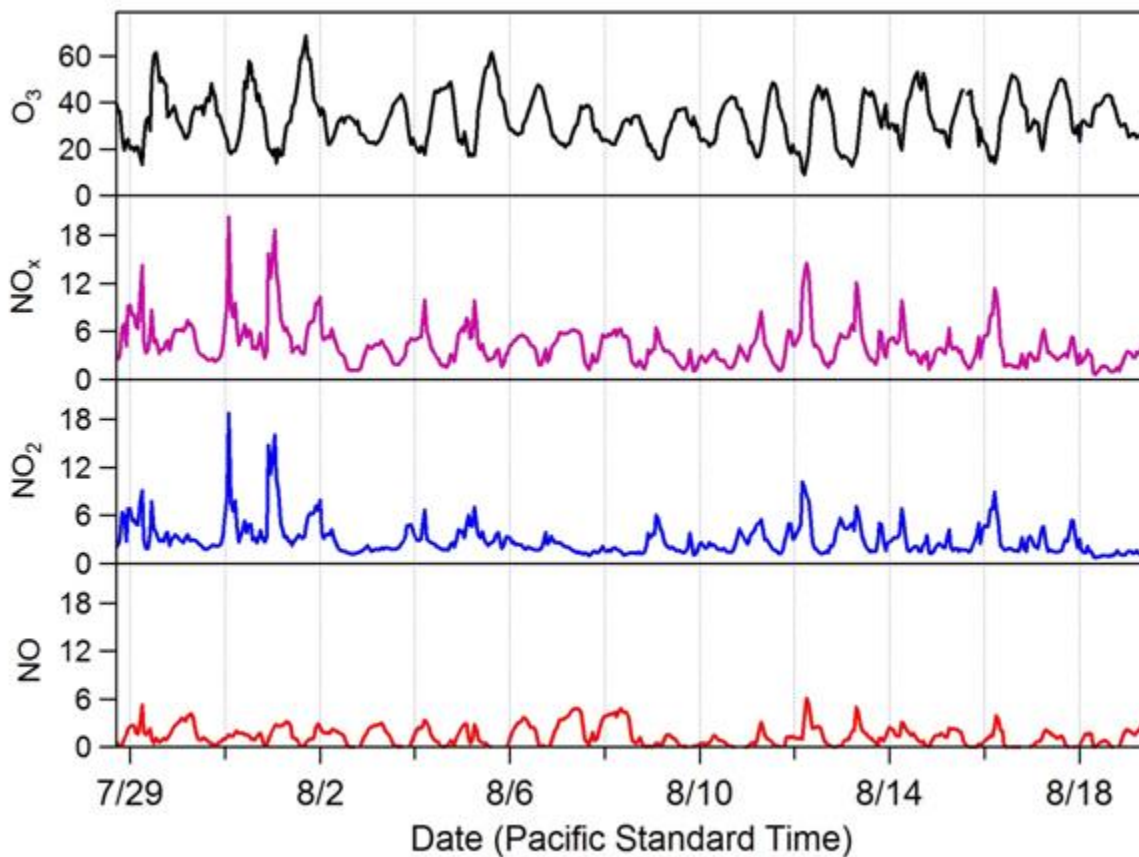


Figure 6.14. Time series of 1-hr averages ozone and NO_x at Horn Rapids. Units are ppbv.

6.8 Pollutant Time Series Burbank

Figure 6.15 shows times series of O₃, CO, and NO_x at Burbank. NO_x concentrations were highly elevated both during morning rush hour and in the evenings. Elevated NO_x (> 15 ppbv) in the evenings was interesting because it was not observed at BCAA, where typical nighttime were less than 5 ppbv. Ozone was elevated over the Columbia Cup boat race weekend, during the wildfire period, and during the mid-August stagnation event. Highest ozone concentrations were observed at Burbank during the mid-August stagnation. Due to the high night time NO_x concentrations, night time ozone was routinely low, often less than 10 ppbv.

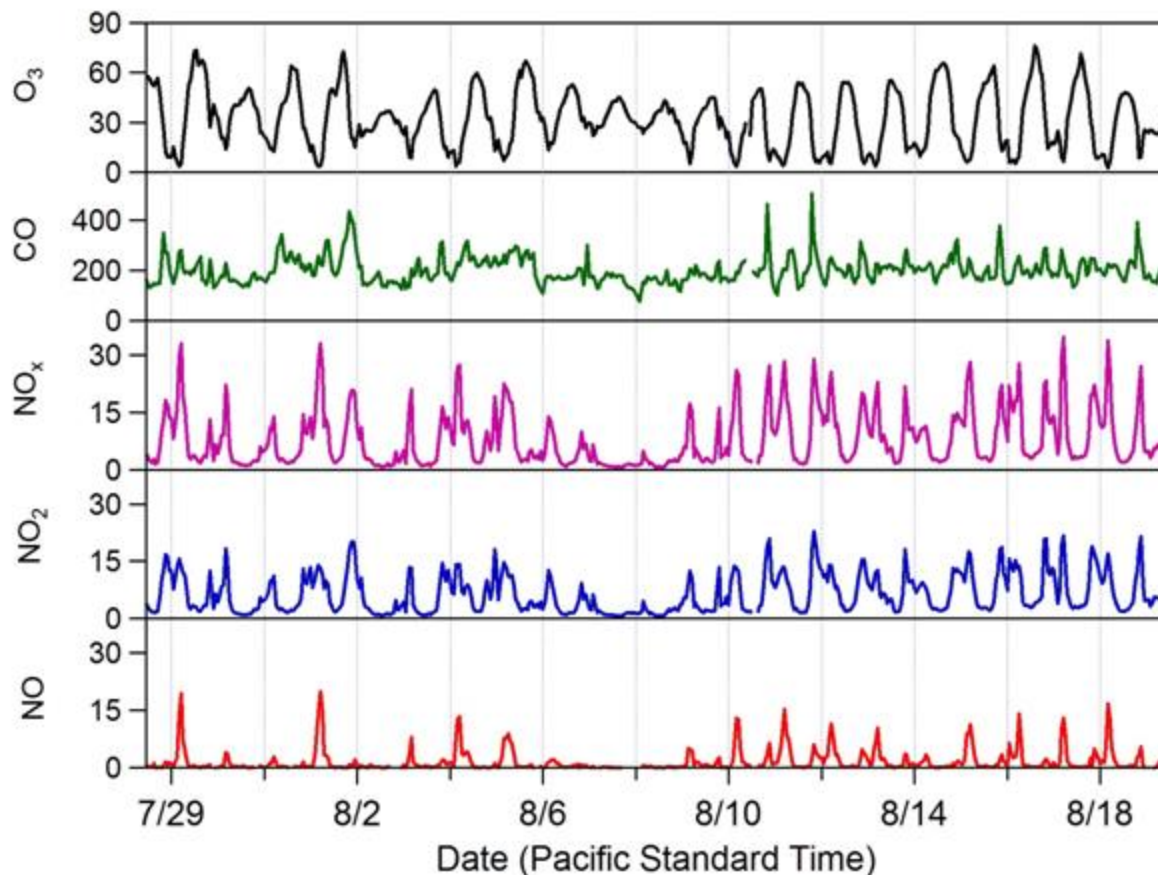


Figure 6.15. Time series of 1-hr averages of ozone, CO and NO_x at Burbank. Units are ppbv.

6.9. Measurements at Burbank in the Summer of 2017

Due to sampling issues at Burbank with the RJ Lee PTR-QMS and DNPH formaldehyde cartridges during the T-COPS study, an additional set of measurements was made from August 17 to August 23, 2017 to characterize VOC and ozone levels at Burbank. Meteorology was characterized by primarily calm winds (<2 m/s) from the west (wind rose shown in Figure 6.16) and daily high temperatures greater than 30 °C. Ozone was relatively low Burbank (< 61 ppbv for 1-minute average data) and never exceeded 60 ppbv at the WA DoE BCAA site (1-hr average). Ozone, wind speed, and temperature shown in Figure 6.17. The wind speeds and direction suggest that the site was mostly influenced by local emissions and transport from the urban center and this calm westerly wind made it impossible to assess the possibility of transport of VOCs into the airshed from the east. Results from the additional sampling are shown in Figures 6.18 and 6.19. Generally, level of aromatics were very low, with afternoon concentrations less than 100 pptv, similar to BCAA in 2016. Interestingly, the highest levels were observed in the evenings, not during morning rush hour. Formaldehyde levels were typically 1-2 ppbv, somewhat lower than those observed at BCAA in 2016. Methanol levels were similar at 5-15 ppbv, while acetaldehyde levels were somewhat higher. Isoprene levels during the day were much lower at Burbank than BCAA during T-COPS, far below 200 pptv. This suggests that local isoprene emissions were negligible and that there was little

isoprene being transported in from the urban center. Evening spikes in the isoprene trace are like due to measurement interferences in the PTR-MS associated with traffic emissions, since the isoprene spike was coincident with spikes in aromatics. Overall, there was no evidence in this set of measurements that Burbank is a hotspot for VOCs. The 2017 measurements were not made during an ozone episode, meaning that it was not possible to assess typical Burbank VOC levels during an ozone episode using this data. The only significant difference between VOC levels measures in 2016 and 2017 at Burbank is the significantly higher acetaldehyde levels in 2017 as shown in Figure 6.20

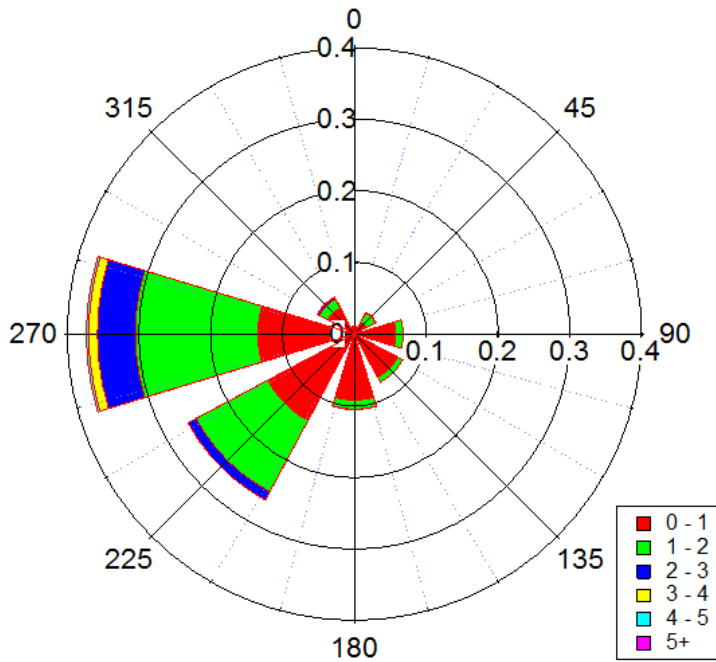


Figure 6.16. Wind rose for Burbank measurements made from 8/17 - 8/23 2017. The wedges represent observations in each wind sector, the colors represents observation in each wind speed range (m/s), and the radial axis represents the fraction of total observations in each wind speed/direction sector.

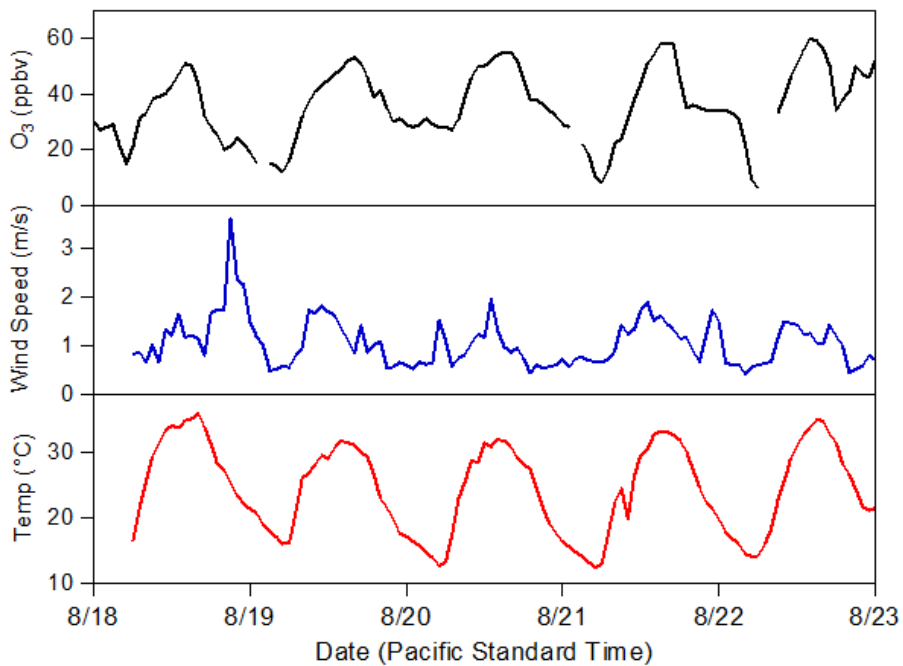


Figure 6.17. Ozone from the Ecology monitor at BCAA, along with Burbank wind speed and temperature from 8/17 - 8/23 2017.

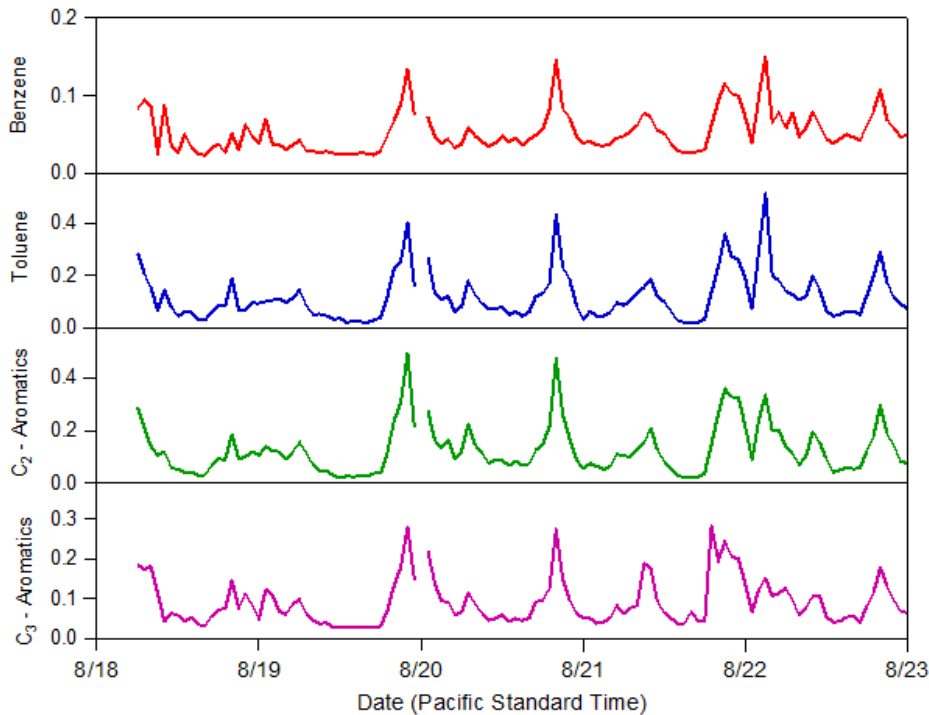


Figure 6.18. Time series of aromatics at Burbank in the summer of 2017. A 1 hour spike was removed on 8/20 at 0:00. Units are ppbv.

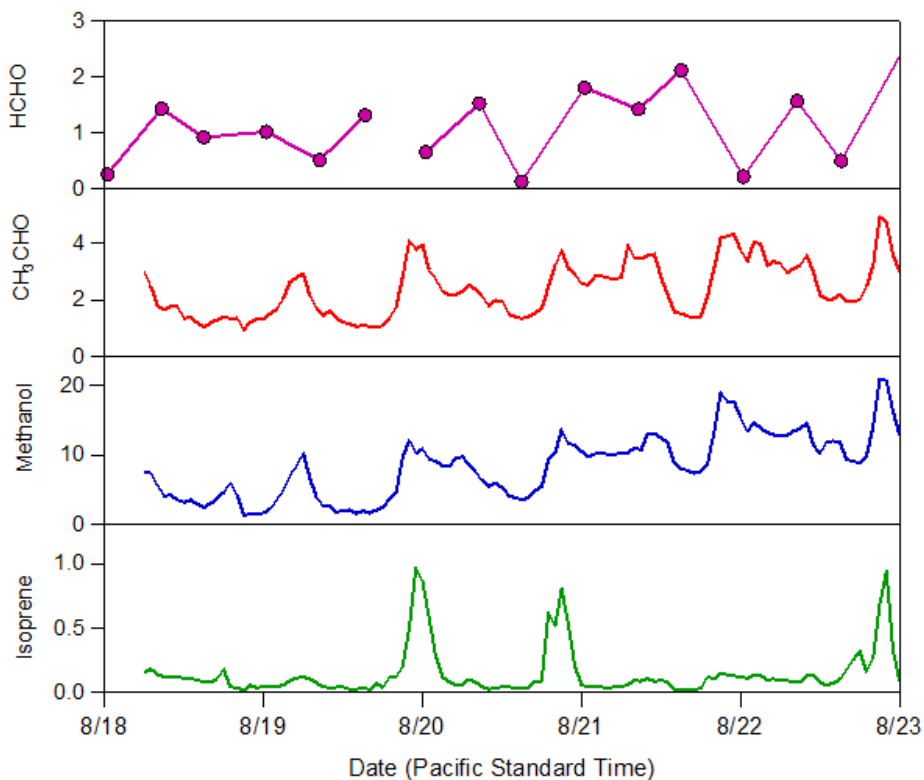


Figure 6.19. Time series of formaldehyde (HCHO), acetaldehyde (CH₃CHO), methanol, and isoprene. Formaldehyde measurements are from DNPH cartridge sampling (morning [~6:00 - 11:00], afternoon [~11:00 - 19:00], and night [~19:00 - 6:00]) and the other species were measured by the PTR-MS. Units are ppbv.

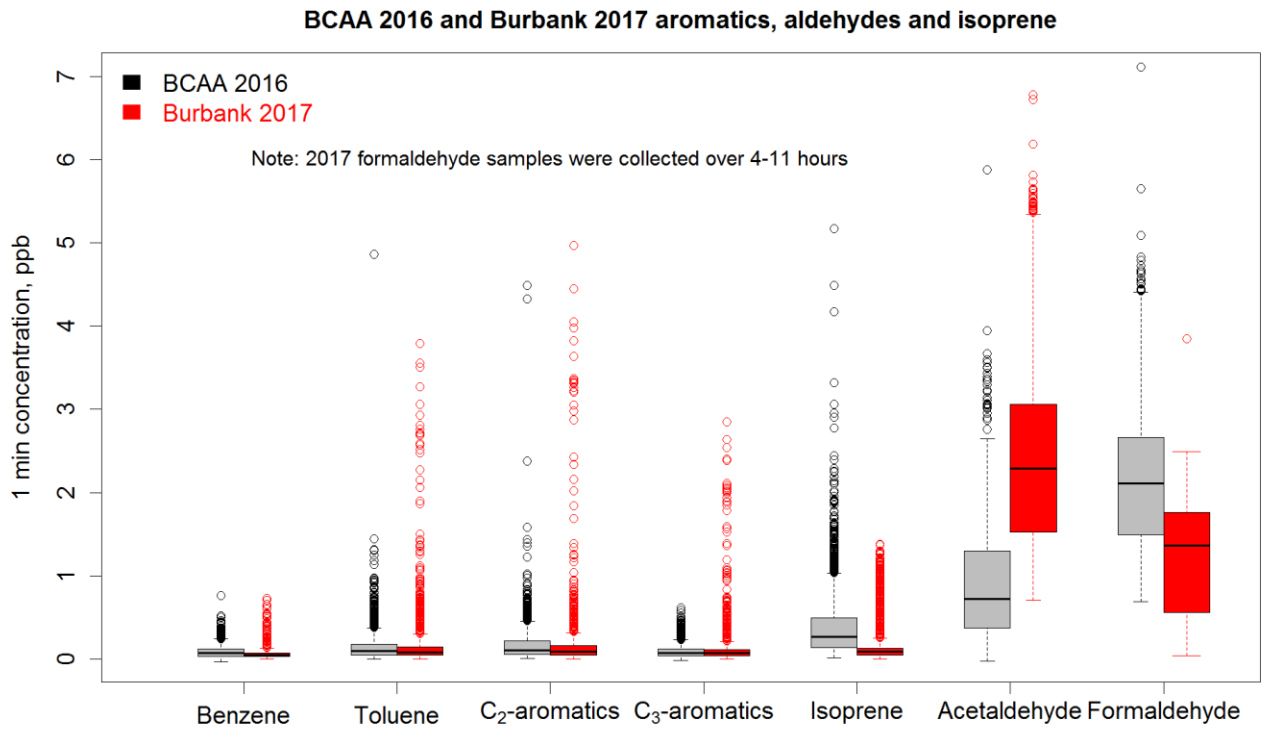


Figure 6.20. Comparison of selected VOCs measured at Burbank in 2016 and 2017.

7. Chemical and Meteorological Drivers of Ozone

7.1 Tri-Cities Regional Ozone

The regional distribution of ozone was of interest to WA DoE to assess whether ozone events were widespread or specific to small “hot spots” where precursor concentrations might be elevated. Ozone mixing ratios at BCAA, Burbank, and Horn Rapids are plotted in Figure 7.1 to illustrate its spatial variation in the Tri-Cities. In general, afternoon ozone mixing ratios at the Horn Rapids site were lower than that of BCAA and the Burbank sites. During periods of wind or rainy weather ozone mixing ratios were similar between the 3 sites. The figure illustrates that there were five different events where the 1 hour average ozone exceeded 70 ppbv for some length of time one of the sites. Four events were identified and labeled in Figure 6.1 for the BCAA data, with the fifth event occurring on Aug 17 at Horn Rapids, where for a about a 1-hr period ozone was ~ 8 ppbv greater than the BCAA site. Table 7.1 summarizes the average ozone concentrations observed during the five events noted in the figure. The length of time when ozone continuously exceeded 70 ppbv at BCAA is given in the table. For the Aug 17 episode, the duration that the Burbank site was above 70 ppbv is given instead. The site ozone averages are taken over the same time interval that the BCAA site or the Burbank site exceeded 70 ppbv. Ozone events #1 (July 29) and #4 (August 16) lasted most of the afternoon. It is clear from the table that ozone at the Horn Rapids site was typically 10 to 20 ppbv lower than at BCAA during these events, a significant concentration gradient. Ozone at Burbank was about 10 ppbv lower than BCAA during event #1, lower by only 3-5 ppbv for events #2, #3, #4, and 8 ppbv greater for event #5.

The first ozone event occurred on Friday, July 29 during the Columbia Cup hydroplane boat race event. The highest observed ozone between the three sites was observed at BCAA, the closest site to the Columbia Cup races and the one most likely to be impacted by an increase in traffic at the Richland/Kennewick urban center. Elevated ozone levels (68 ppbv) were also observed at Burbank, but were significantly lower at Horn Rapids (54 ppbv). This suggested that elevated ozone was prevalent through the eastern part of the urban area, but was not distributed to the western part of the area. Similar differences were observed on the August 16th (event #4) and 17th episode (event #5), where ozone was much higher at BCAA and Burbank than at Horn Rapids. While the average value for the August 16 event was higher at BCAA than Burbank, Burbank displayed the highest short term ozone level. During the period when wildfire smoke impacted the region (7/31 - 8/7) two elevated ozone days were observed on August 1 (event #2) and August 5 (event #3). Interestingly, ozone levels were more spatially uniform during these events. The weaker ozone spatial gradient during the wildfire period suggests well distributed transport of ozone or ozone precursors into the Tri-Cities airshed from the wild fire. The existence of significant spatial gradients in ozone between Horn Rapids and the other two sites suggests ozone is being created in the Tri-Cities airshed.

Figure 7.2 shows a box and whisker plot of ozone mixing ratios measured during T-COPS in comparison with previous measurements made at Mesa, WA and at the DoE Metaline site in Kennewick, WA. Comparison with historical data from July- August indicates the TCOPS study period was likely representative of conditions encountered in past summers. The Kennewick

monitoring site was initially operated as a temporary site at the DoE Metaline station, about 3 miles away and was moved to the current BCAA location in 2015. There was a notable increase in nighttime O_3 concentrations after this move, as evidenced by differences in the bottom whiskers. As explained earlier, nighttime drainage through the Amon Wasteway is likely to prevent NO_x titration of O_3 at the BCAA site and maintain higher background concentrations, while the Metaline site was not prone to this phenomenon. The highest 1-hr average O_3 at BCAA during TCOPS was 81 ppbv, comparable to the summer of 2015 when the max 1-hr average O_3 at BCAA was 89 ppbv. Though Mesa sampling was conducted with the same type of instrument and at two locations a few 100 meters apart, the sampler was only operated there for a total of 10 days during T-COPS. Historical data were collected in the summer of 2015. Given the short period being compared, and that 2015 contained a wildfire-impacted day with 1-hr ozone levels reaching 90 ppb, a median difference of 3 ppb is not unreasonable. Median ozone values in the Tri-Cities are higher than the Mesa site.

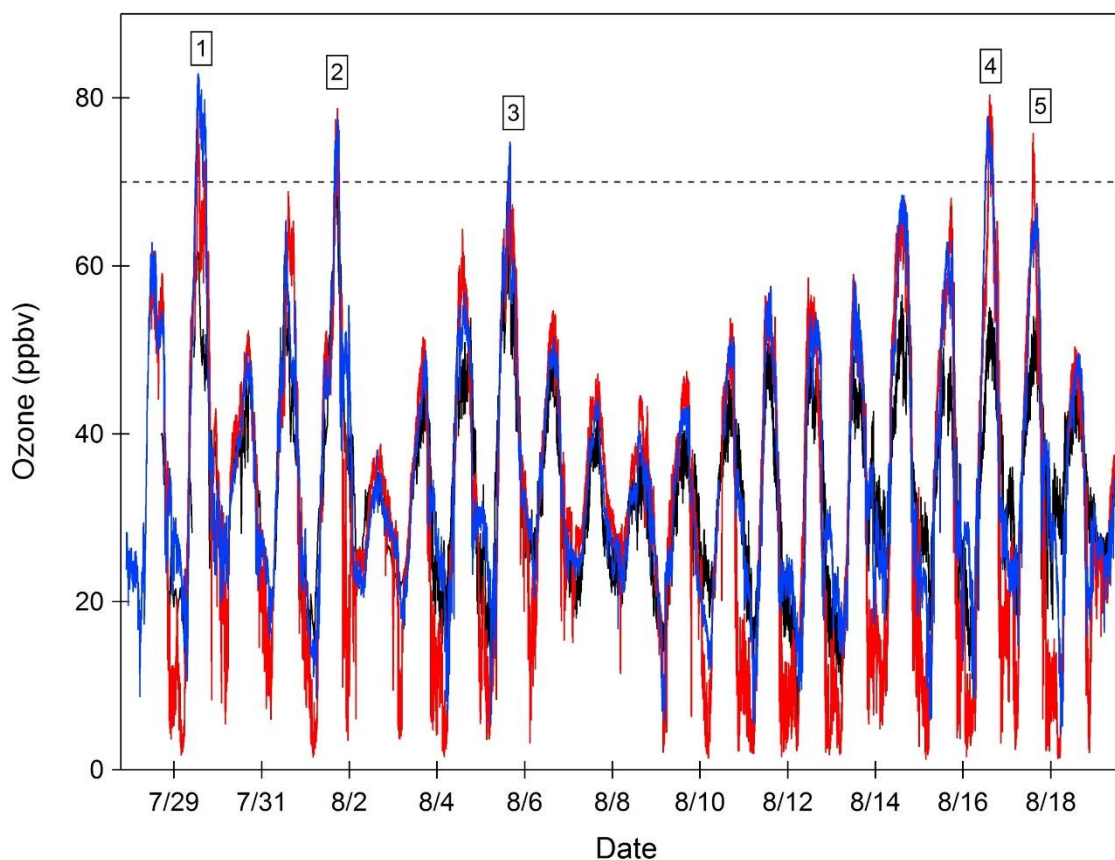


Figure 7.1. Time series of ozone mixing ratios measured at BCAA (blue), Burbank (red) and Horn Rapids (black) during T-COPS. Dashed line indicates 70 ppbv threshold for identifying the ozone events labeled 1 through 5 in the figure.

Table 7.1. Summary of average ozone mixing ratios observed for the 5 ozone pollution events observed during T-COPS.

Event #	Date	BCAA	Horn Rapids	Burbank	# hrs >70 ppb	Note
1	July 29	77 ± 3	54 ± 6	68 ± 4	5.5	boat race weekend
2	Aug 1	74 ± 2	64 ± 5	71 ± 5	2.7	wildfire
3	Aug 5	72 ± 2	62 ± 3	67 ± 4	1.2	wildfire
4	Aug 16	73 ± 2	50 ± 2	69 ± 8	4.0	
5	Aug 17	64 ± 1	50 ± 2	72 ± 1	1.0*	

*duration at Horn Rapids site

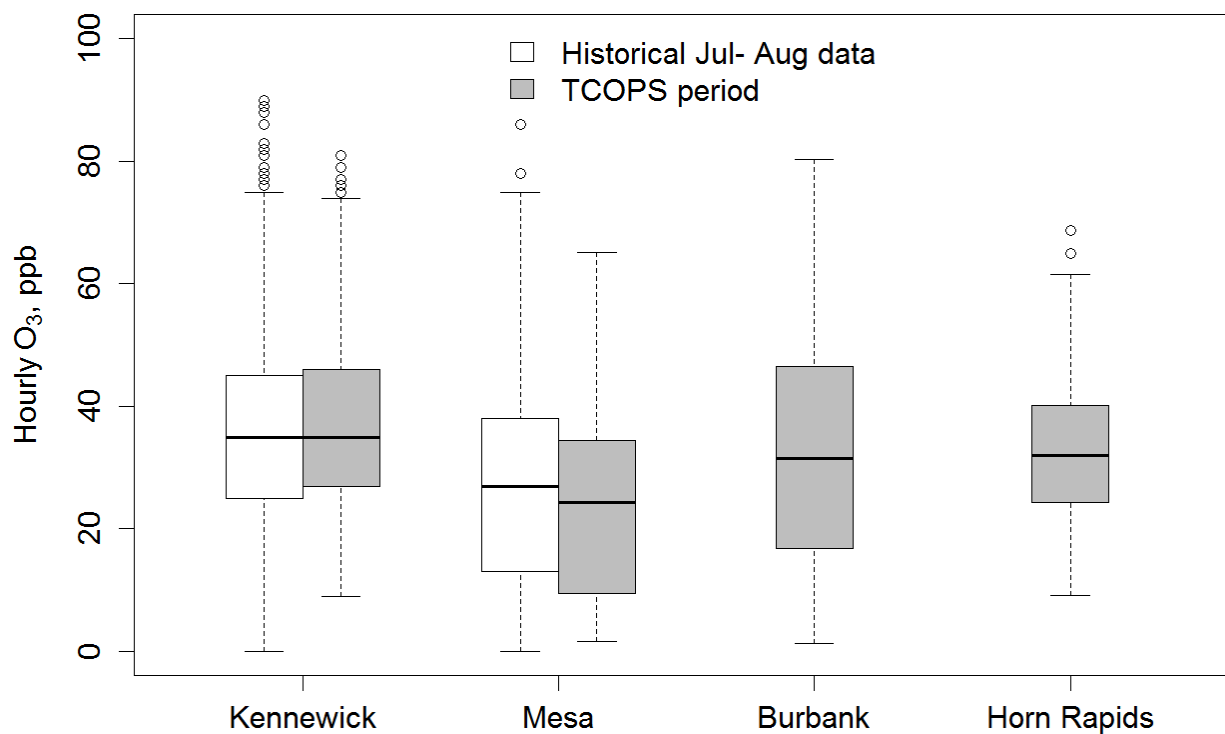


Figure 7.2. Box plots of O₃ at Metaline / BCAA (Kennewick), Mesa, Burbank and Horn Rapids comparing T-COPS observations (shaded box) to historical data (open box). Shown are medians, 25th to 75th percentile and 10th to 90th percentile ranges.

Figure 7.3 displays the time of day variation in ozone mixing ratios at the three sites as a box and whisker plot with a comparison of the medians. The figure illustrates that hat ozone levels were similar at BCAA and Burbank, but were generally lower at Horn Rapids. Afternoon ozone was also more variable at BCAA and Burbank than Horn Rapids. The daily variation is due to both meteorological processes and chemical formation and loss processes.

Figure 7.4 compares the 1/2-hr average ozone mixing ratios as a function of time of day for the 3 sites compared to a typical regional background abundance of ozone of 40 ppbv. This level of ozone would be expected for a clean air site in the afternoon due to transport of ozone from clean tropospheric air and it is inferred from the TCOPS data for very windy days. Typically, the BCAA and Burbank afternoon ozone levels are about 15 ppbv greater than this nominal background level, while the Horn Rapids site was typically only 5 ppbv greater than the background. The ozone minimum for BCAA and Horn Rapids was reached at 05:00 PST on average, due to losses of ozone overnight from dry deposition and reaction with NO. Ozone levels begin to increase in the morning around 06:00 PST at all sites, reaching a maximum typically at about 15:00 PST. The increase of ozone in the early morning is in part attributed to mixing down to the surface of ozone rich air from above as the convective boundary layer grows. Afternoon ozone levels were remarkably similar at BCAA and Burbank, with mean values tracking each other closely. Ozone levels decrease after about 18:00 PST, coincident with the onset of evening rush hour traffic, lower light levels, and the evening collapse of the mixed layer height which leads to higher NO mixing ratios that react with ozone to form NO₂. Nighttime levels of ozone were very similar at BCAA and Horn Rapids. Nighttime ozone levels at Burbank were significantly lower due to much higher NO mixing ratios.

Figure 7.5 compares the ozone time of day variation of ozone in Kennewick with Mud Mountain Dam and Spokane from the summers of 2015 and 2016. Ozone in Kennewick during the day is typically significantly higher (> 10 ppbv) than other sites in Washington. The Mud Mountain Dam site near Enumclaw typically has the highest ozone design levels in the State as a result of transport and photochemical processing of emissions from Seattle and Tacoma. In 2015 the medians and percentile ranges of the Kennewick (BCAA site) and Mud Mountain Dam data were very similar. Both sites had 90th percentile ranges exceeding 70 ppbv in the afternoon. Spokane, a larger urban area than the Tri-Cities, generally had lower ozone levels in the afternoon; the 90th percentile range was just over 60 ppbv. In 2016, Kennewick ozone levels at the 75th and 90th percentile ranges were lower than those in 2015 but the medians and averages were similar. Afternoon ozone levels were also lower at Mud Mountain Dam in 2016 and were substantially lower than those at Kennewick. The afternoon median and average ozone levels in Kennewick are higher than those in Spokane and the 75th and 90th percentile ranges are significantly larger still, with the 90th percentile range about 10 ppbv higher in Kennewick than Spokane in both 2015 and 2016.

In summary, the ozone levels in Kennewick are consistently higher in the afternoon than those observed in Spokane. Afternoon ozone is typically about 15 ppbv higher than the nominal 40 ppbv regional background level, suggesting local production. The afternoon 90th percentile range in 2015 and 2016 was similar to or greater than that of Mud Mountain Dam, the area with the highest ozone design values in the State.

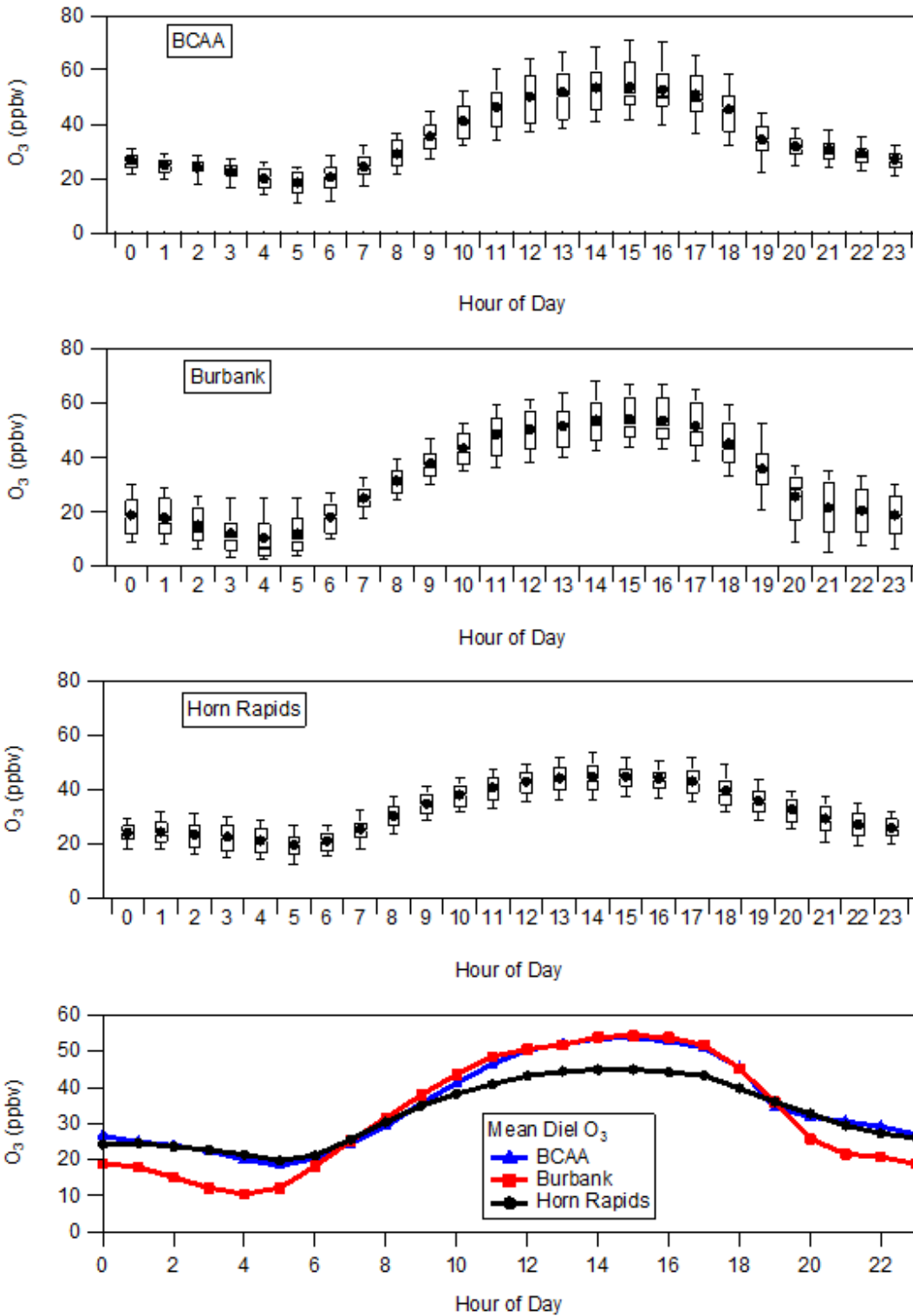


Figure 7.3. Time of day variation of O₃ at Burbank, BCAA, and Horn Rapids. The bottom whisker is 10th percentile, the bottom of the box is the 25th percentile, the bar is the 50th percentile, the top of the box is the 75th percentile, and the top whisker is the 90th percentile. The bottom panel shows the diel means for each site.

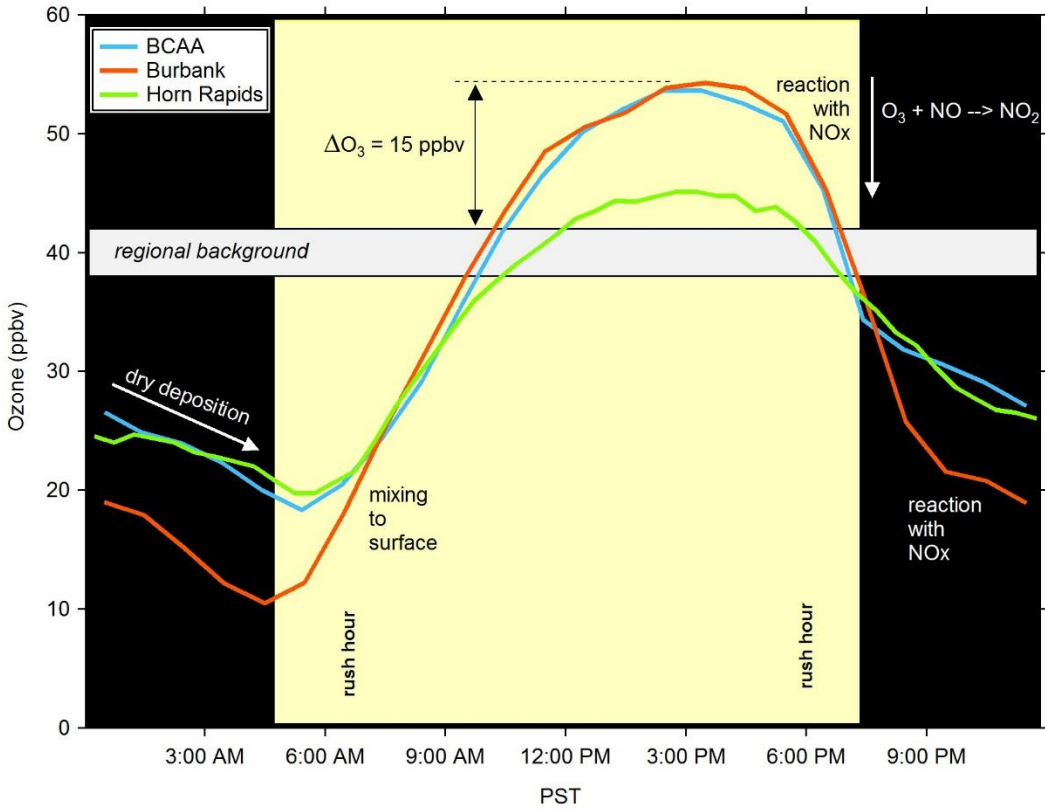


Figure 7.4. Comparison of the time of day variation of ozone at the three fixed sites ($\frac{1}{2}$ -hr averages). Light area of the plot indicates the time period between sunrise and sunset.

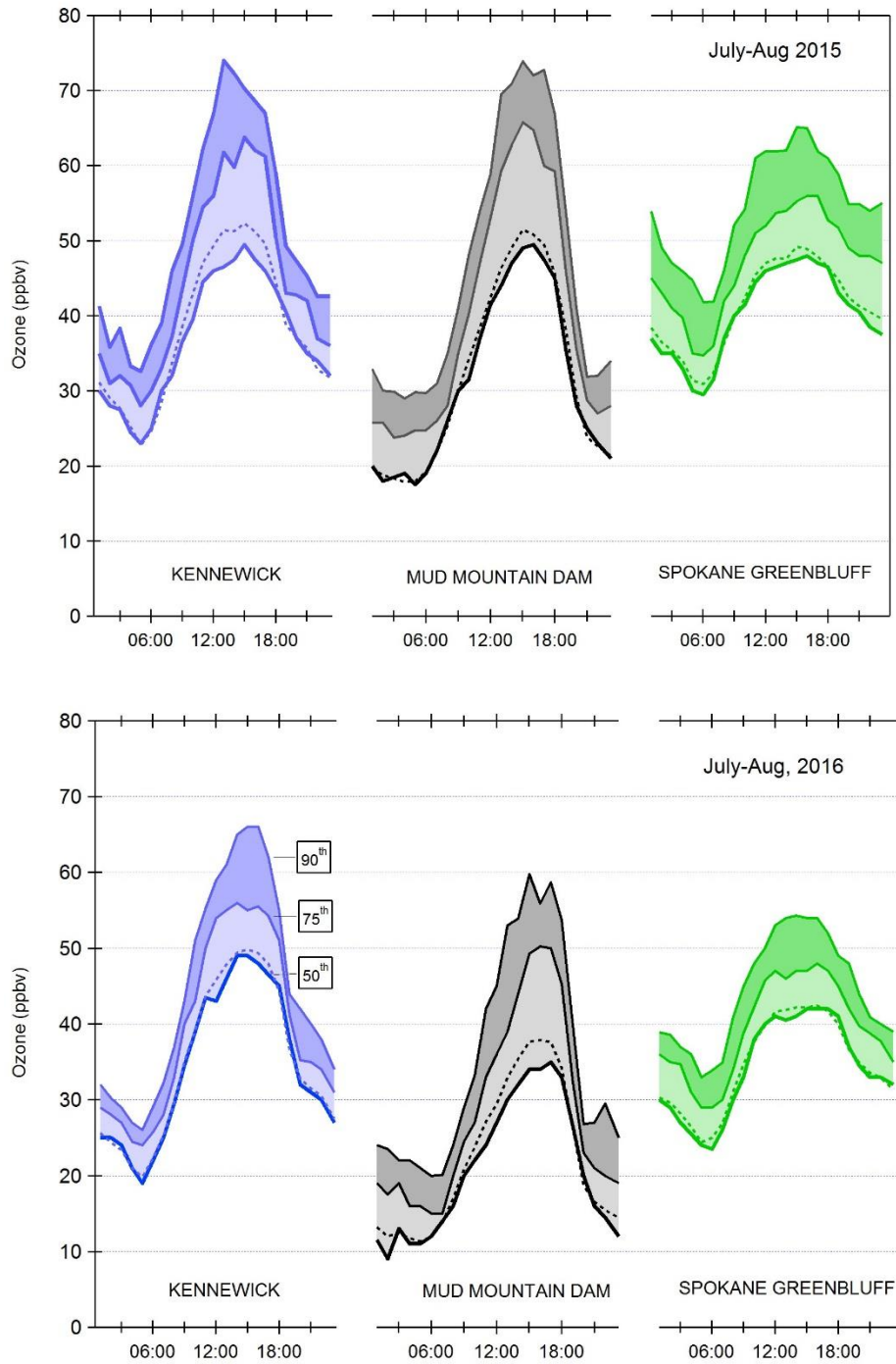


Figure 7.5. Comparison of the Aug-July time of day variation of ozone mixing ratios (1-hr averages) in Kennewick (BCAA) to the Mud Mountain Dam and Spokane (Green Bluff) monitoring locations for the summers of 2015 and 2016. Shown are the 90th, 75th, 50th (median) percentiles as heavy lines with shading, and the average (dashed line).

7.2. Influence of Wildfire

Wildfire emissions significantly affected the area from 7/30 - 8/6, including during two ozone episodes (8/1 and 8/5). Wildfires are known to be a significant source of ozone precursors (Andreae and Merlet, 2001; Jaffe and Wigder, 2012) and elevated ozone is typically observed in wildfire plumes (Jaffe and Wigder, 2012). Therefore, it is likely that ozone levels were affected by some combination of ozone and ozone precursors transported to the airshed from wildfires during this period. Significant differences were indeed observed between the wildfire period and the rest of the study, suggesting that the wildfire smoke significantly affected the chemical composition of the atmosphere. The impact of the wildfires on ozone precursors is evident in the CO-to-NO_x molar ratio. Combustion of any fuel type emits both CO and NO_x, but at different rates depending on combustion temperatures. Emissions from fossil fuel combustion sources such as automobiles tend to have a low CO-to-NO_x ratio, while biomass burning emissions, such as those from wildfires tend to have high CO-to-NO_x ratios. As shown in Figure 7.6, the wildfire period had a much higher CO-to-NO_x ratio (21) than the study on the whole (5.5), suggesting that wildfire emissions of CO had been transported into the airshed.

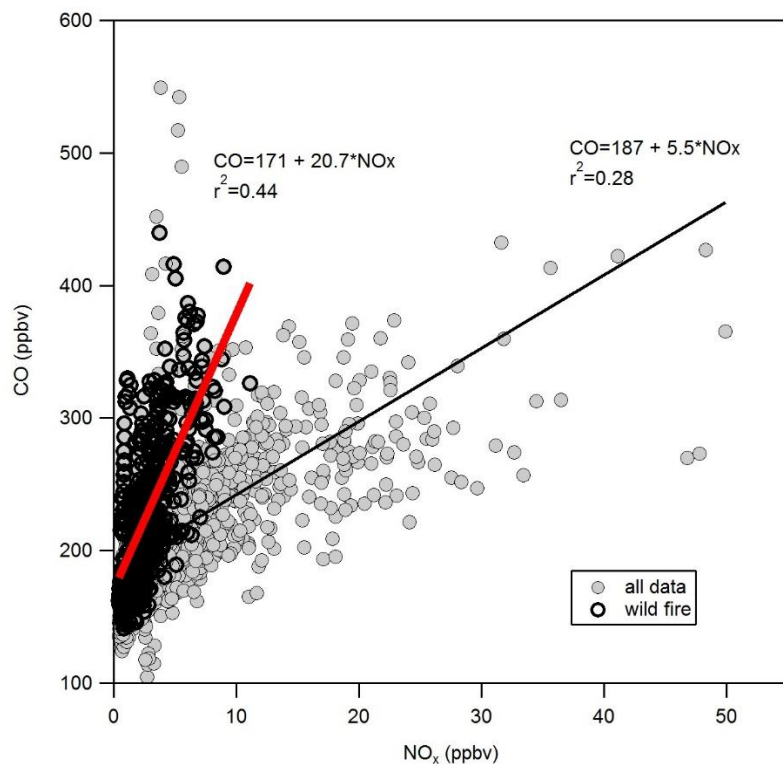


Figure 7.6. Correlations of CO to NO_x for the entire study at BCAA (grey circles and black line), the wildfire period (dark circles and red line). The CO to NO_x ratio is defined as the slope of the correlation and was 5.5 for the entire study, 20.7 for the wildfire period.

Strong correlations between many organic pollutant species and acetonitrile also provided evidence of wildfire impact between 7/30 and 8/1. Acetonitrile is a good tracer for biomass burning and is not typically observed in urban plumes (deGouw, et al., 2003). Therefore, coincident

enhancement of acetonitrile and other pollutants suggests that the pollutants originated from a biomass burning source. Figure 7.7 shows correlations with acetonitrile of organic compounds and NO_x during the wildfire period (rush hours excluded). Strong correlations were observed between acetonitrile and CO, benzene, formaldehyde, and to a lesser extent acetaldehyde. This suggests that wildfire plumes were responsible for elevated levels of CO and some organics during the wildfire period, consistent with reported emissions from wildfires (Andreae and Merlet, 2001). Interestingly, C_2 -alkylbenzenes and NO_x didn't display strong correlations with acetonitrile ($r^2 \sim 0.1$). These poor correlations with acetonitrile for these compounds and others (i.e. toluene, isoprene) imply local urban emissions were a more important source of these compounds than wildfire emissions.

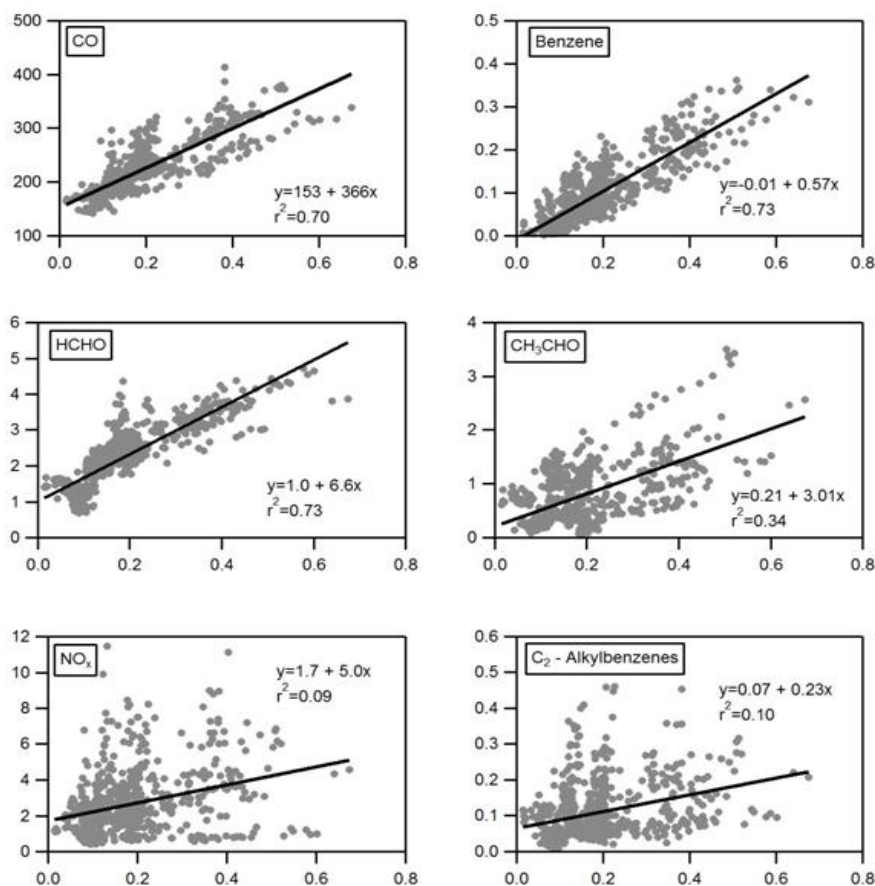


Figure 7.7. Correlations of selected pollutants versus acetonitrile (CH_3CN) at BCAA during the wildfire period. Morning rush hour data are excluded (06:00 - 10:00). Graphs are labeled by pollutant in the upper right corner and in each graph the pollutant is on the y axis and acetonitrile is on the x axis. Units are ppbv.

During the wildfire period ozone mixing ratios were more similar between the sites than at other times of T-COPS. Figure 7.8 shows the two ozone episodes that occurred during the wildfire period (8/1 and 8/5) compared with the other ozone episodes (7/29, 8/16, and 8/17). Ozone levels on

8/1 and 8/5 were similar between the three sites during the high ozone period in the afternoon in contrast to the other three ozone events where significant difference in ozone levels between Horn Rapids and the other sites were observed. The lack of spatial gradients on 8/1 and 8/5 suggests that ozone was transported into the airshed by the wildfire plume and/or that the additional precursors provided by the wildfire smoke was the primary driver of ozone throughout the airshed. Because we believe that transport of NO_x was negligible compared with locally emitted NO_x , the additional VOCs contributed by the wildfire plume along with any ozone produced in the plume during transport were likely the reasons for the widespread elevated ozone episode in the airshed. Correlations of ozone with acetonitrile during the afternoons in the wildfire period displayed in Figure 7.9 demonstrate a relationship between ozone and acetonitrile, suggesting that elevated ozone was associated with the wildfire plumes. Because the wildfires clearly had an impact on ozone in the airshed, we chose to analyze these days separately from days that were more typical of conditions in the Tri-Cities. It important to note, however, that wildfires could be important contributors of ozone and precursors on high ozone days.

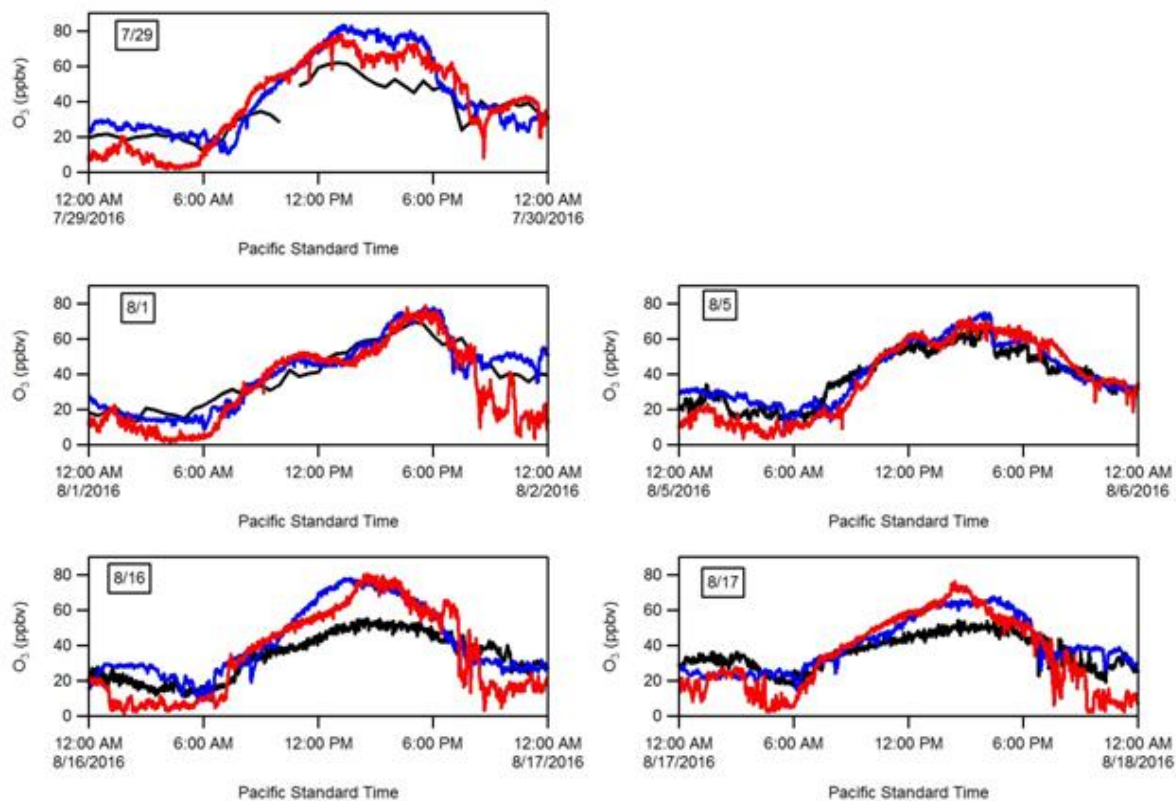


Figure 7.8. Comparison of ozone mixing ratios for the ozone event days. Blue trace is BCAA, red trace is Burbank, and black trace is Horn Rapids. Ozone was very similar between the sites during the wild fire period events of 8/1 and 8/5.

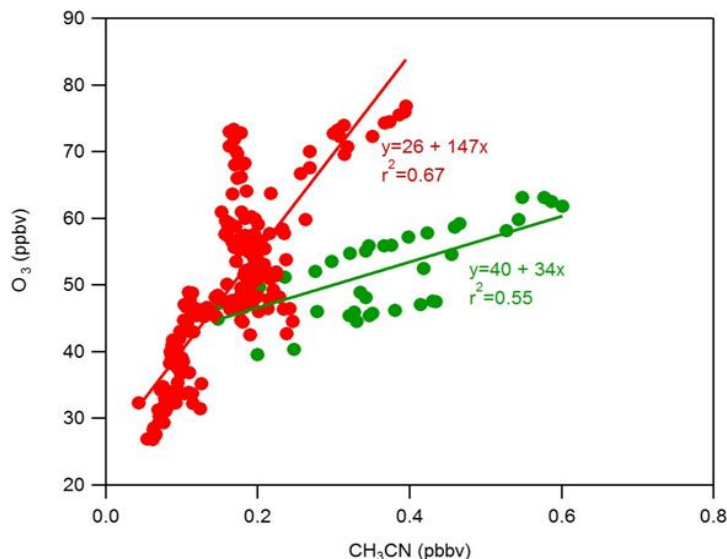


Figure 7.9. Correlations between ozone and acetonitrile during photochemically active hours (10:00 - 18:00) at BCAA during the wildfire period (10 min average data). The green points are 7/31 data and the red points are data from 8/1 - 8/5.

7.3. Ozone Precursor Emissions Inventory

Table 7.2 shows the combined CO, NO_x, and VOC emissions for Benton and Franklin counties. The emissions inventory was obtained from the AIRPACT 5 emissions tool for early August 2016. The major limitation of using the emission inventory is that it is a county wide, meaning that emissions from outside the Tri-Cities airshed are included. We expect that a majority of traffic related emissions (on-road vehicles) to be located in the Tri-Cities airshed since it is the major population center for both Benton and Franklin counties. On-road vehicle emissions are important sources of NO_x and VOCs at the county level, and it is reasonable to assume traffic related emissions in the Tri-Cities are a major source of these precursors. Non-road vehicle emissions (i.e. farm equipment, trains, boats, lawnmowers) are also a significant source of VOC and NO_x at the county level. Biogenic VOC emissions are distributed throughout the county and are dependent on the types of vegetation (crops, trees) growing in an area.

The major anthropogenic emission categories of ozone precursors (NO_x and VOCs) were mobile sources (on-road and off-road vehicles), point sources, and solvent volatilization (VOCs). Table 7.3 shows the total anthropogenic emissions from each sector and their percentage contributions. By far the largest anthropogenic source of NO_x in the three county area are on road vehicles at 50% of total emissions. Point sources accounted for only 10% of NO_x emissions (notably the Boise Cascade paper mill in Wallula) with the remainder originating from other sources (mostly smaller scale fuel and waste combustion). Vehicles sources were also a major source of VOCs, but solvent volatilization was also a major source in the region, contributing 43% of anthropogenic VOC emissions. Point sources made up 15% of VOC emissions in the area.

Table 7.2. Benton and Franklin County ozone precursor emissions for August 2016,

Category	CO (tons)	NO _x (tons)	VOC (tons)
On-Road Vehicles	89.67	16.14	7.86
Non-Road Vehicle	40.62	6.98	5.84
Point Sources	2.03	1.03	1.47
Biogenic	14.73	1.14	31.63
Fires	43.89	0.88	21.17
Solvents	0.00	0.00	16.37
Other Sources	1.68	5.86	2.25
Total	192.62	32.02	86.58

Table 7.3. Total emissions (in tons per day) for the major anthropogenic emission categories excluding fires and biogenic emissions for Benton and Franklin Counties for August 2016.

	CO		NO _x		VOC	
	Tons/Day	%	Tons/Day	%	Tons/Day	%
On Road Vehicles	89.67	65	16.14	50	7.85	21
Non-road Vehicles	40.62	30	6.99	22	5.84	15
Point Sources	5.46	4	3.26	10	5.84	15
Solvents pesticides	0	0	0	0	12.6	33
Solvents other	0	0	0	0	3.8	9.9
Other Sources	1.68	1	5.86	18	2.25	5.9
Total	137.4		32.2		38.2	

Solvents and Pesticides

The solvent category is the largest source of VOCs. A detailed examination of the sources in this category reveals that 77% of the emissions are from agricultural use of pesticides, amounting to 12.6 tons per day compared to 3.8 tons per day for all other solvent categories combined (i.e. architectural surface coatings, household cleaning products, cosmetics and toiletries). Many

pesticide active ingredients are not volatile and would have little influence on local atmospheric chemistry but may be formulated with inactive ingredients such as light petroleum distillates that are volatile and photochemically reactive. These distillates are accounted for in the solvent category. Table 7.4 lists the major pesticides used in Benton and Franklin counties. The data are annual use estimates of 219 pesticides as determined by the United States Geological Service (USGS) for the year 2015. Total annual pesticide use in Benton and Franklin counties is estimated to range from 6.3 million to 8.6 million kg per year. The top 3 pesticides collectively account for 70-80% of the total mass of pesticide applied. Several of the pesticides are formulated with a petroleum solvent that has the potential to volatilize and be a source of VOCs. The source profile (3001) used by the US EPA to speciate this “solvent” lists alkanes as being the principal VOC in pesticide formulations. Material safety data sheets (MSDS) from pesticide manufacturers were examined to better determine actual pesticide composition. The most heavily used pesticides that are relevant as a source of ozone precursors are 1,3-dichloropropene, metam, and horticultural oil.

The compound 1,3-dichloropropene (trade name Telone, Dow Chemical Company) is the most heavily used pesticide with annual application rate for the 2 counties combined to be approximately 2 million kilograms. This is comparable to the total annual VOC emissions from on-road traffic in Benton and Franklin counties of 2.5 million kg. Dichloropropene is used as a pre-plant fumigant and applied as a liquid into the soil. It rapidly evaporates to a gas and diffuses through the soil. It has been estimated that 25% to 60% is lost from the field due to diffusion from the soil to the air; most of this loss occurs in the first 4 days after application (EPA, 1998; Kim et al. 2003). Dichloropropene has been shown in smog chamber experiments to be an efficient ozone precursor (Carter and Malkina, 2007). The Washington State Department of Agriculture lists the majority of its use in potato and carrot crops. Benton and Franklin counties have the state’s largest potato production. However the application of 1,3-dichloropropene for potato crops occurs in October through February, outside of summer ozone season.

Horticultural oils (example trade name Orchem 796, Calumet Specialty Products) are light petroleum distillates (mineral oil) primarily composed of alkanes (> 60%). A major use in the State of Washington is in orchard pest and disease management. The hydrocarbon compounds associated with light petroleum distillates would also be found in diesel fuel and diesel exhaust emissions and thus it would be difficult to identify occurrence of this pesticide in urban air sampling. By design these oils have lower volatility but once volatilized would act as ozone precursors.

Metam (trade name Vapam, AMVAC Chemical Corporation) is also used as a soil fumigant. Metam is an organo sulfur compound that is not volatile and not an ozone precursor itself. Metam rapidly breaks down in soil upon hydrolysis to produce methyl isothiocyanate, the volatile, biologically active compound in the pesticide application. MSDS sheets from AMVAC Chemical Corporation lists inert ingredients as ~50% by weight of the formulation but do not specify what they are. Methyl isothiocyanate is photochemically reactive and can act as an ozone precursor (Carter and Malkina, 2007). Metam is widely used for potato crops in Benton and Franklin counties and is applied in the fall (September and October) by center pivot irrigation (Merriman and Hebert, 2007). Thus use of metam based pesticides and horticultural oil application may be a source of

chemically reactive hydrocarbons that could serve as ozone precursors toward the end of the summer ozone season.

Table 7.4. USGS estimated annual pesticide usage in millions of kilograms for Benton and Franklin counties in 2015.

Compound	Low	High	Comment
1,3-dichloropropene	2.11	2.23	ozone precursor but applied in fall & winter
Metam	2.04	3.10	methyl isothiocyanate is an ozone precursor but applied in fall
Horticultural oil	0.715	0.715	100% mineral oil: alkanes + cycloalkanes. Ozone precursor with potential summertime application.
Sulfur	0.304	0.314	
Calcium polysulfide	0.129	0.140	
Mancozeb	0.134	0.138	
Glycophosphate	0.0864	0.0865	
EPTC	0.0601	0.0601	
Oxamyl	0.0516	0.0525	petroleum solvent
Pendimethalin	0.0472	0.0482	petroleum solvent
2,4-D	0.0276	0.0455	petroleum solvent
DCPA	0.0270	0.0270	

The impact of agricultural pesticide application as a source of hydrocarbon precursors to the Tri-Cities airshed is difficult to assess. Annual application data from USGS are for the entire county and so the bulk of the usage may not impact the Tri-Cities airshed. Much of Franklin County immediately north of Pasco and along the Columbia River is under agricultural production with center pivot irrigation (CropScape, National Agricultural Statistical Service). Pesticide use in this region likely impacts the Tri-Cities airshed. A map of the area around the Tri-Cities showing agriculture land and associated crop type is shown in Figure 7.10. In Benton County much of the productive agricultural land is further away from the Tri-Cities and thus may not have much impact. There is extensive viticulture to the west of the Tri-Cities along the Yakima River valley (Prosser,

WA), and center pivot cropland 25 to 60 km away to the south along the Columbia River. Pesticide application in Walla Walla County, where there is extensive irrigated croplands running south along the Columbia River might also be a more significant influence on the Tri-Cities airshed.

The AIRPACT emissions inventory currently allocates the annual agricultural pesticide use (SCC 2461850000) evenly across all months and days except for Sunday. Clearly many agricultural pesticides are not used this way. Based on conversations with WA Dept. of Agriculture staff and WSU Tri Cities researchers, not many volatile agrochemicals are applied during the summer ozone season. This appears to be the case for 1,3-dichloropropene and metam with application being done in late fall through winter for 1,3-dichloropropene and in fall for metam. Horticultural oil however is applied to foliage and summer applications would be higher than other times of year. Given the low and high use estimates, metam and 1,3-dichloropropene account for approximately 64% of total pesticide emissions. Uncertainty in the temporal profile use for pesticides makes the solvent emission inventory for VOC ozone precursors highly uncertain.

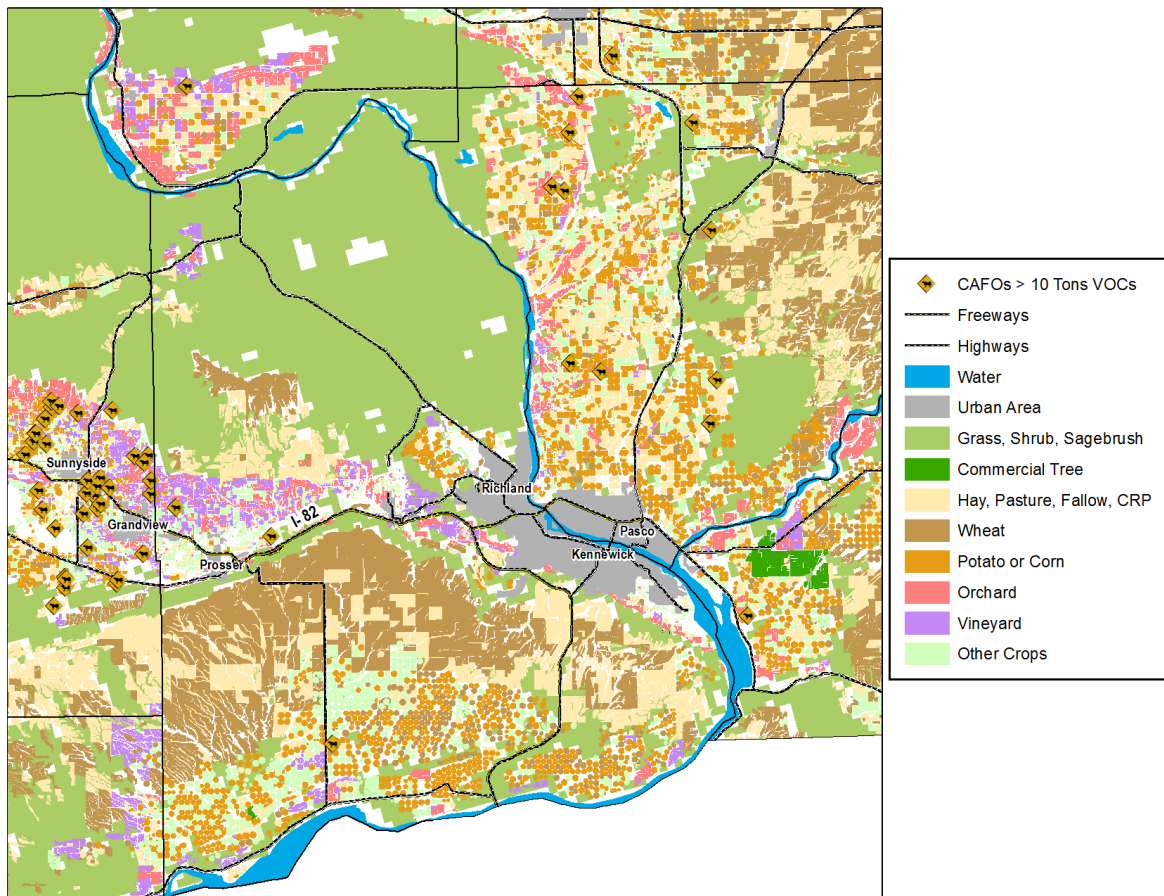


Figure 7.10. Land use map of the area surrounding the Tri-Cities showing crop type. Center pivot irrigation for potato and hay crops is extensive to the immediate north of Pasco. Vineyards and fruit crops are common to the west of Richland.

Point Sources

Specific information on individual point source locations and emissions are shown in Table 7.5. The largest point sources reside in Walla Walla County, associated with industries along the Columbia River to the south of the Tri-Cities area. The table lists sources emitting more than 0.05 tons/day or more of VOCs or NO_x. Locations of these sources are shown in Figure 7.11. The largest emitter by far is the Boise Cascade paper facility, which contributed 5.4% of the NO_x and 11.3% of the VOCs in the Benton and Franklin including major nearby point sources from Walla Walla County. The Boise paper facility was somewhat removed from the airshed (about 8 miles southeast of Burbank on the Columbia River), but may be a major source of precursors when there are southeast winds blowing up the Columbia River. The other point sources are generally small in magnitude relative to mobile emissions suggesting that they may make strong local influences, but are much less important than mobile sources at the airshed scale.

To better understand the impact of point sources on the ozone monitoring location during T-COPS, atmospheric dispersion of emissions from the above list of NO_x point sources were modeled using the EPA- approved AERMOD steady-state Gaussian modeling system. The salient inputs to AERMOD v16216r were:

- Point sources emitting over 0.05 tons/ day, along with their stack parameters
- Tyson Fresh Meats and Pasco airport were modeled as an area source and a line of volume sources respectively, assuming very low release heights
- Actual 2014 summertime emissions reported to Ecology spread evenly over all summertime hours to derive a static hourly emission rate
- Modeling domain was about 40km x 40km
- Gridded receptors were 300m apart.
- Discrete receptors at the BCAA and Burbank monitoring sites
- AERMAP supplied with 1 arc-sec (~ 30m) resolution digital terrain data
- AERMET inputs:
 - On-site meteorological data from BCAA monitor, for T-COPS period
 - Relative humidity, pressure and cloud cover data obtained from Pasco airport.
 - AERMINUTE run on Pasco airport data to minimize instances of calm winds.
 - Twice- daily upper air soundings from Spokane

The 2nd highest 1-hour NO_x mixing ratio during the 3 weeks of T-COPS is shown in Figure 7.11. With the exception of the area right next to Boise Cascade in Wallula, all impacts over 10 ppb occur between 7PM- 9AM. Even if all NO_x emissions from these sources were assumed to be in the form of NO₂ (a gross over-estimate) it is clear that the BCAA and Burbank monitors would be impacted by less than 5 ppb from all sources. So although point and area source emissions do contribute toward NO_x in the airshed, we conclude that point source emissions likely had little impact on measured NO_x levels at the BCAA and Burbank sites.

Table 7.5. Summary of major point sources and their contribution to total CO, NO_x and VOCs. The percentages are of total airshed emissions (Franklin and Benton Counties and the Boise Paper, Tyson Meats, and Gas Transmission Northwest Station 8 facilities).

Source	CO		NO _x		VOC	
	Tons/day	Pct	Tons/day	Pct	Tons/day	Pct
Boise Cascade	2.761	2.01%	1.72	5.35%	4.32	11.33%
Williams Pipeline	0.024	0.02%	0.18	0.57%	0.01	0.01%
Agrium US Inc	0.003	0.00%	0.13	0.39%	0.00	0.00%
Penford Food Ingredients	0.064	0.05%	0.11	0.34%	0.01	0.03%
ConAgra Foods Lamb Weston	0.074	0.05%	0.09	0.27%	0.03	0.07%
Tree Top Inc	0.06	0.04%	0.06	0.19%	0	0.00%
Greenbrier Rail Services	0.024	0.02%	0.00	0.01%	0.05	0.13%
Tesoro Logistics	0	0.00%	0	0.00%	0.09	0.25%
Tidewater Terminal Company	0	0.00%	0	0.00%	0.08	0.22%
ConAgra Foods Lamb Weston - Pasco	0.081	0.06%	0.10	0.30%	0.08	0.22%
Tri-Cities Airport	0.642	0.47%	0.09	0.28%	0.04	0.11%
Gas Transmission Northwest Station 8	0.61	0.44%	0.46	1.42%	0.03	0.09%
Tyson Fresh Meats	0.064	0.05%	0.05	0.17%	0.01	0.03%

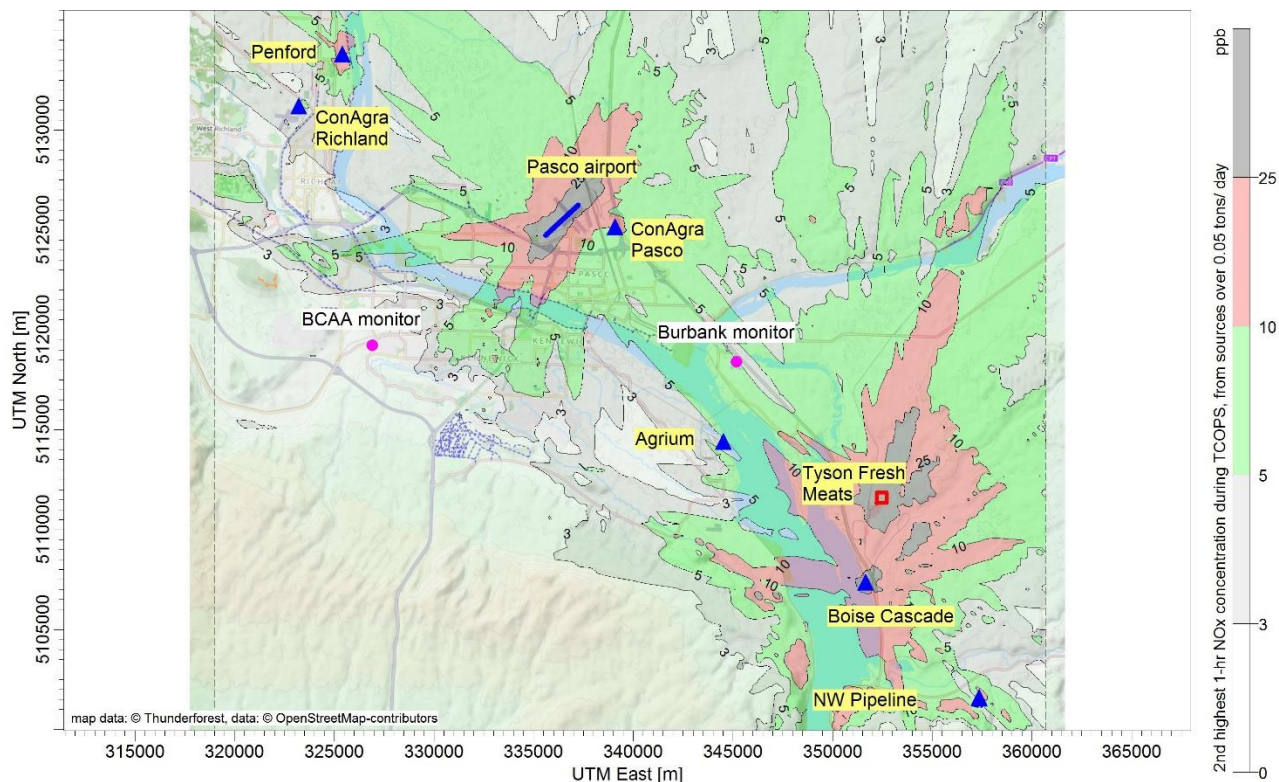


Figure 7.11. Map of AERMOD- modeled 2nd highest NO_x impacts from point sources during T-COPS. All sources emitting more than 0.05 tons per day were considered.

7.4 Time of Day Trends in Vehicle Traffic Pollutants

The emission inventory shown in Tables 7.2 and 7.3 reveal that on a county level, excluding biogenic and wildfire emissions, on-road vehicles are a major source of CO, NO_x, and VOCs. If pesticide emissions of VOCs could be excluded, then on-road vehicles would be most important source of CO, NO_x and VOCs. The impact of vehicle emissions as a source of ozone precursors should be apparent in the temporal variation and relationships between CO, NO_x, and VOCs during T-COPS.

Roadway traffic is monitored in the Tri-Cities area by the Washington State Department of Transportation (WSDOT) at 4 locations with automated traffic recorders (PTR sites) shown in the road map displayed in Figure 7.12. The figure displays the locations of the automatic traffic counters and major roads color coded for traffic volume. Traffic volume is greatest along the Columbia Park Trail in Kennewick, along highway 182 in Pasco and Richland, and along state highway 395 connecting Pasco to Kennewick. Traffic volume along highway 12 past the Burbank site is noted by WSDOT to be approximately 13,000 vehicles per day. Urban vehicle traffic has a strong time of day dependence that would impact ozone precursor concentrations. Figure 7.13 shows the average hourly traffic volume for the months July and August 2016 for site 2 on the Columbia Park Trail (PTR site R062W) together with total daily traffic volume. Similar vehicle

traffic patterns are also observed at sites 1 and 3. Weekday morning rush hour traffic volumes are about 4,000 to 5,000 vehicles per hour at site 2, while evening rush hour traffic is between 6,000 to 8,000 vehicles per hour. The onset of the morning and evening rush hours occur when mixed layer heights are rapidly changing as a result of changes in surface heating. Figure 7.14 shows the time of day variation of NO_x mixing ratios measured at BCAA with an estimate of PBL height variation and the average weekday traffic count on the Columbia Park Trail. The PBL height for this area was obtained from the AERMOD model (more specifically, diagnosed from AERMET's SFC file) described above. NO_x typically displays a large peak in the morning around 8:00 PST (~ 10 ppbv), an afternoon minimum (~2 ppbv), and a smaller evening peak at 19:00 PST (~ 5 ppbv). The diel variation in NO_x is consistent with the expected time of day variation in vehicle emissions and PBL height. The onset of the morning rush hour occurs within a shallow PBL resulting in a rapid increase in NO_x and a peak in abundance around 8:00 PST. NO_x mixing ratios decrease steadily through the late morning and afternoon as a result of a growing convective boundary layer even though vehicle traffic is reasonably constant if not increasing through the afternoon. The convective boundary layer reaches a maximum height in the afternoon of ~2 km around 15:00 PST. During this time NO_x mixing ratios are at a minimum consistent with greater dilution of surface emissions. In the late afternoon just before sunset, the mixed layer height rapidly shrinks just as the evening rush hour begins. The result of a shallower mixed layer height is an evening peak in NO_x mixing ratios around 19:00 PST when the PBL height is estimated to be ~ 150-m.

Figure 7.15 shows that CO, NO_x and the sum of aromatic hydrocarbons (benzene, toluene, C₂-alkylbenzenes, and C₃-alkylbenzenes) have a similar time of day variation in their abundance, consistent with the expectation from the emission inventory that motor vehicles are a major source of these ozone precursors. Figure 7.16 shows the correlation between CO and NO_x for the morning rush hour data excluding the wild fire impacted period (7/30 to 8/6) and the period of low CO and NO_x mixing ratios during the windy rainy period (8/8 to 8/10). The morning rush hour data have an average CO-to-NO_x molar ratio of 4.1, consistent with vehicle exhaust sources (Wallace et al. 2012). In summary the diel variation of the ozone precursors CO, NO_x, and aromatic hydrocarbons are consistent with road-way vehicle emissions.

Figure 7.15 also shows the time of day variation of isoprene, an important ozone precursor. This compound is largely emitted from vegetation such as trees, and its emissions are light and temperature dependent. Isoprene thus displays a different time of day variation; mixing ratios are higher in the afternoon when light levels and temperatures are at a maximum. An early evening peak is also apparent, likely also due to a collapsing mixed layer height as the sun sets. PTR-MS based measurements of isoprene in urban areas likely have interferences from other hydrocarbons (Gueneron et al., 2013), especially when isoprene levels are low as in the evening. Positive interferences at night are one reason why isoprene levels do not fall to zero in the evening.

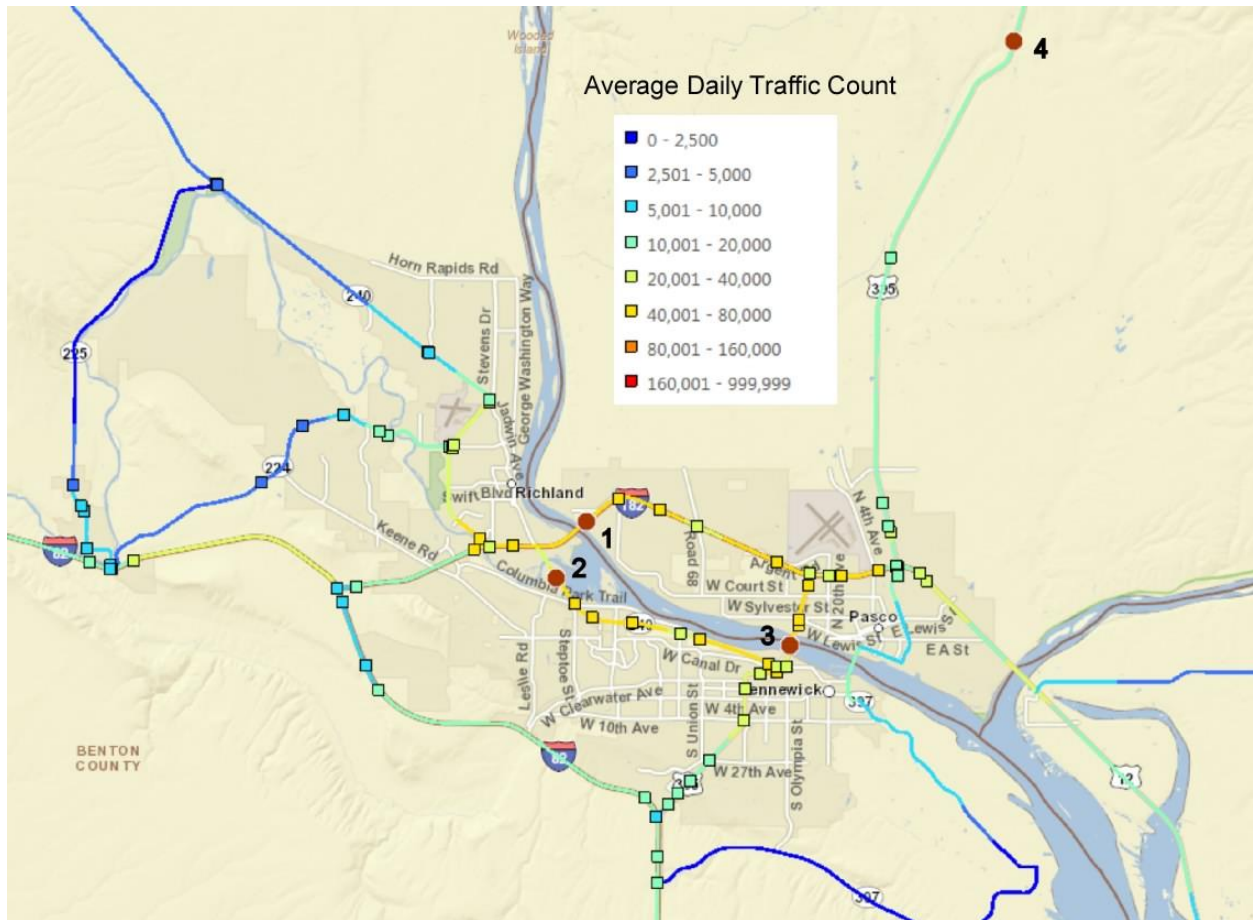


Figure 7.12. Annual average daily traffic count as reported by WA Department of Transportation. Road segments are color coded for average daily traffic volume. Automatic Traffic Recorders are labelled 1 through 4. Annual average traffic counts in 2015 were 60,000 for site 1 (PTR site R081, SR -182, Pasco), 74,000 at site 2 (PTR site R062W, Columbia Park Trail, Richland), and 63,000 vehicles per day at site 3 (PTR site R087, SR-395, Columbia River Bridge). Traffic volume at site 4 (PTR site R061, SR- 395, milepost 36) is 15,000 vehicles per day. Traffic volume along Highway 12 into Burbank was reported as 13,000 vehicles per day.

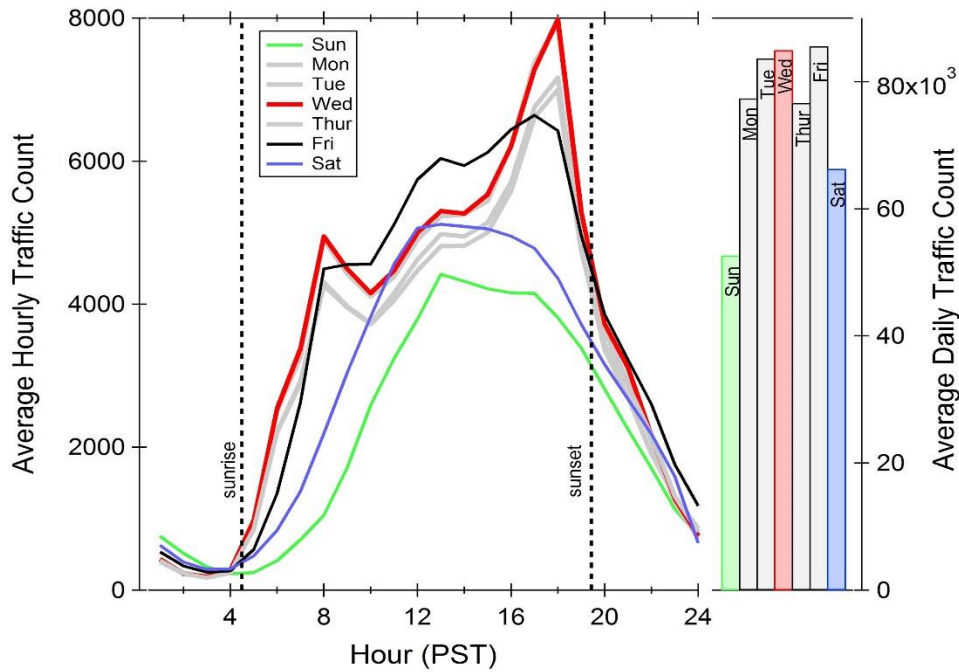


Figure 7.13. Day of week hourly average traffic counts for July-Aug, 2016 at WA Department of Transportation automated traffic recorder site R062W (SR-240) together with average daily total traffic counts for each day of the week.

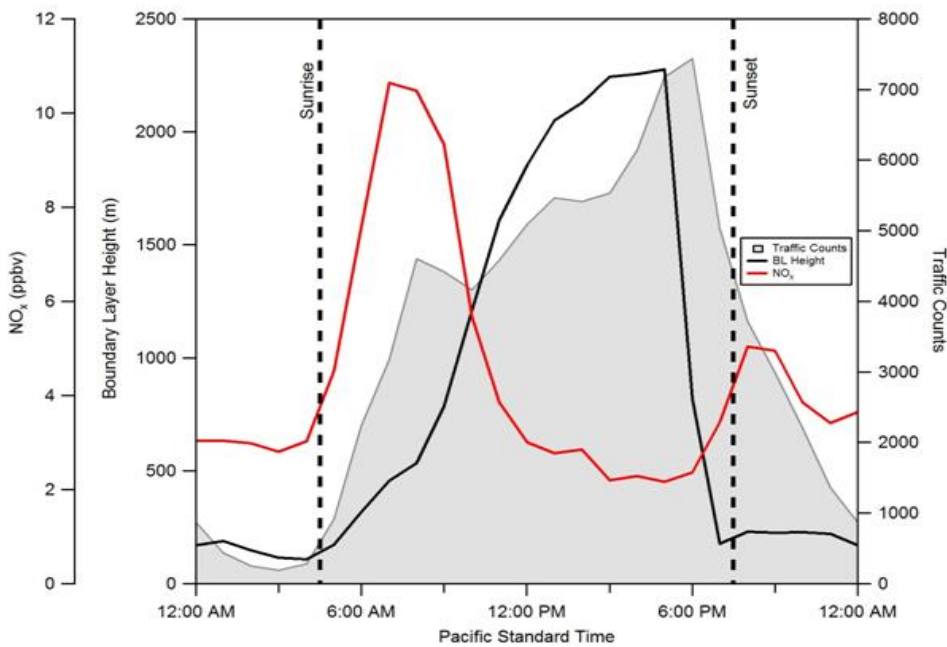


Figure 7.14. Diel variation of boundary layer height from the AERMET model (black trace), averaged weekday hourly traffic counts from the Columbia Park Trail (shaded trace) and 1/2-hr averaged NO_x mixing ratios from BCAA (red trace).

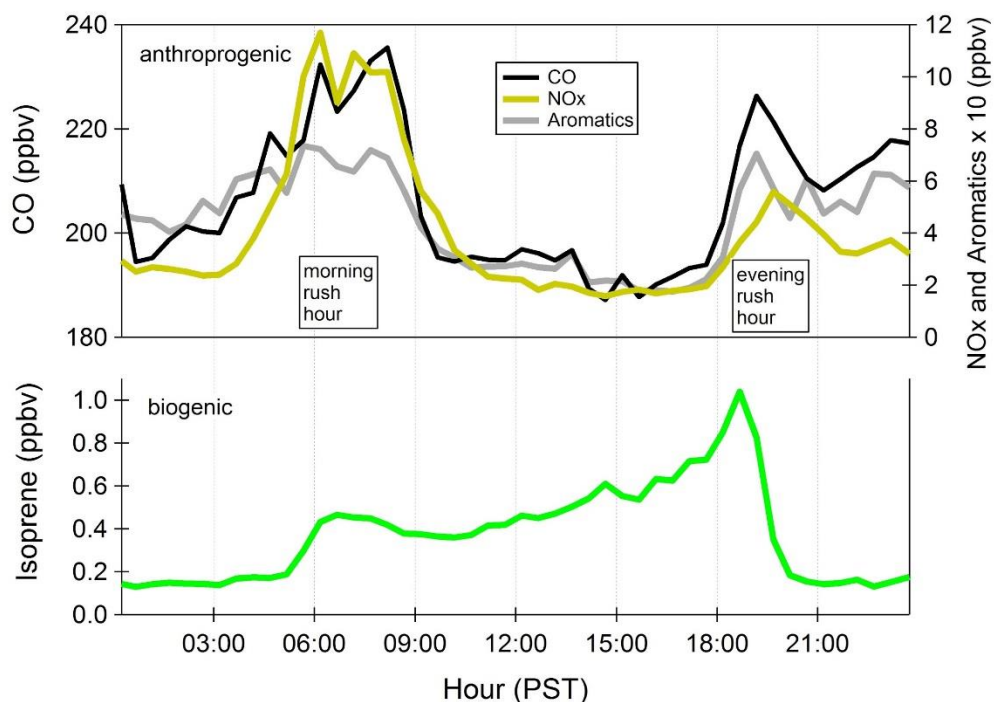


Figure 7.15. Diel variation of CO, NO_x, isoprene, and sum of aromatic compounds measured at BCAA. Shown are ½-hr averages. Aromatic hydrocarbon abundance has been multiplied by 10 to fit the scale. CO, NO_x and aromatic hydrocarbons display similar time of day variation which is consistent with on-road vehicles as the major source.

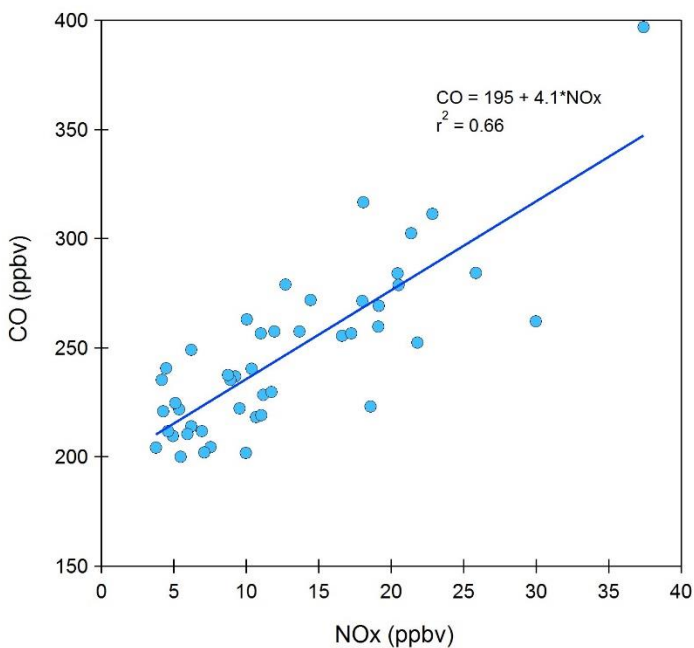


Figure 7.16. CO to NO_x correlation for BCAA for morning rush hour hourly average data (5:00 - 09:00 PST) excluding the wild fire period (7/30 to 8/6) and the rainy and windy period (8/8 to 8/10).

7.5. Spatial Distribution of NO_x

NO_x measurements from all three sites are shown as a time series in Figure 7.17. Some difference between the sites is evident. It is clear from the figure that there were many periods of elevated NO_x at Burbank that were not accompanied by elevated NO_x at the other two sites. Additionally, morning rush hour NO_x spikes were typically larger at BCAA than at Horn Rapids. Highest NO_x levels at BCAA were observed during the morning rush hour of Thursday Aug 18 (peak of 54 ppbv, 10 min average) at 06:30, and similar levels on Friday morning at 07:15 on July 29 (peak of 46 ppbv, 10-min average). Figure 7.17 displays the time of day variation of NO_x as a box and whisker plot and a comparison of the average hourly values for the three sites. Night time levels at BCAA are strongly influenced by the drainage flow along the Amon wasteway and therefore do not really reflect Tri-Cities nighttime airshed NO_x concentrations. This drainage flow effect is a likely explanation for why BCAA typically had the lowest nighttime NO_x levels of the 3 sites. Interestingly, Burbank had much higher NO_x levels at night and displays a maximum around 04:00, much earlier than what would be expected due to the onset of urban morning rush hour traffic (see Figure 7.13). Consistent with its distance from the urban traffic center, the Horn Rapids site shows no pronounced morning or evening rush hour peaks. In the afternoon NO_x levels between all the sites are quite similar, approximately 2 ppbv. The NO_x data are summarized and compared as a box and whisker plot in Figure 7.19. The 75th and 90th percentile range of NO_x levels at Burbank were much higher than BCAA and Horn Rapids, suggesting impact of nearby local sources.

To put the Tri-Cities NO_x abundance into perspective, the BCAA site was compared to the NO_x data collected by WA DoE from the Tacoma (36 Street site) and Seattle (10th and Weller site). These are the only sites in Washington where NO_x is routinely measured near roadways. The time of day variation of NO_x (1-hr averages) for these sites are compared in Figure 7.20. NO_x abundance in Kennewick is much lower than these other urban areas. Morning rush hour values at BCAA were a factor of 4 and 8 lower than Tacoma and Seattle respectively. Afternoon NO_x values at BCAA were about factor of 12 lower than Tacoma's and about a factor of 25 lower than Seattle's.

The higher NO_x mixing ratios at Burbank are somewhat unexpected given that this site is also removed from the major urban traffic center of the Tri-Cities. The AERMOD simulation does not indicate substantial impacts from point sources. Using the NO-to-NO_x ratio as an indicator of the freshness of emissions (with higher ratios indicating nearby sources), and wind directions at each site, the polar annuli plots in Figure 7.21 were constructed to compare BCAA and Burbank NO_x sources during the stagnant period toward the end of T-COPS. Each annular ring in the plot represents an hour of the day. Empty space (white) implies the wind rarely blew from that direction during those hours. Burbank data show the freshest NO_x (highest ratios) occurs mostly during east-vector winds about 1-2 hours earlier in the morning than the BCAA site. The latter is impacted by fresh NO_x from all directions, consistent with urban morning rush hour traffic. A likely explanation for the high NO_x mixing ratios at Burbank is the fact that the site is in close proximity to State Highway 12, approximately 250-m to the north east, and could be influenced by early morning road traffic. WSDOT traffic count data for highway 12 near the Burbank site (mile post 296) for the year 2015 is reported to be 13,000 vehicles per day with 19.9% being transport truck traffic. Early

morning transport truck traffic might be influencing the site as the passenger vehicle traffic would be expected to be low at 04:00 in the morning. One influence of diesel truck traffic would be on the CO-to-NO_x molar ratio. Diesel engine exhaust has lower CO-to-NO_x molar ratios than gasoline vehicles. Consistent with diesel truck traffic emissions, the Burbank site has a lower CO-to-NO_x molar ratio (2.4) as shown in Figure 7.22 than BCAA rush hour data (4.1) shown previously in Figure 7.16. The pattern of truck traffic on the highway was assessed using the automated traffic recorder data from Highway 395 (WSDOT PTR B03; site 4 in Figure 7.12) for July and August 2016; these data are shown in Figure 7.23. We infer that similar patterns would be observed along Highway 12 as some of the Highway 395 traffic would flow through Burbank along Highway 12 to and from the industries on the Columbia River between Burbank and Wallula. Transport truck traffic is a large fraction of the traffic volume between 01:00 and 05:00, as high as 56% on the weekdays and higher on the weekends. We conclude that the proximity of the Burbank site to the highway, and the higher frequency of early morning truck traffic is a plausible explanation for the early morning peak in NO_x and lower CO-to-NO_x molar ratio.

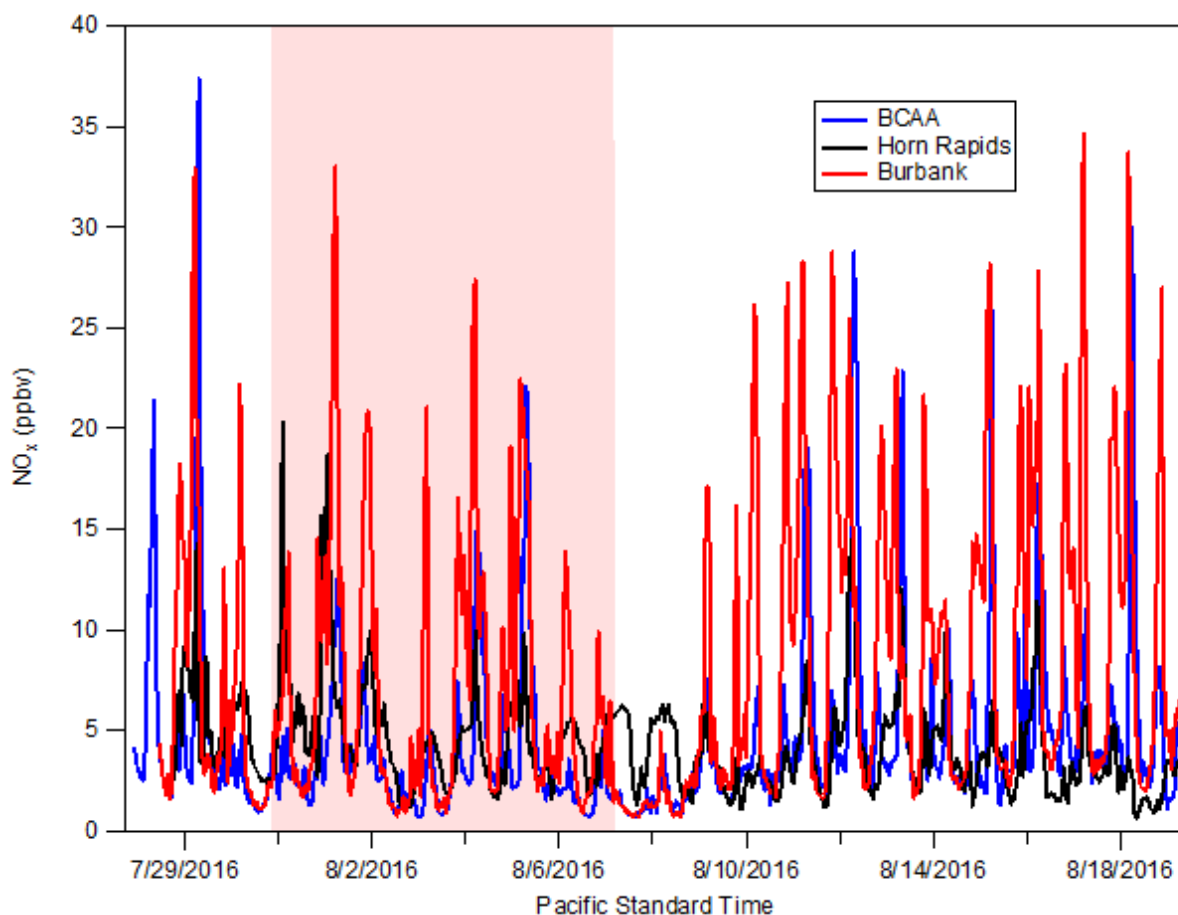


Figure 7.17. Comparison of NO_x mixing ratios at BCAA, Burbank, and Horn Rapids sites. The red shaded area indicates the period influenced by wildfires.

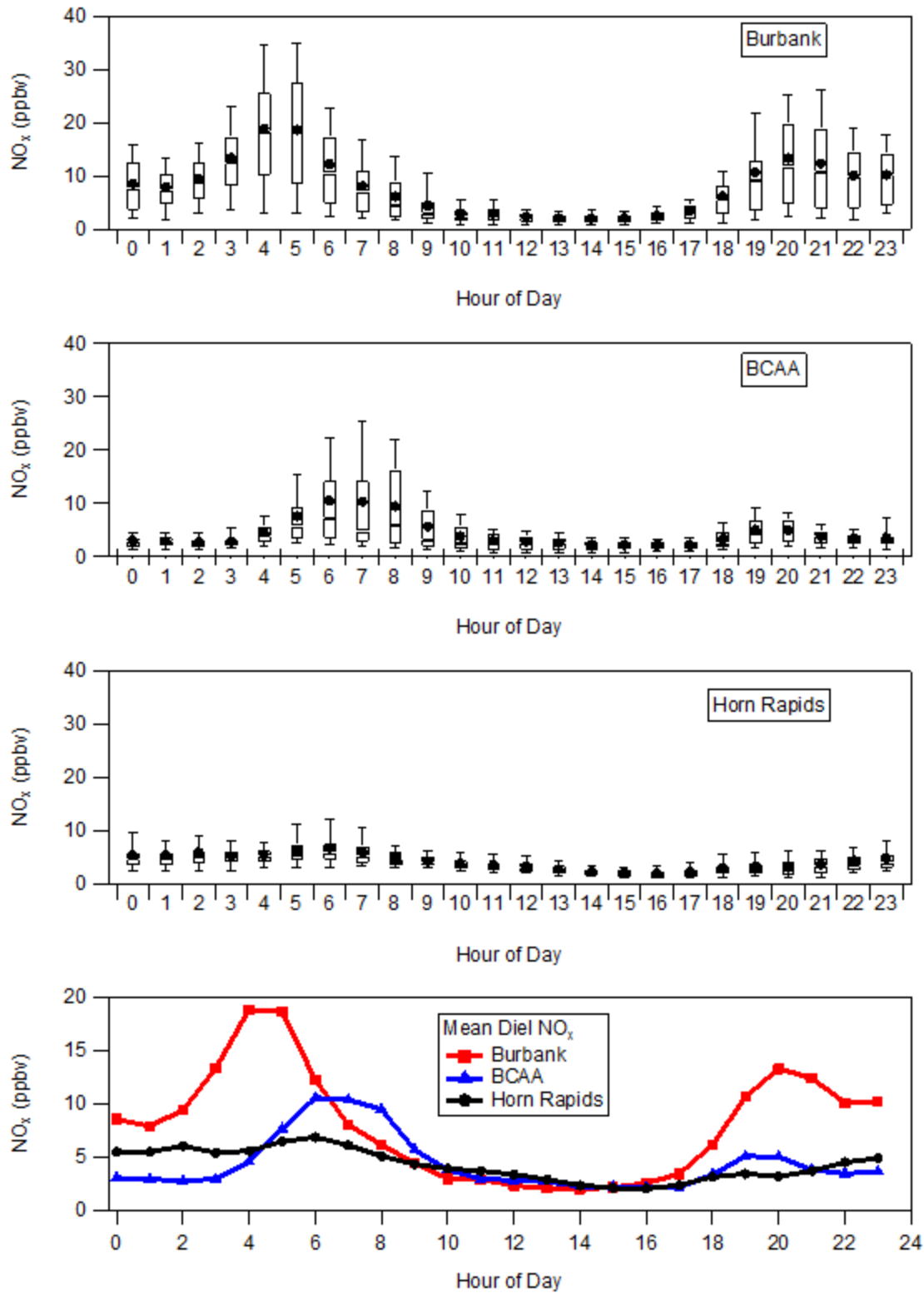


Figure 7.18. Time of day variation of NO_x mixing ratios at the Burbank, BCAA, and Horn Rapids sites. Bottom plot compares averages.

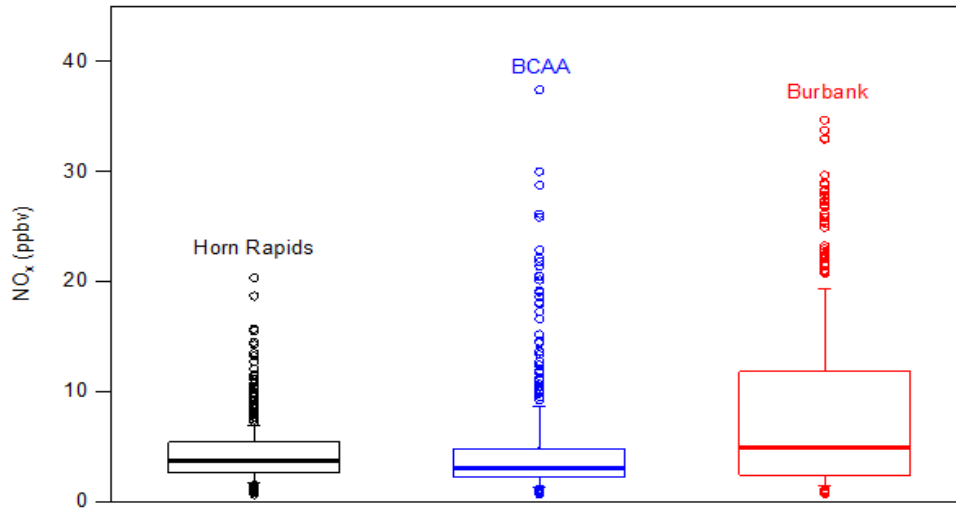


Figure 7.19. Box plots of 1/2-hr averaged NO_x data at Horn Rapids, BCAA, and Burbank. The bottom whisker is 10th percentile, the bottom of the box is the 25th percentile, the bar is the 50th percentile, the top of the box is the 75th percentile, and the top whisker is the 90th percentile.

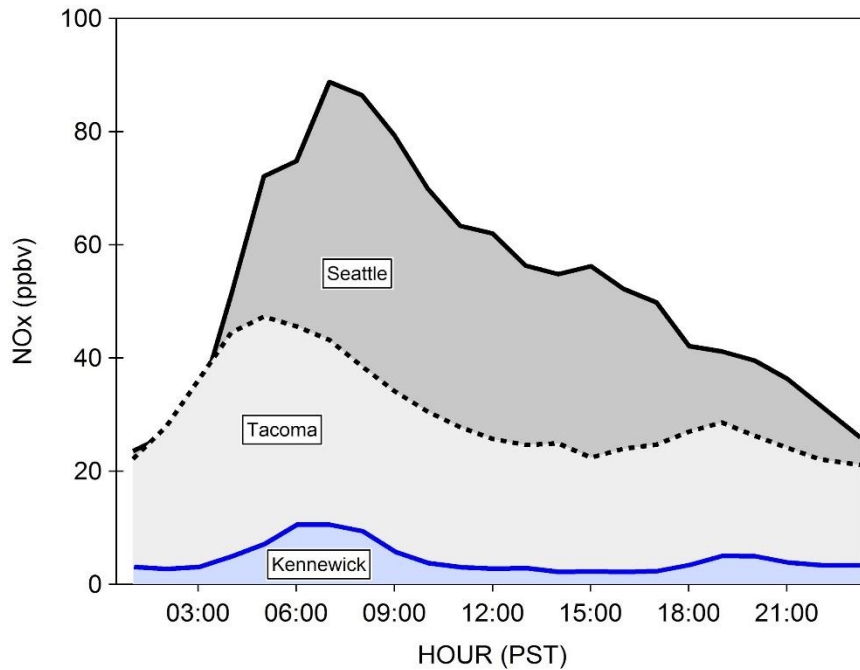


Figure 7.20. Comparison of the time of day variation of NO_x mixing ratios (1-hr average) between Seattle and Tacoma for July and August 2016 and the BCAA site T-COPS data (Kennewick).

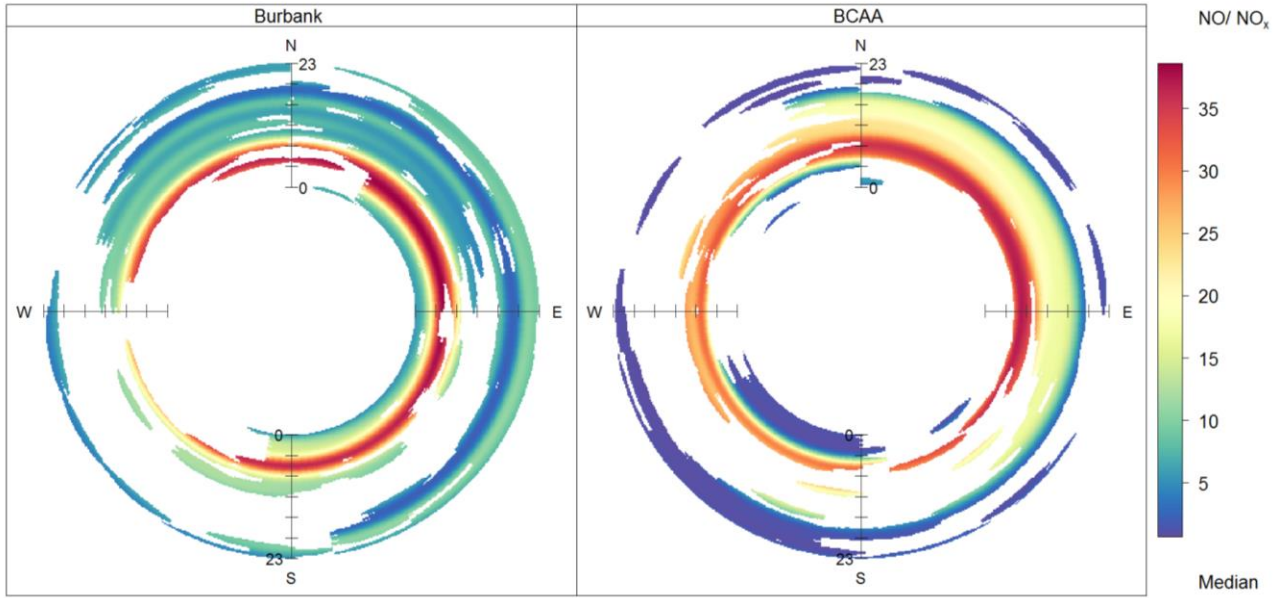


Figure 7.21. Polar annuli of median NO-to-NO_x ratios at BCAA and Burbank during the stagnant period.

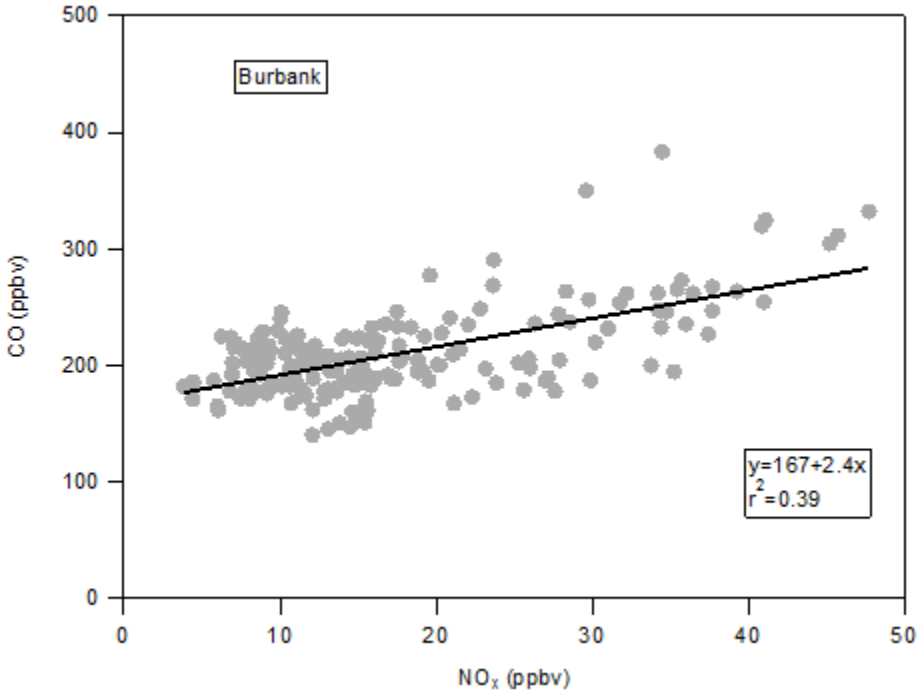


Figure 7.22. CO to NO_x correlation for Burbank morning maximum (3:00 - 8:00 PST).

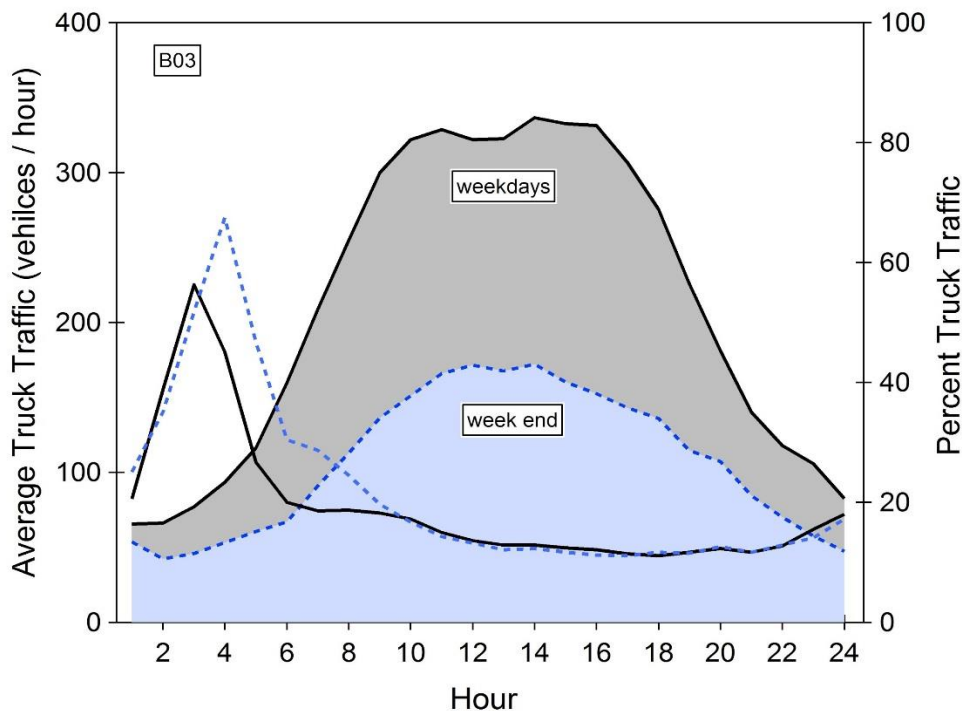


Figure 7.23. Time of day variation of transport truck traffic on state highway 395 (WSDOT PTR site B03) showing average weekday (black shaded area) and week end traffic counts (blue shaded area) for July and August 2016. Percentage of truck traffic to total vehicle traffic is shown as lines (solid black is weekday, dashed blue line is week end traffic).

7.6. Ozone Episodes: Analysis of mid-August Stagnation Period

The stagnation period at the end of the study was the best representative period during T-COPS of summertime meteorological conditions in the Tri-Cities that foster high ozone. The stagnation period occurred from 8/10 - 8/17 and was characterized by low wind speeds (< 3 m/s) and relatively high temperatures, with daily highs exceeding 30 °C on all days except for 8/10. Figure 7.24 shows the ozone mixing ratio, temperature and wind speed during the stagnation period. Ozone was relatively low during the first half of the stagnation period (8/10 - 8/13, daily maxima between 50 and 55 ppbv) and higher during the second half of the stagnation period (8/14 - 8/17, daily maxima between 60 and 75 ppbv). August 16th in particular stands out as a significant ozone episode, as hourly averaged ozone exceeded 70 ppbv as discussed in section 7.1. This ozone episode day (8/16) was compared to the rest of the stagnation period to determine whether there were noticeable differences in ozone precursors or other conditions that highlight factors that cause elevated ozone on particular days.

The time of day variation of NO_x and ozone mixing ratios at the sites for the stagnation period are compared to the Aug 16 data in Figures 7.25, 7.26, and 7.27 as box and whisker plots. The BCAA data, in Figure 7.25, shows that afternoon ozone on Aug 16 was higher than other days during this period, and that the largest differences in abundance were observed for the early

afternoon. In contrast, the time of day variation in NO_x mixing ratios for Aug 16 was very similar to the average trend; thus there is no difference in NO_x abundance that could explain differences in ozone.

The data for Burbank are shown in Figure 7.26. The Aug 16 data trend for ozone and NO_x was similar to typical values during the morning to early afternoon, but a sudden increase in ozone mixing ratios occurred ~ 13:00 PST, accompanied by an increase in NO_x. At this time the wind direction shifted from SSE to northerly. The change in wind direction and abrupt change in ozone abundance suggests a change in air mass origin. The ozone abundance at Burbank after the wind direction change was similar to that of BCAA, suggesting that the Tri-Cities urban area as the air mass origin. At Horn Rapids, shown in Figure 7.27, ozone levels were somewhat elevated on 8/16, but NO_x levels were a little lower than the average. Overall, it did not seem like local enhancement of NO_x was a significant driver of the high ozone episode that was observed at any of the sites on 8/16.

Time of day trends of organic compounds (sum of benzene, toluene, C₂-alkylbenzenes, and C₃-alkylbenzenes), NO_z, CH₃OOH, and water vapor during the stagnation period are compared to the 8/16 data in Figure 7.28. The photoproducts NO_z and formaldehyde were clearly elevated on Aug 16 compared to the stagnation period average trend. The abundance of CH₃OOH, a HO_x radical chain termination product was slightly elevated in the afternoon compared the stagnation period average. Isoprene, an important ozone precursor, did not substantially vary from the stagnation period average. Interestingly, afternoon mixing ratios of aromatic compounds were about 50% to a factor of 2 larger on 8/16 than typically seen during the stagnation period. The higher mixing ratios of aromatic compounds on Aug 16 suggests their influence as ozone precursors. Water vapor was also elevated on Aug 16 compared to the stagnation period average. Water vapor and formaldehyde participate in HO_x radical production. Higher radical production rates on Aug 16 would enhance ozone production rates compared to other days.

Figure 7.29 displays the relationship between maximum daily ozone and the average afternoon from 10:00 to 18:00 PST of water vapor, formaldehyde, aromatic compounds, isoprene NO_x, and wind speed during the stagnation period. Different relationships were observed for the first 4 days of this period (8/10 to 8/13) compared to the last 4 days (8/14 to 8/17) which were generally warmer and had higher ozone levels. The last 4 days show a positive correlation between max ozone and water vapor, formaldehyde, and aromatic compounds. The first 4 days, which were less photochemically active by virtue of their lower maximum ozone abundance displayed no relationship. The positive correlation with aromatic compounds can be contrasted with the poor correlation between ozone and isoprene. Likewise, the correlation between maximum ozone and NO_x is much poorer than between ozone and aromatic hydrocarbons. This suggests that ozone photochemistry was more sensitive to the abundance of hydrocarbons and radical precursors. The afternoon of Aug 16 had a slightly lower average wind speed (1.70 m/s) than the other 3 stagnation days with elevated ozone (range 1.85 to 1.95 m/s). Afternoon wind speeds for Aug 14, 15, 17 were similar to Aug 10, 11, and 13. The afternoon of August 12 had the highest wind speeds, (2.3 m/s).

We conclude from the analysis the August stagnation period that elevated ozone on Aug 16 was associated with elevated water vapor, formaldehyde, and aromatic hydrocarbons and a slightly lower wind speed while NO_x levels remained the same. The higher abundance of ozone on Aug 16 is qualitatively consistent with our understanding of the chemical and meteorological process that impact ozone abundance. On Aug 16 lower average wind speeds combined with higher concentrations of HO_x radical precursors (H_2O and HCHO) and aromatic hydrocarbons (an ozone precursor).

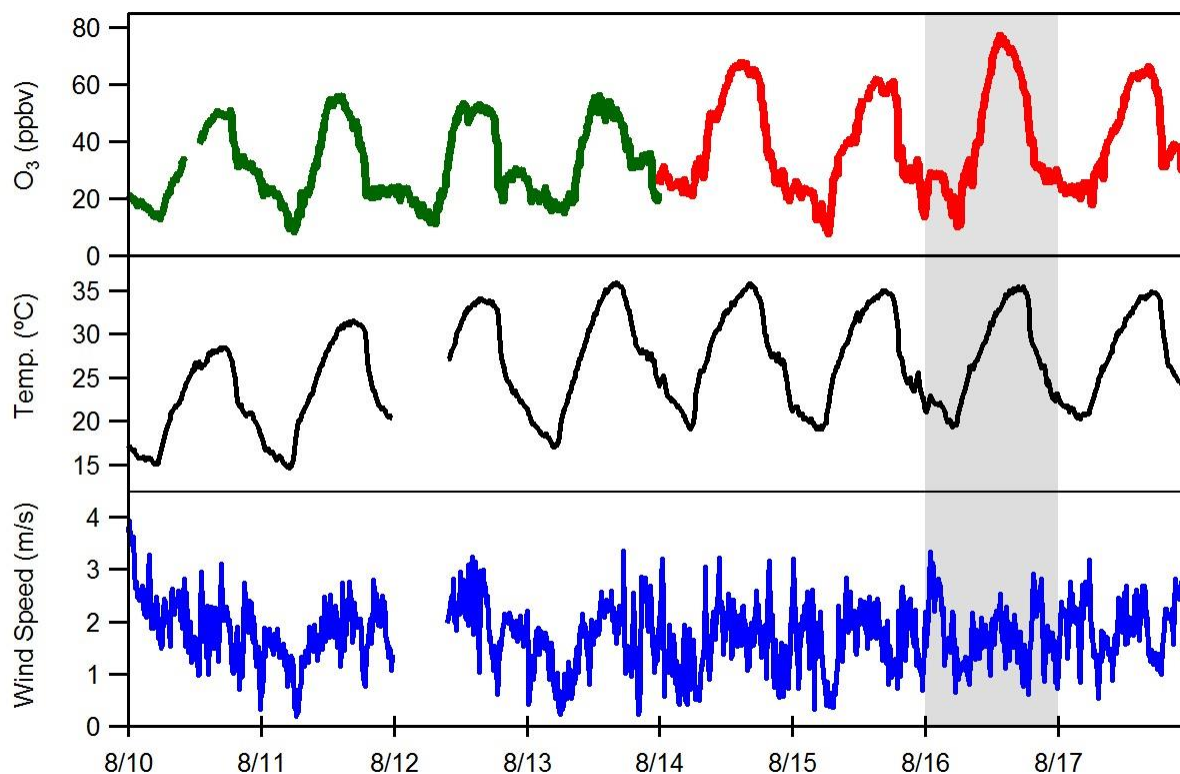


Figure 7.24. Ozone at BCAA during the stagnation period at the end of the study (8/10 - 8/17). The green trace represents the cooler, lower ozone period (8/10 to 8/14), and the red trace represents the higher ozone period (8/14 – 8/17). The shaded area is the high ozone day (8/16) where hourly ozone at BCAA exceeded 70 ppbv.

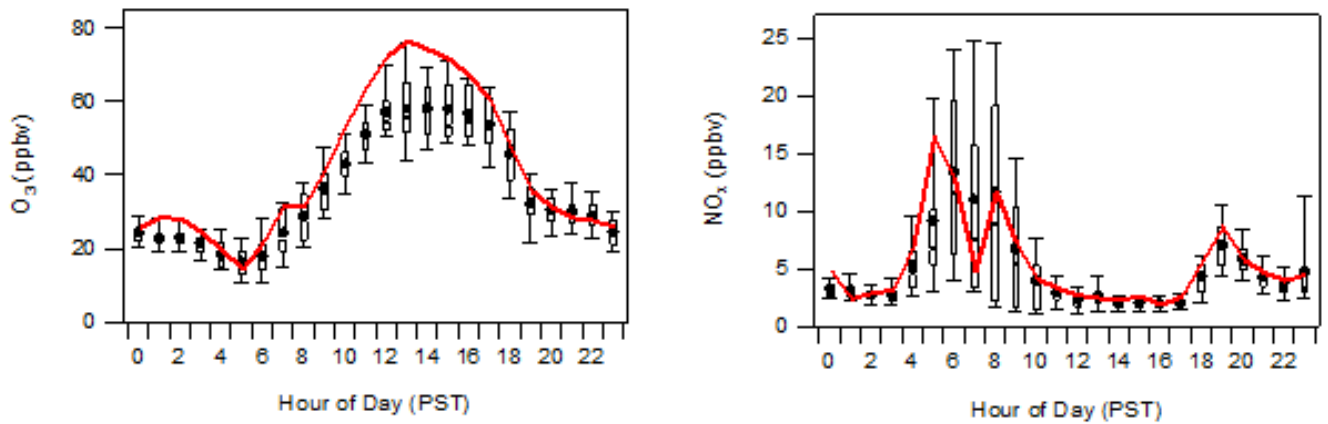


Figure 7.25. Ozone and NO_x at BCAA during the stagnation period. The boxes represent the 25th to 75th percentile of observations and the whiskers represent the 10th to 90th percentiles. The dot is the mean. The red trace represents the hourly averaged concentration on the high ozone day (8/17) where hourly ozone exceeded 70 ppbv at BCAA.

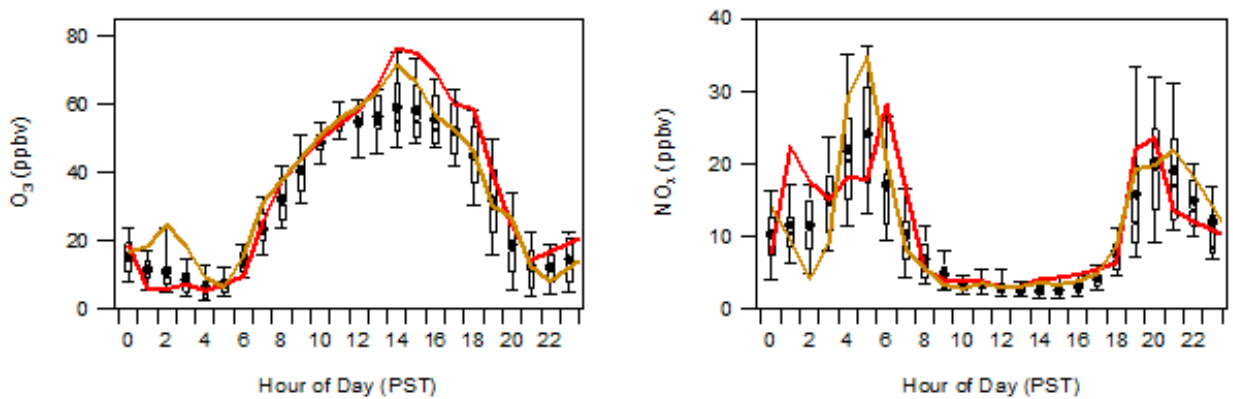


Figure 7.26. Ozone and NO_x at Burbank during the stagnation period. The boxes represent the 25th to 75th percentile of observations and the whiskers represent the 10th to 90th percentiles. The dot is the mean. The red trace represents the hourly averaged concentration on the high ozone day (8/16) where hourly ozone exceeded 70 ppbv at BCAA. The orange trace is the high ozone day at Burbank when hourly ozone exceeded 70 ppbv at Burbank (8/17).

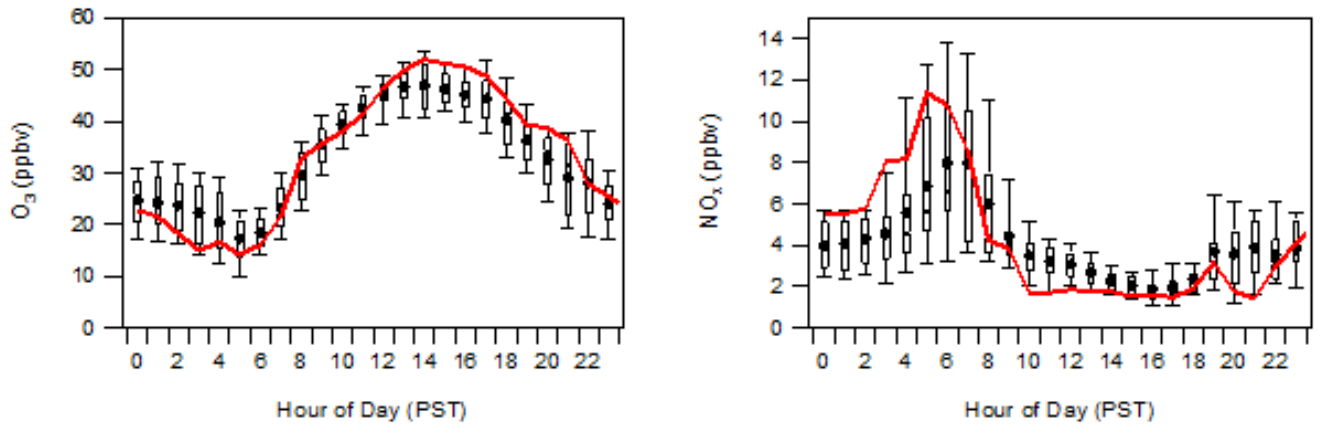


Figure 7.27. Ozone and NO_x at Horn Rapids during the stagnation period. The boxes represent the 25th to 75th percentile of observations and the whiskers represent the 10th to 90th percentiles. The dot is the mean. The red trace represents the hourly averaged concentration on the high ozone day (8/16) where hourly ozone exceeded 70 ppbv at BCAA.

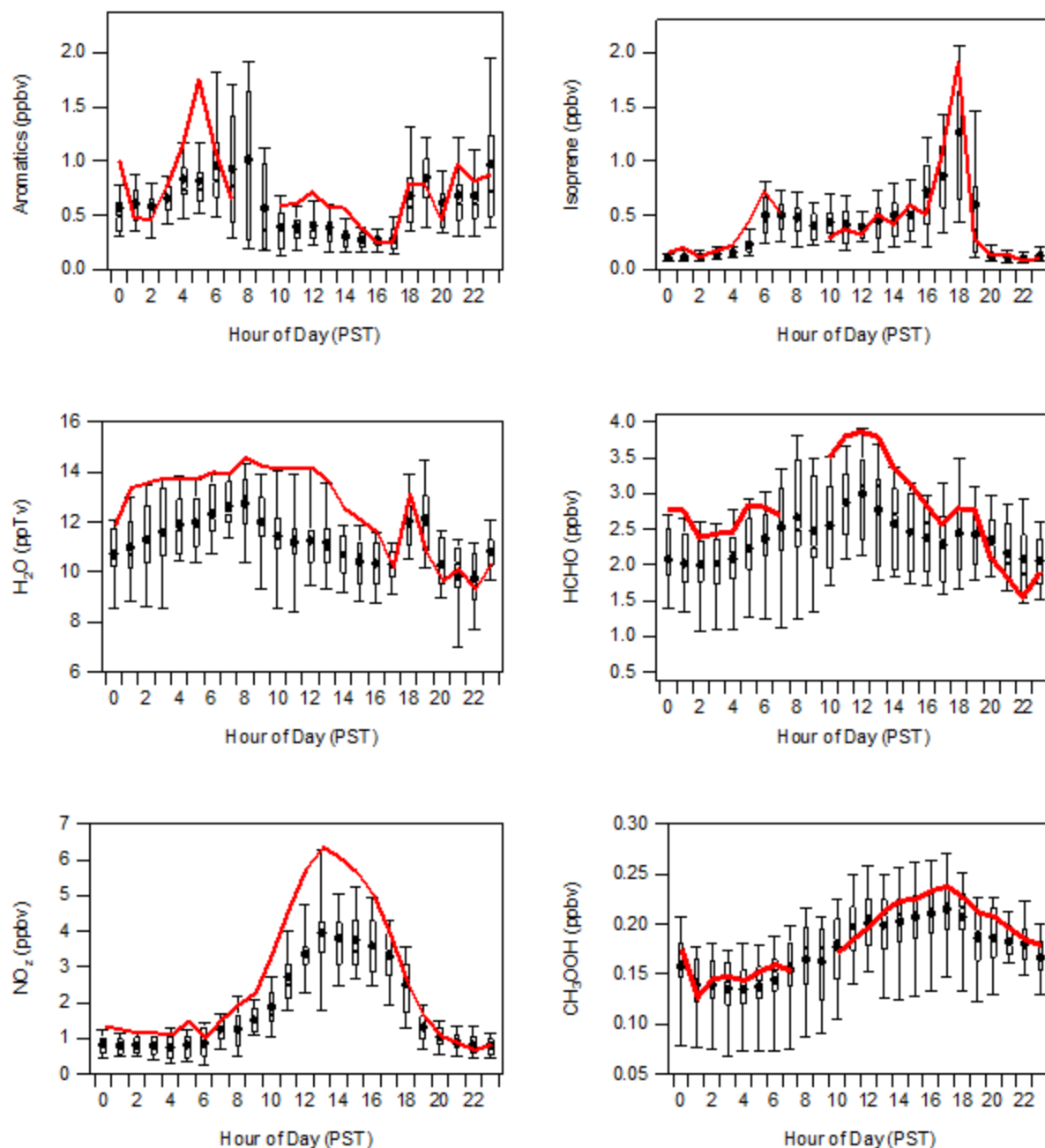


Figure 7.28. Time of day trends of aromatics, isoprene, H₂O, HCHO, NO₂, and CH₃OOH for the stagnation period. The boxes represent the 25th to 75th percentile of observations and the whiskers represent the 10th to 90th percentiles. The dot is the mean. The red trace represents the hourly averaged concentration on the high ozone day (8/16) where hourly ozone exceeded 70 ppbv at BCAA.

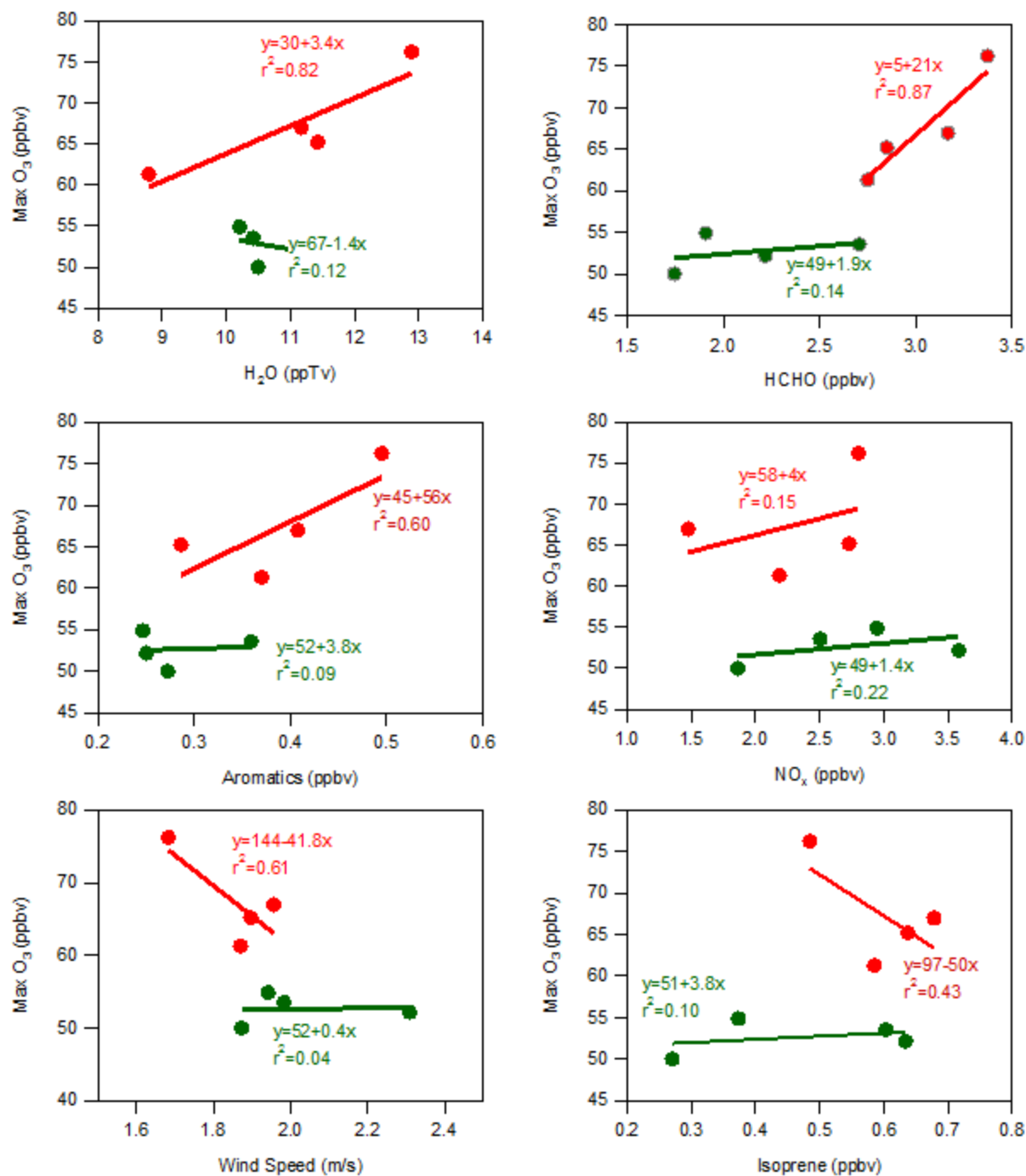


Figure 7.29. Daily maximum ozone vs afternoon average (10:00 - 18:00) abundance of H₂O, HCHO, aromatic compounds, NO_x, wind speed, and isoprene for the stagnation period (8/10 - 8/17). Green symbols are the first 4 days of the period (8/10 to 8/13) and red symbols are the last 4 days (8/14 to 8/17) when ozone levels were typically higher.

7.7 Analysis of VOC and NO_x Limitation

To assess whether the airshed was VOC or NO_x limited based on observations at BCAA, indicator species ratios were examined. Indicator ratios are metrics of ozone formation chemistry that have been developed from analysis of 3-D photochemical transport modeling and analysis of radical budgets (Milford et al. 1994; Kleinman 1994; Sillman, 1995; Tonnesen and Dennis, 2000). Indicator ratios are typically longer lived secondary products that are formed in the ozone formation process and accumulate over the course of the day. Several different ratios have been proposed and used in field observations to assess VOC or NO_x sensitivity. Such ratios tend to provide clear distinctions between very VOC or very NO_x limited regimes but have more difficulty consistently defining conditions near the O₃ ridge line (Tonnesen and Dennis, 2000). Photochemical model analysis has shown urban areas can transition from one regime to another over the course of the day, typically VOC limited (or radical limited) in the morning and early afternoon to NO_x limited in the later afternoon (Ren et al., 2013). Indicator ratios and attribution of ratio values to NO_x or VOC sensitivity may vary regionally as a result of different source and sink processes influencing species concentration. Thus indicator ratios are not perfect predictors of ozone sensitivity. Indicator ratios that have provided consistent insight on ozone formation chemistry are O₃/HNO₃ or O₃/NO_z, H₂O₂/HNO₃, HCHO/NO₂, and O_x/Peroxides (Tonnesen and Dennis, 2000). Urban areas have been found to display both VOC and NO_x limited chemistry based on indicator ratios. For example, Sillman et al. (1997) reported the city of Atlanta to have NO_x sensitive chemistry, suggest that Los Angeles and Phoenix have VOC sensitive chemistry (Sillman et al., 1997; Kleinman et al., 2005). In the state of Washington, Xie et al. (2011) examined measured and modeled urban plume O₃/NO_y ratios downwind of Seattle and concluded that peak ozone was associated with VOC sensitive conditions but that ozone formation was close to showing equal sensitivity to VOC and NO_x.

The indicator ratios evaluated for T-COPS were O₃/NO_z and HCHO/NO_y, and HCHO/NO₂ measured at BCAA. These choices were made based on the measurement data available. The indicator ratios O₃/NO_z and HCHO/NO_y were calculated from a linear regression between the two indicator species with the slope being the indicator ratio. Examples of these correlations for O₃/NO_z are shown in Figure 7.30. The analysis was performed on data from the photochemically active period of the day, between 10:00 - 18:00. Indicator ratios were compared to those from photochemical transport model simulations reported by Sillman (1995) in the Lake Michigan region and Northeast corridor, to those reported by Sillman et al. (1998) for Nashville, TN, and to those reported by Tonnesen and Dennis (2000) for regional grid model of the eastern US. O₃/NO_z values indicative of NO_x or VOC sensitivity are listed in Table 7.6 together with values of other indicator ratios. There is a range of O₃/NO_z values from the different models that indicate a NO_x sensitive regime (low of 5.8 to high of 9.5).

Table 7.7 shows the T-COPS O₃/NO_z indicator ratios for the entire campaign, the Columbia Cup boat race high ozone day (7/29), the period of wildfire influence where acetonitrile was elevated (7/31-8/1 and 8/4 - 8/6) and the end of the campaign stagnation period (8/10 - 8/18). As illustrated in Figure 7.30, the O₃/NO_z analysis yielded strong correlations for all periods ($r^2 > 0.79$). Observed O₃/NO_z values ranged from a low of 6.5 ± 0.2 during the August stagnation period (8/10 - 8/19

period) to a high of 9.5 ± 0.5 on the Friday of the boat race weekend (7/29). Compared to the O_3/NO_z values reported by Sillman in Table 7.6, the BCAA values suggest a chemical regime that is neither very VOC nor NO_x limited. Most values in Table 7.7 fall within either the upper range of VOC limited values or lower range of NO_x limited values. Compared to the O_3/NO_z ratios reported by Tonnesen and Dennis (2000), the BCAA data for all periods were greater than the 5.8 ratio that is indicative of NO_x sensitive chemistry.

An examination of the $HCHO/NO_y$ ratio yielded similar results as O_3/NO_z , that the BCAA chemical regime is neither strongly VOC nor NO_x sensitive. As an indicator ratio, $HCHO / NO_y$ does not have as sharp a delineation between VOC and NO_x sensitive chemistry as O_3 / NO_z , thus indicator ratio values from chemical transport models have some overlap between VOC and NO_x sensitive chemistry as shown in Table 7.6. For the T-COPS data, correlations between $HCHO$ and NO_y were much weaker than the correlations between O_3 and NO_z . This is likely due in part to the fact that a substantial fraction of $HCHO$ and NO_y are primary in origin, while O_3 and NO_z are almost exclusively secondary. The T-COPS $HCHO/NO_y$ ratios ranged from 0.23 to 0.35, values that fall within the transition range between VOC and NO_x sensitive chemistry for both of Sillman's (1995) model scenarios. The highest ratio during T-COPS was the Friday of the Columbia Cup race weekend (7/29), suggesting more strongly NO_x sensitive chemistry, consistent with the O_3 / NO_z ratio.

The $HCHO/NO_2$ ratios were examined for daytime periods (10:00 to 18:00 PST) when O_3 exceeded 50 ppbv and these ratio values are shown for a number of different periods in Table 7.9. The average ratio was calculated from the individual 10-minute data averages rather than from a regression fit. The ratio typically increased slightly over the course of the day, suggesting that conditions were more VOC sensitive in the morning and more NO_x sensitive in the afternoon, consistent with observations in other urban areas (Ren et al., 2013). Based on the Tonneson and Dennis (2000) analysis, ratios < 0.8 indicate a VOC sensitive regime, and ratios greater than 1.8 indicate a NO_x sensitive regime with ratios in between indicating an airshed that could be equally VOC or NO_x sensitive. The $HCHO/NO_2$ ratios displayed a modest range of values, from a low of 1.27 ± 0.26 (8/1 wild fire event) to a high of 1.78 ± 0.51 (7/29 Columbia Cup event). These values suggests the airshed is not strongly VOC or NO_x limited, and that it exists in a regime of near equal VOC and NO_x sensitivity. The boat race weekend had the highest value and was close to the value identifying NO_x limited chemistry, consistent with the O_3/NO_z analysis and $HCHO/NO_y$ analysis.

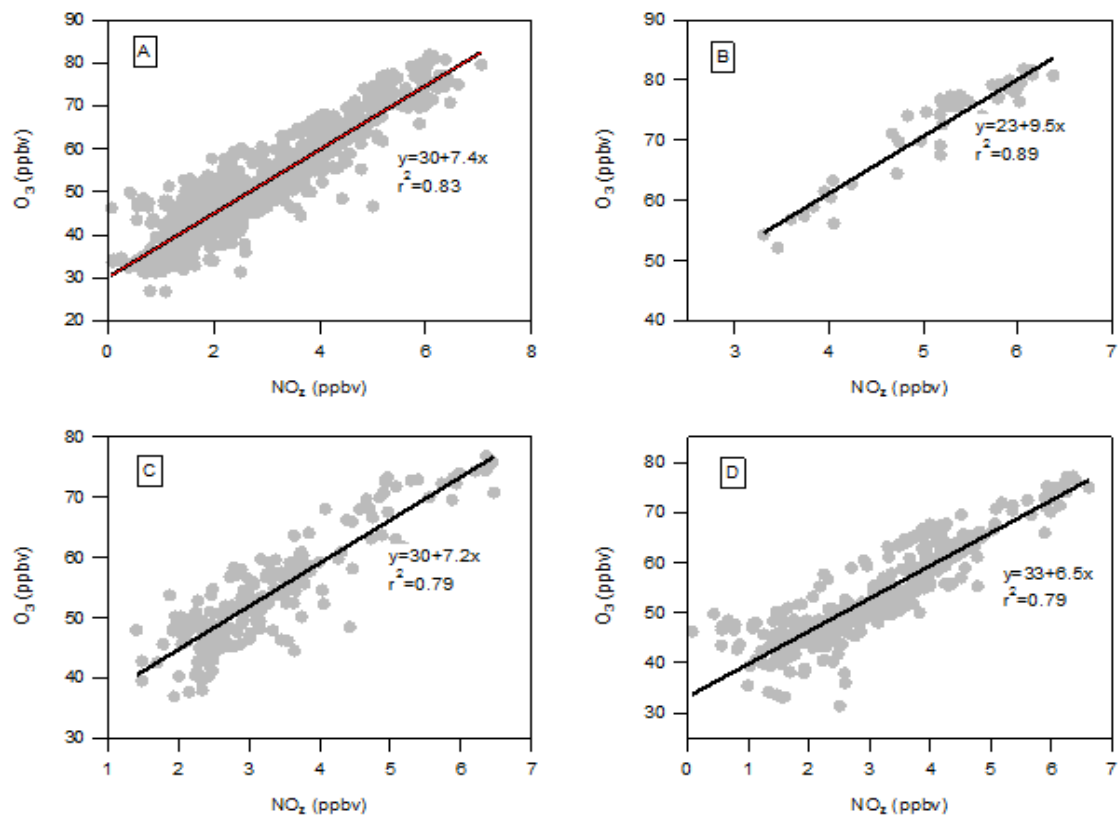


Figure 7.30. Correlations between ozone and NO_z for the entire campaign (A), the boat race day (B), the wildfire period (C), and the end of the campaign (D).

Table 7.6. Reported indicator ratios for VOC and NO_x limitation from photochemical models.

	O_3 / NO_z		$\text{HCHO} / \text{NO}_y$		$\text{HCHO} / \text{NO}_2$	
	VOC Limited	NO_x Limited	VOC Limited	NO_x Limited	VOC Limited	NO_x Limited
Sillman (1995) Lake Michigan	3.5-8.4	9.5-19	0.14-0.31	0.29-0.67		
Sillman (1995) Northeast Corridor	6.2-8.6	7.9-21	0.23-0.42	0.26-1.2		
Sillman et al. (1998) Nashville	6.6-6.9	8.6-12.5				
Tonnesen and Dennis (2000) Eastern US	< 5.8	> 5.8			< 0.8	> 1.8

Table 7.7. Correlations of O₃ to NO_z for data between 10:00 - 18:00 PST

Period	O ₃ / NO _z		
	Intercept	Slope	r ²
all T-COPS data	30.0 ± 0.3	7.4 ± 0.1	0.83
Boat Race Day (7/29)	23.3 ± 2.5	9.5 ± 0.5	0.89
Wild Fire (7/31 - 8/1 & 8/4 - 8/6)	30.3 ± 0.8	7.2 ± 0.2	0.79
Stagnation Period (8/10 - 8/18)	33.2 ± 0.6	6.5 ± 0.2	0.79

Table 7.8. Correlations of HCHO to NO_y for data between 10:00 - 18:00 PST.

Period	HCHO / NO _y		
	Intercept	Slope	r ²
Whole Campaign	0.88 ± 0.04	0.3 ± 0.01	0.59
Boat race day (7/29)	0.85 ± 0.30	0.35 ± 0.04	0.67
Wildfire (7/31 - 8/1 & 8/4 - 8/6)	1.24 ± 0.10	0.26 ± 0.02	0.49
End of Camp. (8/10 - 8/18)	1.30 ± 0.10	0.23 ± 0.02	0.31

Table 7.9. Average HCHO / NO₂ molar ratio measured between 10:00 and 18:00 PST for periods with O₃ > 50 ppbv.

Period	HCHO / NO ₂ ratio
Whole Campaign	1.76 ± 0.85
Boat race day (7/29)	1.78 ± 0.51
Aug 1 wildfire episode	1.27 ± 0.26
Aug 5 wildfire episode	1.62 ± 0.64
Stagnation (8/10 to 8/18)	1.66 ± 0.64
Aug 16 episode	1.55 ± 0.36

7.8 VOC Reactivity

VOC reactivity is a metric that describes the HO radical loss frequency to volatile organic compound reactions. It is a product of the VOC abundance and its HO reaction rate coefficient given in equation (2) in Chapter 1. The metric identifies which VOCs are the most important ozone precursors. VOCs that are both abundance and reactive with HO are the most important precursors. As discussed in section 7.3, vehicle emissions are a significant source of reactive VOCs in the airshed. The impact of vehicle exhaust was clear in the relative abundance of aromatic hydrocarbons. For example, the abundance of C₂-alkylbenzenes relative to toluene matched closely the ratio expected from gasoline vehicle exhaust as displayed in Figure 7.31. The two species were strongly correlated ($r^2=0.87$) suggesting that they were co-emitted. The observed molar ratio of 1.09 was similar to the 0.96 ratio given by the EPA speciation profile used in MOVES (profile #8757, EPA SPECIATE 4.5) for gasoline vehicles burning E10 gasoline. There are many compounds important for ozone formation in vehicle exhaust that the PTR-MS cannot measure and need to be accounted for. To estimate the contribution of unmeasured VOCs originating from vehicle exhaust to VOC reactivity at the BCAA site, the molar abundance of those hydrocarbon in the exhaust profile relative to C₂-alkylbenzenes was calculated. Given the measured abundance of C₂-alkylbenzenes at BCAA, the abundance of other exhaust components such as ethylene and propylene were estimated from the molar ratios in the exhaust profile.

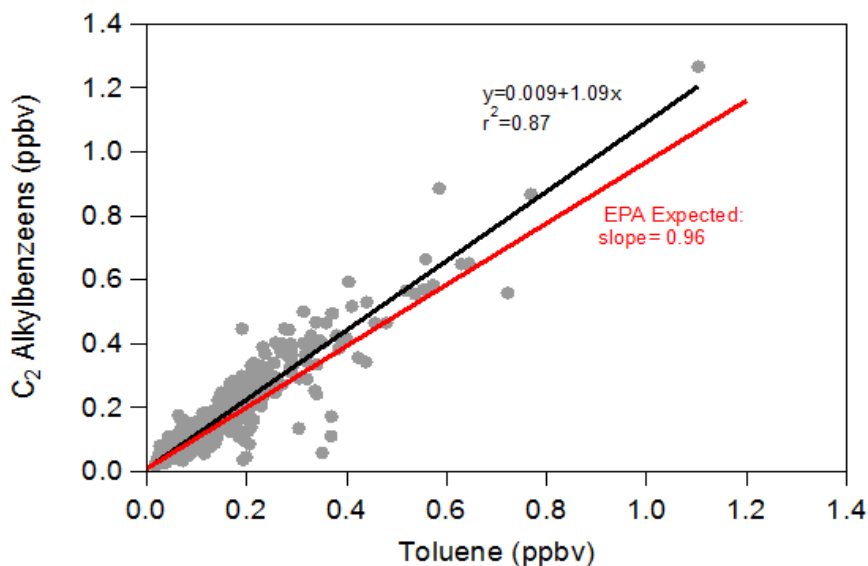


Figure 7.31. Correlation of hourly C₂-alkylbenzenes to toluene at BCAA. The abundance of C₂ alkylbenzenes relative to toluene was 1.09, within 15% of the expected ratio in the EPA gasoline exhaust emissions profile.

VOC reactivity was calculated from measured VOC abundance and from the unmeasured exhaust components to assess their relative importance as ozone precursors. The HO reaction rate constants were taken from primary literature where available (Atkinson and Arey, 2003; Aschmann

et al., 2013) and from the SAPRC 11 chemical mechanism where experimentally determined rate constants were not available (Carter, 2011). The HO loss frequencies (units of s^{-1}) were calculated by multiplying the hydrocarbon concentrations by their reaction rate constants with HO (Jobson et al., 2004). Table 7.10 shows important vehicle exhaust compound groups, the molar fraction of each compound group within the exhaust, the average hydrocarbon reactivity during the photochemically active period of the day (10:00 - 16:00), and the percentage contribution of each compound group to the total reactivity contributed by the exhaust. The largest contributors to total reactivity were alkenes (57.7 %) followed by aromatics (21.7 %), alkanes (10.9 %), and aldehydes (6.7 %). Of these compound groups, only aromatics and aldehydes can be reliably measured by the PTR-MS, so at best, the PTR-MS was capturing about 28% of the total hydrocarbon reactivity from vehicle exhaust.

Table 7.10. VOC reactivity of compound groups within gasoline exhaust. Shown are the molar fraction of each compound group within the exhaust, the average reactivity for each group, and the percentage of the total reactivity associated within each compound group within gasoline exhaust. Gray cells indicate compound groups measurable by PTR-MS.

Compound Group	Mole Fraction in Exhaust	Group Reactivity (s^{-1})	% of Total Reactivity
Methane	0.400	0.0002	0.0
Alkanes	0.176	0.0044	10.9
Alkenes	0.179	0.235	57.7
Acetylene	0.056	0.0025	0.6
Cycloalkanes	0.011	0.0042	1.0
Cycloalkenes	0.001	0.0024	0.6
Aromatics	0.126	0.0089	21.7
Ethanol	0.015	0.0029	0.7
Aldehydes	0.036	0.0027	6.7
Ketones	0.001	0.0	0.0

The most important VOC precursors based on VOC reactivity are shown in Table 7.11. These values were determined from the photochemical active period of the day (10:00 – 16:00 PST) for the stagnation period (8/10 – 8/17) which we believe best represents typical Tri-Cities area conditions during T-COPS. The list includes compounds measured by the PTR-MS and inferred from the auto exhaust emissions profile. The most important precursor is the biogenic compound isoprene,

followed by formaldehyde, acetaldehyde, and methanol. The large difference between measured formaldehyde and acetaldehyde and that inferred from exhaust emissions suggest these compounds have larger sources from elsewhere, such as secondary sources. For example, formaldehyde is a common photoproduct of hydrocarbon oxidation, in particular, isoprene oxidation initiated by the HO radical. The large reactivity of isoprene means that even modest abundances can have a significant impact on urban air ozone chemistry. Determining typical isoprene levels in an urban airshed can be problematic with surface based measurements. Close proximity of measurement sites to isoprene emitting vegetation such as trees can have a significant impact on local concentrations and may not be reflective of typical abundances elsewhere. In the Tri-Cities known isoprene emitting vegetation includes the Sycamore tree (*Platanus occidentalis*) which is commonly found in parks and residential property as a shade tree. The Russian Olive (*Elaeagnus angustifolia*) is also common along waterways as an invasive species (Ammon Wasteway, Yakima and Columbia rivers) but is not an isoprene emitter. Urban emission inventories for isoprene are likely poor due to limited survey data on vegetation types and mass. The table also shows that the estimated VOC reactivity of vehicle exhaust constituents (including formaldehyde and acetaldehyde) is 0.407 s^{-1} , less than half of the isoprene reactivity (1.1 s^{-1}) and less than half of the measured formaldehyde and acetaldehyde (0.89 s^{-1}).

The HO loss frequency values are relatively small owing to low abundances of the VOCs. These loss frequencies can be compared to methane and CO, long lived constituents of the troposphere that have abundances in the afternoon in the Tri-Cities that are slightly above background tropospheric levels. While methane was not measured during T-COPS, methane was measured by WSU personnel connected with T-COPS in a separate study at the Horn Rapids site in August 2016. In that experiment methane was measured and found to vary from afternoon mixing ratios of ~ 1.9 ppmv to night time highs of 2.2 ppmv. Typical tropospheric background levels of methane are ~ 1.8 ppmv, so methane mixing ratios are only slightly elevated at this location. Given the 1.9 ppmv mixing ratio and an HO rate coefficient of $5.0 \times 10^{-14} \text{ cm}^3 \text{ molecule}^{-1} \text{ s}^{-1}$ at 300 K, the HO loss frequency to methane is 2.2 s^{-1} . This is twice the value of the HO loss frequency attributed to isoprene (1.11 s^{-1}) shown in Table 7.10. That methane is an important sink for HO highlights that VOC mixing ratios are low and that even background levels of methane and CO are important reactants. The HO loss frequency to CO, using typical daytime mixing ratios of 203 ppbv and an HO rate coefficient of $6.44 \times 10^{-14} \text{ cm}^3 \text{ molecule}^{-1} \text{ s}^{-1}$ yields an HO loss frequency of 0.30 s^{-1} , about one third that of isoprene.

The day time (10:00 to 16:00 PST) reactivity for selected organics are shown in Figure 7.32 to illustrate day-to-day variation and contribute to total reactivity by CO, aldehydes (formaldehyde + acetaldehyde), isoprene, methanol, and the sum of the aromatic compounds (toluene, C2-alkylbenzenes, C3-alkylbenzenes). Isoprene and aldehydes contribute a large fraction of the overall reactivity of compounds measured at BCAA. The variability of isoprene and aldehyde concentration are a significant driver for day-to-day variability in reactivity. The wild fire events days (#2 and #3) had lower reactivity than the other event days. Ozone event days were not always associated with days of highest reactivity.

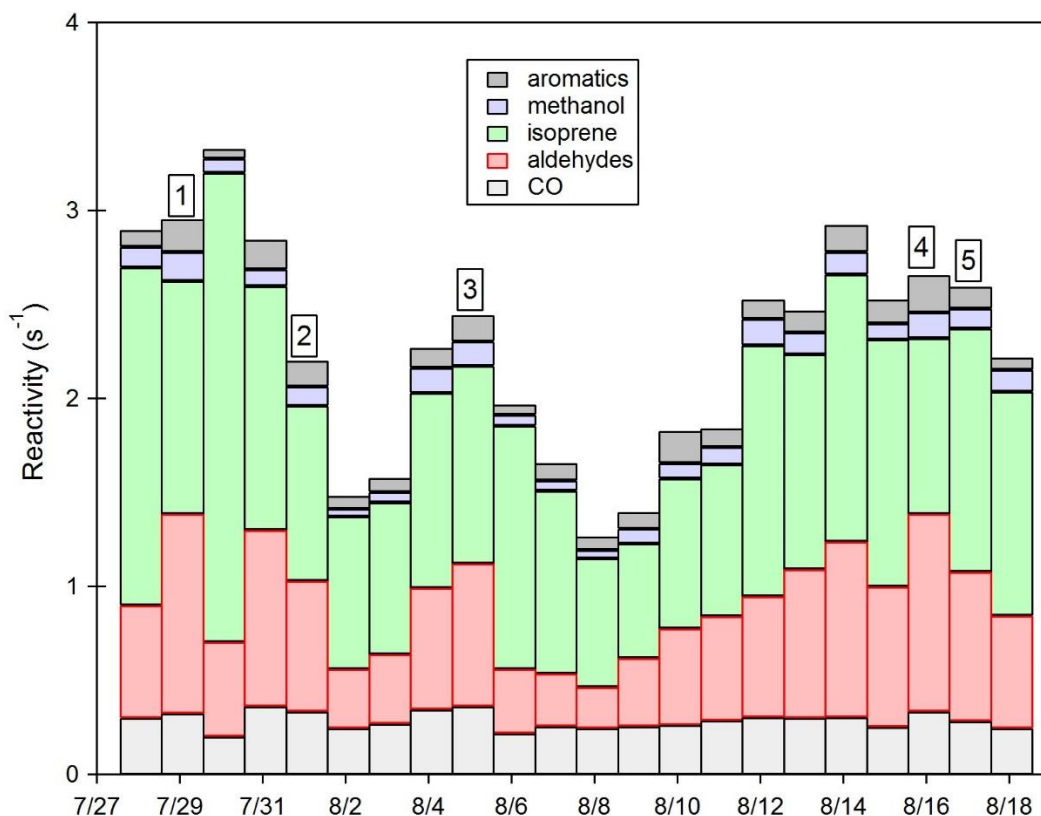


Figure 7.32. Average day time reactivity (HO loss frequency) for compounds measured at BCAA. Numeric labels identify days that were ozone events.

The relationship between daily maximum ozone and primary VOC reactivity is shown in Figure 7.33. Shown are the relationships between methanol, isoprene, and total VOCs reactivity inferred from gasoline exhaust based on data from the photochemically active period (10:00 to 16:00 PST) during T-COPs. Also included is the HO loss frequency to reaction with NO₂; this reaction would be a major radical chain termination reaction. The HO loss frequency to NO₂ is comparable to the loss frequency to gasoline VOCs, and is typically less than the loss frequency to isoprene. The daily maximum ozone displays a reasonably strong positive correlation with gasoline VOC reactivity inferred from the abundance of C₂-alkylbenzenes ($r^2 = 0.67$). The variation in the abundance of gasoline exhaust compounds, hence loss frequency shown in Figure 7.33, is driven more by differences in dispersion rates than variation in emission rates. Vehicle traffic emissions would be expected to be reasonably similar from one day to the next, although there are differences between weekday and weekend hourly traffic count profiles. Max daily ozone also displays a reasonably strong positive correlation with methanol reactivity ($r^2 = 0.53$). A much more scattered relationship is observed for isoprene ($r^2 = 0.18$), including 2 outliers that were not included in the regression fit. The poor fit to isoprene is likely due to strong local concentration variance due to local sources and wind direction influences. The fit to NO₂ is also scattered ($r^2 = 0.28$) but displays a general positive correlation. If the system was very NO_x limited an inverse relationship would be anticipated based

on equation R4 in Chapter 1. The positive corrections observed for both VOC and NO₂ reactivity suggest that ozone production rates can be enhanced by increasing both VOC and NO₂ abundance. The stronger correlation between daily max ozone and VOC reactivity compared to NO₂ suggests that hydrocarbon concentration variability is a more significant driver of elevated ozone than NO_x variability. This may be due to VOCs enhancing radical production rates through the formation of photo labile products like aldehydes.

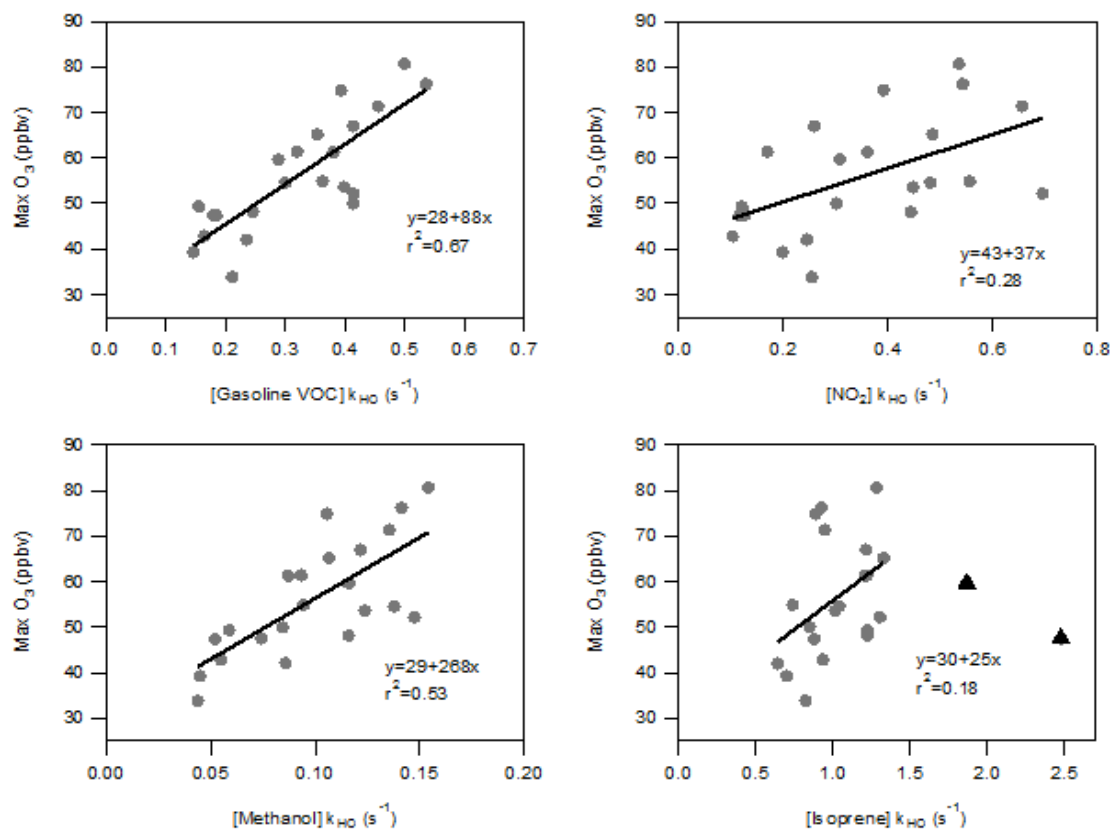


Figure 7.33. Maximum daily ozone versus VOC and NO₂ reactivity. Loss frequencies are averaged during the post rush hour photochemically active period (10:00 - 16:00). The triangles in the isoprene plot indicate outliers that were not included in the linear regression.

Table 7.11. Compound abundance (ppbv), HO rate coefficient, and reactivity (inverse milliseconds) based on average mixing ratios from the photochemically active period of the day (10:00 - 16:00) during the stagnation period (8/10 - 8/17).

Compound or Group	Average (ppbv)	Rate Coefficient ($10^{12} \text{ cm}^3 \text{ molec}^{-1} \text{ s}^{-1}$)	Reactivity (ms^{-1})
<i>Measured</i>			
isoprene	0.453	101	1114
methanol	5.1	0.9	118
benzene	0.065	1.2	2
toluene	0.123	5.6	17
C ₂ -alkylbenzenes	0.091	15.0	34
C ₃ -alkylbenzenes	0.080	24.9	49
formaldehyde	2.70	9.4	623
acetaldehyde	0.73	15.0	268
CO	203	0.06	300
methane	1900	0.05	2200
<i>Inferred</i>			
propylene	0.103	26.3	67
ethylene	0.238	8.5	50
1-butene & isobutene	0.041	31.4	32
m,p-xylene	0.052	18.7	24
1,3-butadiene	0.011	66.6	18
toluene	0.094	5.6	13
1,2,4-trimethylbenzene	0.015	32.5	12
formaldehyde	0.051	9.4	12
acetaldehyde	0.032	15.0	12
<i>Vehicle Exhaust Total</i>	<i>1.502</i>	-	<i>407</i>

7.9. Results of Mobile Monitoring for O₃, NO_x and VOCs

Mobile data collected by the RJ Lee van were aggregated first from 1-second to 15-second averages and then into a grid of 1750-m diameter hexagons. This temporal and spatial aggregation was applied to concentrations of NO_x, O₃ and select VOCs: isoprene, monoterpenes, toluene, C₂-alkylbenzenes, C₃-alkylbenzenes, C₄-alkylbenzenes, acetaldehyde, and methylvinyl ketone + methacrolein. Within each hexagon, the 75th percentile NO_x, O₃ and VOC concentrations were calculated as well as the median VOC-to-NO_x ratio. Summary statistics were only calculated for hexagons containing a minimum of eight 15-second average data points. Only O₃ data collected from 10:00 through 19:59 and VOC data collected from 5:00 through 19:59 were included in the aggregation. As the VOC-to-NO_x ratios were only calculated using the subset of VOCs listed above, they may not be directly comparable to ratios published elsewhere. Further, some hexagons such as NO_x near the Agrium facility or along some roads are only based on a few minutes of data and do not capture the variability in concentrations.

In general, NO_x mixing ratios observed throughout the study area were relatively low as displayed in Figure 7.34. It must be noted that the Hanford Nuclear Reservation operated at a reduced capacity due to a labor dispute during T-COPS. The highest concentrations of NO_x were found downwind of the Agrium facility near Finley, along SR-240 in Richland, and at select points along US 395 north of Pasco. Agrium is a nitric acid facility and gaseous HNO₃- which likely offgases during loading operations- is known to positively bias chemiluminescence- based NO_x measurements (Dunlea et al., 2007).

Ozone mixing ratios were highest in Burbank and north of Pasco as displayed in Figure 7.35. Ozone abundance declined rapidly in West Pasco west of US 395. Elevated ozone mixing ratios do not extend far north or west of the Tri-Cities but moderately elevated levels were observed around Burbank and Wallula. This is conceivable given the north sector winds accompanying high ozone events (Figure 1.2).

Maps of total VOCs were stratified by time period in order to isolate the spatial patterns from the temporal variation in abundance throughout the study. The maps below show the sum of the VOC species analyzed during the wildfire period (8/1 - 8/6/2016), the low concentration period (8/7 - 8/11/2016) and the high ozone period (8/12/2016). Mobile data were not available before 8/1/2016. The color scale reflects the quantiles of total VOC data in the larger dataset and is held constant across the three maps. During the low concentration period, VOCs showed greater spatial heterogeneity. The highest concentrations of VOCs were observed north of the Tri-Cities at Hanford, in Mesa, and along US 395. Some high concentrations were also observed along I-182 between Pasco and Richland. The lowest concentrations were measured along Ice Harbor Dr. east of Burbank, though a localized relative hotspot was still observed in the immediate vicinity of the poplar tree farms. Total VOC concentrations were highest during the high ozone period. They followed a similar spatial pattern to that seen during the low concentration period, with the highest concentrations observed north of the Tri-Cities along US 395 toward Mesa. This is consistent with increased biogenic emissions on hotter days, as well as poorer dispersion on such days.

Only data with NO_x levels above 1 ppb were considered in calculating VOC-to-NO_x ratios. Median VOC-to-NO_x ratios throughout the central Tri-Cities and along US 395 north of Pasco were generally below 5. Higher ratios were observed farther outside the Tri-Cities, with ratios along US 240 northeast of Richland generally between 5 and 8. Typically VOC/NO_x ratios below 5.8 suggest VOC limitation while ratios above 8 suggest NO_x limitation. Because only a subset of all reactive VOCs were sampled during TCOPS, the above map presents a lower limit of true VOC-to-NO_x ratios. Therefore, while it is not possible to comment on VOC limitation within the area, it is likely that dark green hexagons (tree farm) are located in NO_x limited areas. It is very likely that highways are NO_x-rich and areas close to CAFOs and orchards are not lacking VOCs.

In summary, besides the ubiquitous but relatively low levels of NO_x, spatial monitoring does not indicate the presence of widespread ozone precursor hotspots.

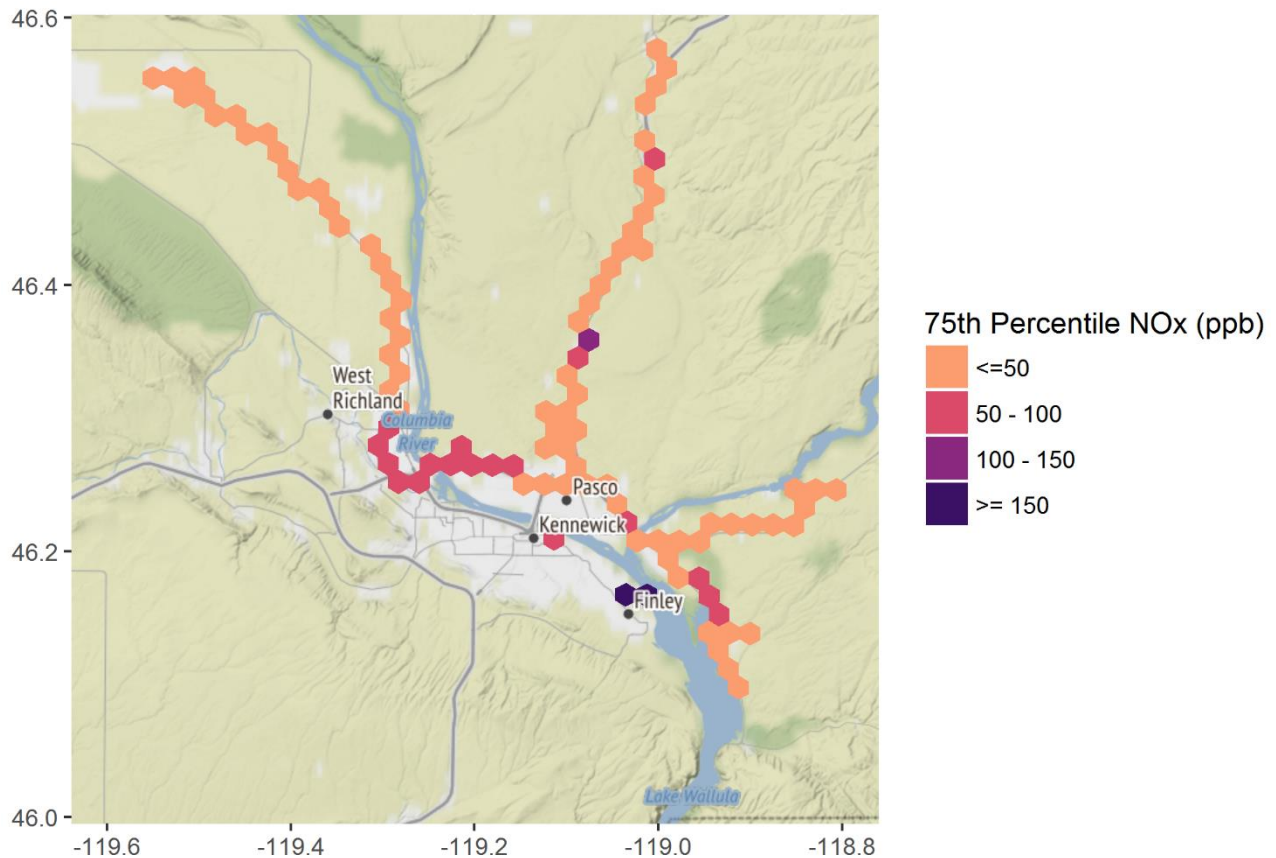


Figure 7.34. 75th percentiles of NO_x concentrations measured during TCOPS

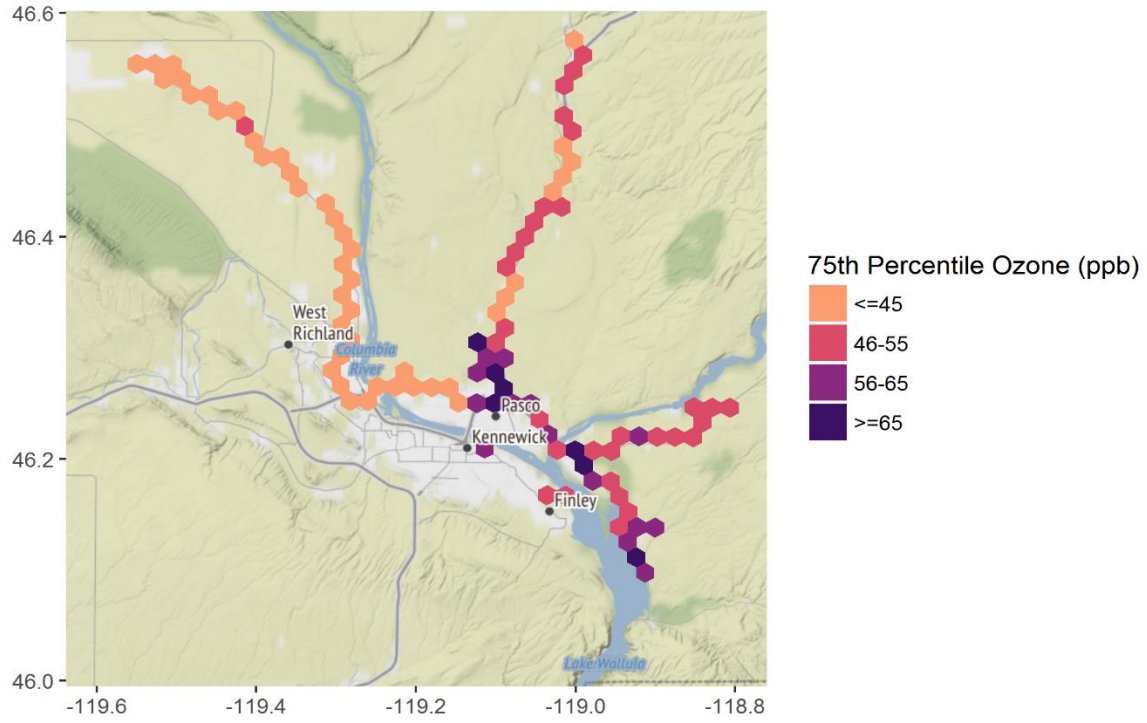


Figure 7.35. 75th percentiles of ozone concentrations measured during TCOPS

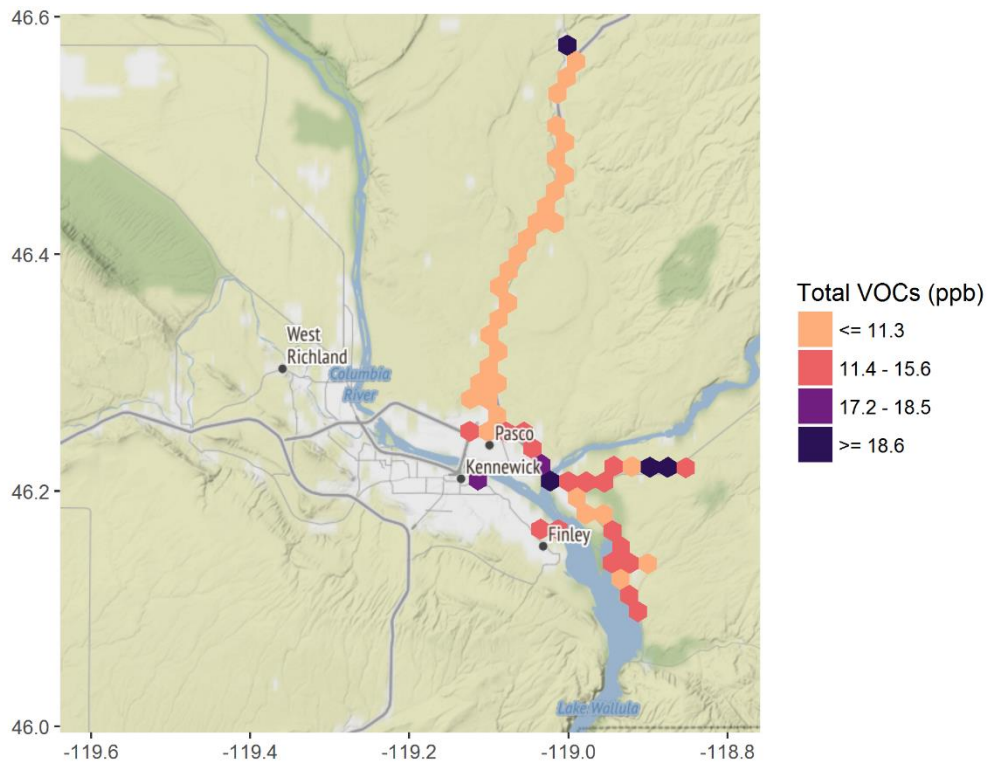


Figure 7.36. Total VOCs measured during the wildfire smoke episode (8/1- 8/6)

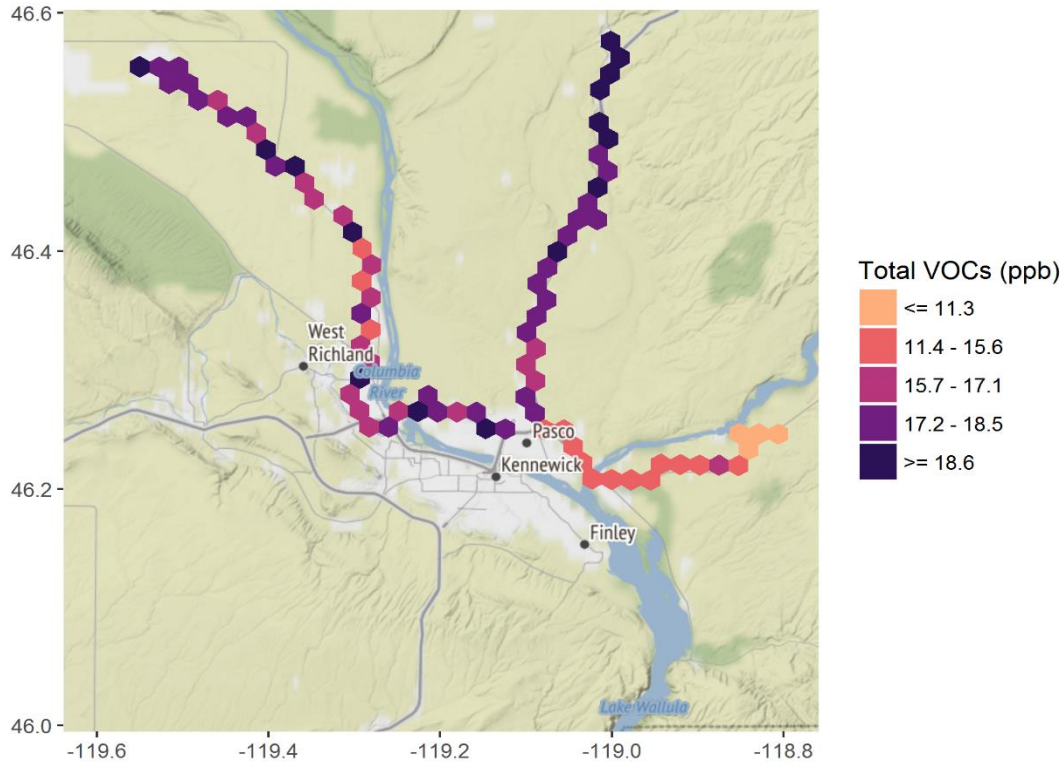


Figure 7.37. Total VOCs measured during the low concentration period of TCOPS (8/7- 8/11)

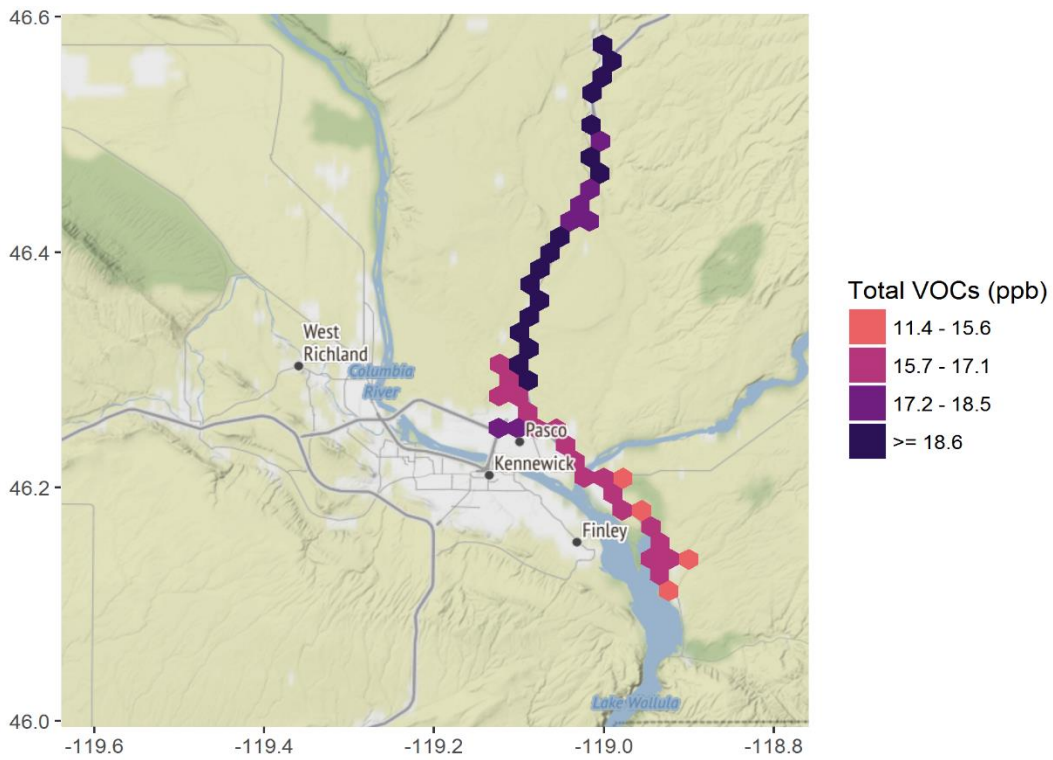


Figure 7.38. Total VOCs measured during the high ozone period (8/12- 8/16)

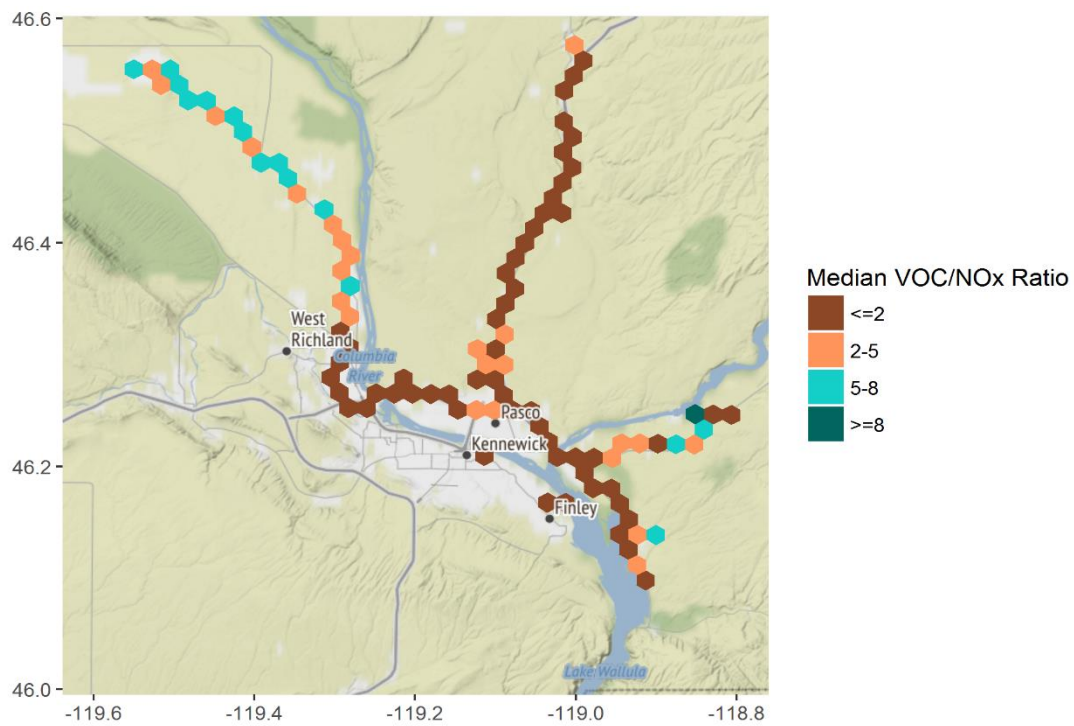


Figure 7.39. Median VOC-to-NOx ratios measured during all of TCOPS

7.10. Comparison to AIRPACT 5

AIRPACT 5 is a photochemical grid model providing daily air quality forecasting for the Pacific Northwest. T-COPS provided an opportunity to compare model results to observations as a way to assess the model's accuracy. The model results are from the lowest model layer from a 4 km x 4km grid that is centered over the western side of Kennewick, with the BCAA site near the southern edge of the grid. Time series of model predictions and measurements for O₃, NO_z, CO and NO_x are shown in Figure 7.40. Correlations between modeled and measured mixing ratios are shown in Figure 7.41 and mean bias and mean errors are shown in Table 7.12. The mean bias and error for the daily maximum concentrations for O₃ and NO_z were also calculated and shown in Table 7.13 to shed light on the model's ability to predict the afternoon maxima (since model – observed agreement is less relevant overnight). It is clear that AIRPACT 5 underestimated afternoon O₃ during the T-COPS study. In Figure 7.40, the daily maxima are clearly lower in the model predictions than in the measurements and the slope of the modeled measured correlation, shown in Figure 7.41, was 0.43. In addition, the mean ozone bias was -4.1% over the entire study and the mean error was 23.6%, but more notably, the mean bias for the daily maxima was -23.2% and the mean error was 24.5%. Interestingly, the model would not have predicted any ozone episodes during the T-COPS study, which is notable because the model was originally used to identify the ozone hot spot in the Tri-Cities as discussed in Chapter 1. The model did transition from AIRPACT version 4 when the hotspot was originally identified, to version 5 in Spring 2016. This transition also switched from the SAPRC chemical mechanism to Carbon Bond VI. Changes to emissions processing modules (newer versions of MOVES and MEGAN) occurred as well.

Modeled NO_z was also severely underestimated. Ozone and NO_z are photoproducts formed in the volume of the convective boundary layer. Their afternoon abundance is a function of both photochemical production rates and dispersion rates. Differences between observations must be due to one or both of these factors. The mean bias for NO_z over the entire study was -45.0% and -55.7% in the afternoons indicating that NO_z was severely under predicted.

The modeled to measured comparisons for CO and NO_x provide evidence that the precursor abundances were not predicted correctly. Some care must be taken here in comparing a point measurements at the surface to model results that smooths emissions into a 16 km² model layer. For CO there is significant off-set between the model and observations. The model routinely under predicted NO_x and CO, with a mean bias of -50.6% for NO_x and -35.6% for CO and mean errors of 56.2% and 35.6% respectively. NO_x is severely under predicted during morning rush hour. Additionally, NO_x abundances appeared to often be under predicted in the afternoon, which could partially explain the discrepancy in NO_z in the afternoons. The CO-to-NO_x ratio can provide more insight into whether the relative emissions of CO and NO_x are correct. Correlations of modeled and measured CO to NO_x during morning rush hours are shown in Figure 7.42. Excluded were data from the wildfire impacted period (7/30 to 8/6) where CO emissions from wild fire impacted the Tri-Cities and the BCAA are clearly much larger than the AIRPACT predictions as shown in Figure 7.39. Also data from the windy and rainy period (8/8 to 8/10) that had low CO and NO_x was excluded. Morning rush hour was chosen because NO_x abundances were less likely to be affected

by chemistry than in the afternoon, providing the best opportunity for measured – model agreement. The AIRPACT trend yields a slope of 12.2 while the BCAA data yield a much smaller slope of 4.1. These molar ratios suggest that the model underestimated NO_x emissions relative to CO.

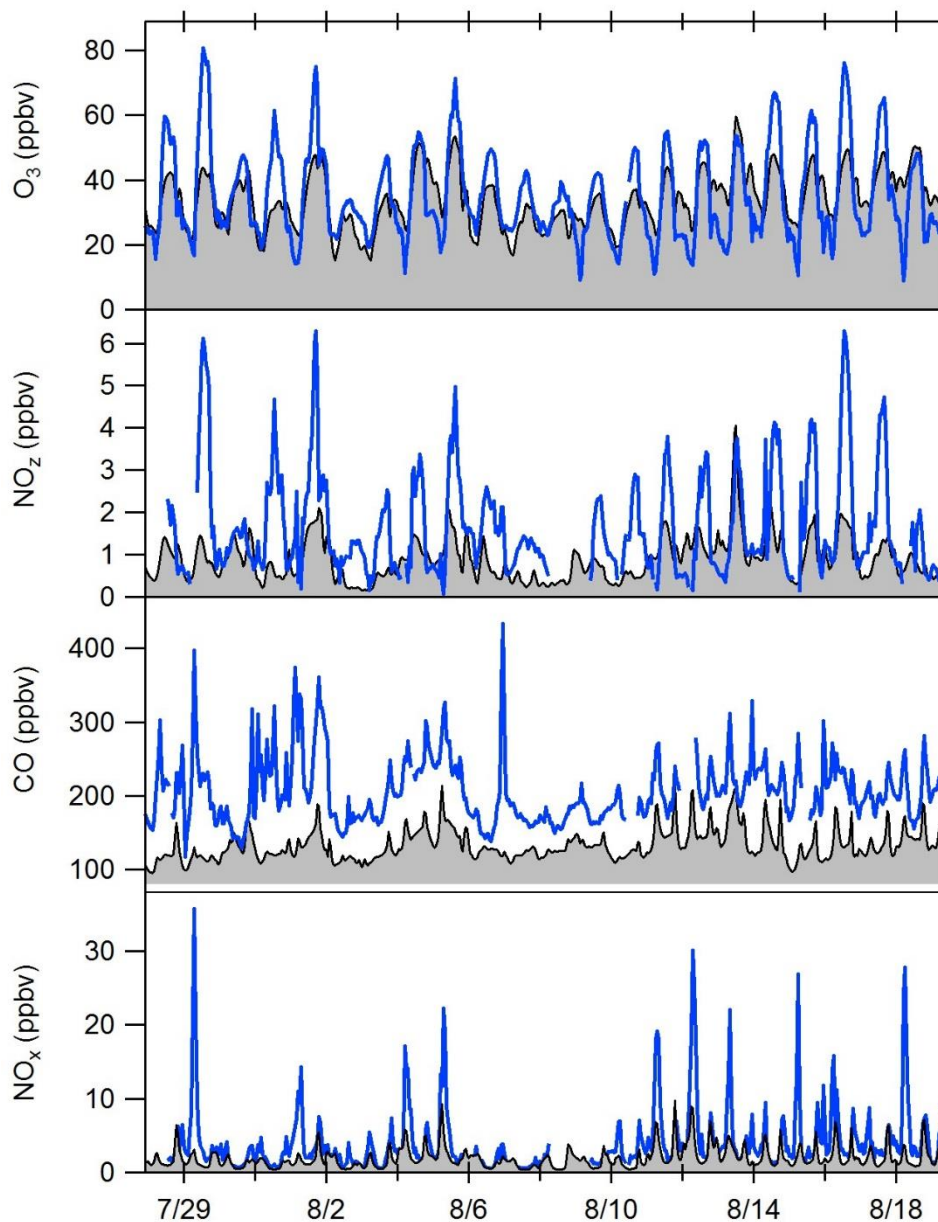


Figure 7.40. Time series comparison of BCAA data (blue line) and AIRPACT 5 data (grey shading) of O_3 , NO_2 , CO, and NO_x .

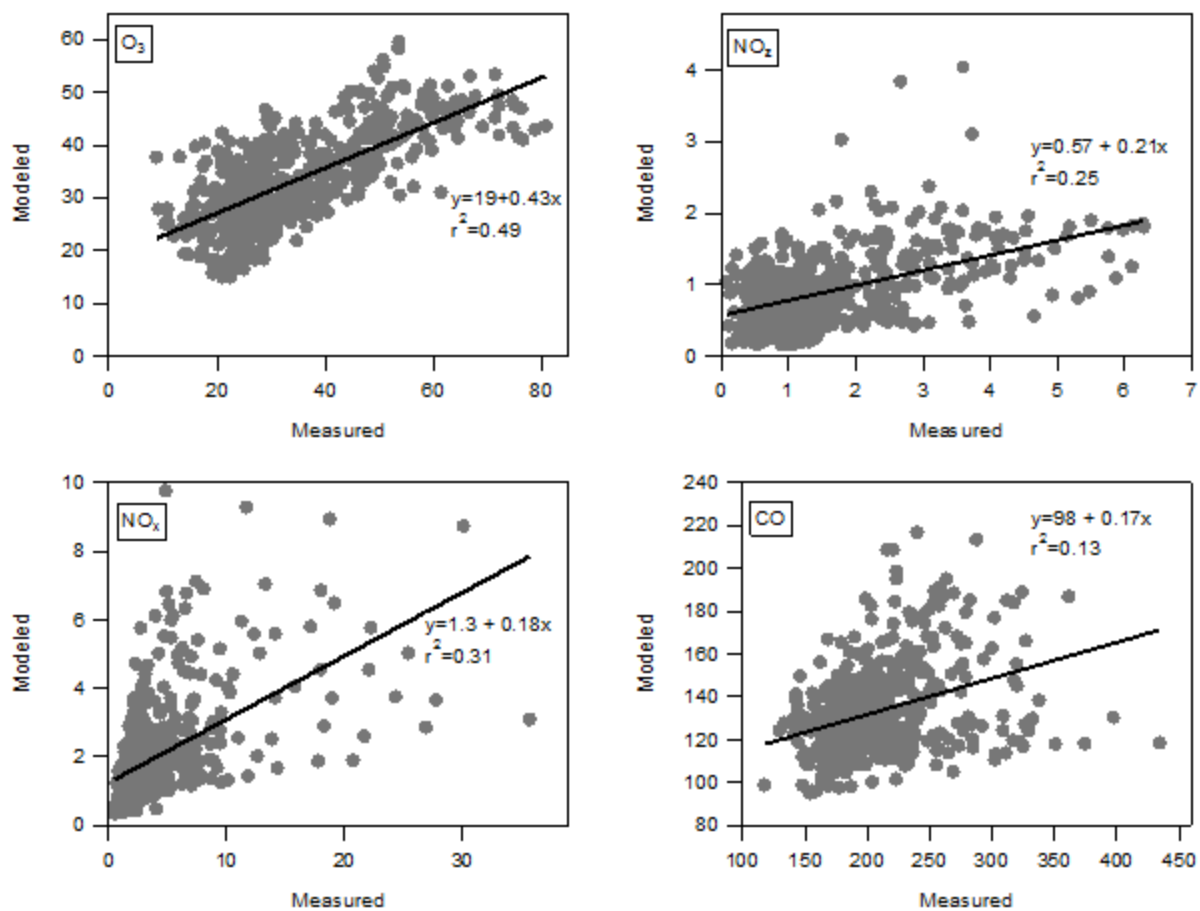


Figure 7.41. AIRPACT 5 hourly average predictions of O₃, NO₂, NO_x, and CO versus measured values at BCAA.

Table 7.12. Mean bias and mean error between AIRPACT 5 and measured parameters for the T-COPS period.

	Mean Bias	Mean Error
O ₃	-4.1	23.6
NO _x	-50.6	56.2
CO	-35.6	35.6
NO ₂	-45.0	55.7

Table 7.13. Mean bias and error for maximum daily concentrations (1 hour average) of O₃ and NO_z for the T-COPS period.

	Mean Bias	Mean Error
O ₃	-23.2	24.5
NO _z	-55.7	56.6

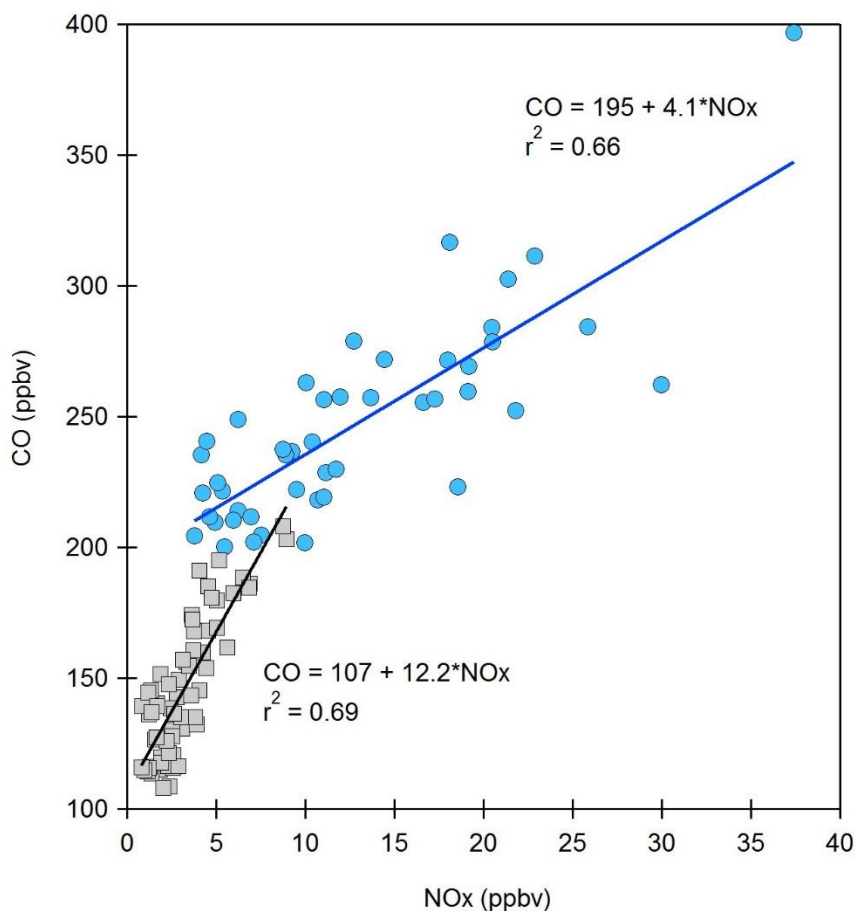


Figure 7.42. CO to NO_x relationship for AIRPACT 5 (grey squares) and BCAA data (circles) for rush hours (5 am to 9am PST) excluding wild fire period days (7/30 to 8/6) and days of rainy windy weather (8/8 to 8/10).

8. Summary and Conclusions

- Air quality managers have been paying close attention to ozone levels in the Tri-Cities airshed since predictions of elevated levels were observed in the AIRPACT model. The fourth highest daily 8 hour maximum concentration was 75 ppbv in 2015 and 68 ppbv in 2016, motivating the Department of Ecology to commission this study to investigate the causes of high ozone in the Tri-Cities.
- This study was conducted from July 27, 2016 - August 18, 2016 and involved making a suite of air quality and meteorological measurements at 4 different sites around the Tri-Cities. The main site was at the Benton Clean Air Agency (BCAA), where Washington State University (WSU) stationed their mobile atmospheric chemistry lab (MACL). MACL made measurements of O₃, NO_x, NO_y, CO, SO₂, VOCs, and surface meteorology. A satellite site was established by WSU in Horn Rapids to measure surface meteorology, ozone and NO_x. A second satellite site was operated in the town of Burbank, where the Department of Ecology measured ozone, NO_x, and CO. The RJ Lee Group performed one week of VOC measurements during August of 2017 that are presented in this report at Burbank as well. Finally, periodic VOC, NO_x, and O₃ measurements were made at Mesa by the RJ Lee group.
- The study was characterized by four distinct sets of conditions. First, the Columbia Cup hydroplane races (7/29-7/31) took place, during which extra traffic was present in the region over the weekend. One ozone episode (one hour average ozone greater than 70 ppbv) occurred during the race weekend (7/29). Secondly, wildfires impacted the site periodically from 7/31-8/7 likely affecting the levels of ozone and precursors in the region. Two ozone episodes occurred during the wildfire period (8/1 and 8/5). This was followed by a wet/windy period (8/7 - 8/10) where pollutant concentrations were low. At the end of the study (8/10 - 8/17), there was a period of high temperatures, low winds, and clear skies, which we refer to as the stagnation period. Ozone concentrations appeared to build up during the stagnation, and two ozone episodes occurred (8/16 and 8/17).
- During the three ozone episodes not influenced by wildfire, ozone levels were relatively similar at BCAA and Burbank but significantly lower (15 – 20 ppbv) at Horn Rapids which is further way from the urban center. This suggests that, under normal conditions, local emissions of precursors from the Tri-Cities urban area are the source of elevated ozone.
- Based on the emissions inventory, mobile source emissions were the primary source of NO_x, and CO during the T-COPS study. Though the emissions inventory cites solvents as a large source of VOCs, agricultural pesticides are the main emission in the solvent category. Given that the emissions inventory is for the entire county, only a fraction of the emissions would impact the Tri-Cities airshed. Additionally, the temporal allocation in the inventory (day of week and time of year) is not accurate given actual pesticide application times. The estimates for agricultural pesticide emissions in the county level emission inventory need refinement for their use in air quality modeling.

- When compared with the rest of the stagnation period, the ozone episode on August 16 had elevated levels of water vapor, aromatics, formaldehyde, and NO_z but not NO_x or isoprene. This suggests that elevated levels of anthropogenic VOCs and moist conditions, coupled with low wind speeds were contributing factors to elevated ozone.
- Examination of modeled vertical wind profiles of the atmosphere and back trajectories, as well as mobile measurements made at the outer extents of the airshed, showed no evidence of long range transport of ozone or ozone precursors to explain elevated ozone levels in the Tri-Cities. The exception maybe wildfire events which appear to be sources of ozone precursors and perhaps ozone.
- Based on emission inventories and observations of CO and NO_x , traffic emissions are a major source of NO_x in the Tri-Cities. Isoprene emitted from vegetation, and the aldehydes, formaldehyde and acetaldehyde, which have both primary and secondary sources, were the most significant VOC precursors. It is estimated that vehicle emissions of CO, aromatics, alkenes and alkanes would collectively comprise a hydroxyl radical reactivity comparable to isoprene. Thus traffic emissions of hydrocarbons and CO have a similar importance as ozone precursors as isoprene at the BCAA site. We note that isoprene mixing ratios are likely to be highly variable in the airshed, reflecting spatial variations in tree density amongst neighborhoods and commercial areas, and emission rate variation among tree species.
- Through modeling of NO_x emissions from large point and area sources, we conclude that while these sources do not impact NO_x concentrations enough to create large “hot spots”, they do contribute towards overall NO_x levels in the airshed.
- Application patterns of agrochemicals containing photochemically active ingredients was investigated. Though not measured directly during TCOPS, horticultural oils could possibly exacerbate ozone formation if sprayed during summer months. It is recommended that alkanes- associated with horticultural oil application- and chemically reactive light alkenes (i.e. ethylene and propylene) - associated with traffic emissions- be measured in future studies in this airshed to better understand the roles of ozone precursors not measured during T-COPS.
- However there is no evidence to suggest that point sources of NO_x or agricultural emissions of VOC are solely responsible for elevated ozone in the airshed
- Indicator ratios (O_3/NO_z , HCHO/NO_y , and HCHO/NO_2) were used to assess whether ozone production was VOC or NO_x sensitive. The results of this analysis suggested that the airshed was neither VOC nor NO_x sensitive based on comparisons of these indicator ratios to literature values. These results suggest that conditions in the area produce ozone very efficiently relative to the abundances of precursors and that the chemistry is not skewed dramatically towards sensitivity to one precursor or the other. A numerical modeling study would be necessary to determine the most efficient strategy for regulating precursors to reduce ozone levels.
- In the interim, strategies to achieve moderate reductions of NO_x and VOCs throughout the airshed could be pursued. In particular, such strategies could be rigorously implemented

when days conducive for ozone formation are forecast. Because reactive species tend to accumulate and carry over into the next day during such episodes, targeted emission reductions should commence the day prior to episode onset.

- When compared with observations at BCAA, the AIRPACT 5 model generally under predicted ozone, CO, NO_x, and NO_z in the surrounding grid cell. This suggests that there are some problems with the emissions, chemical mechanism, or dilution in the model, or that real world heterogeneity within the grid cell led to differences in the model predictions compared to observations.

9. References

Andreae, M O, and P Merlet. "Emission of Trace Gases and Aerosols from Biomass Burning." *Biogeochemistry* 15.4 (2001): 955–966.

Aschmann, Sara M, Janet Arey, and Roger Atkinson. "Rate Constants for the Reactions of OH radicals with 1,2,4,5-tetramethylbenzene, pentamethylbenzene, 2,4,5-trimethylbenzaldehyde, 2,4,5-trimethylphenol, and 3-methyl-3-hexene-2,5-dione and Products of OH + 1,2,4,5-tetramethylbenzene." *Journal of Physical Chemistry*, 117.12 (2013): 2556–2568. Web.

Atkinson, Roger, and Janet Arey. "Atmospheric Degradation of Volatile Organic Compounds." *Chemical Reviews* 103.12 (2003): 4605–4638. Web.

Carter, William, "SAPRC11 Chemical Mechanism." 2014. <http://www.cert.ucr.edu/~carter/SAPRC/>.

Carter, William and Irina L. Malkina, *Investigation of Atmospheric Ozone Impacts of Selected Pesticides*, Final Report to the California Air Resources Board, No. 04-334, January 2007.

de Gouw, J. A., C. Warneke, D. D. Parrish, J. S. Holloway, M. Trainer, and F. C. Fehsenfeld (2003), Emission sources and ocean uptake of acetonitrile (CH₃CN) in the atmosphere, *J. Geophys. Res.*, 108(D11), 4329, doi:10.1029/2002JD002897.

de Gouw, Joost, and Carsten Warneke. Measurements of Volatile Organic Compounds in the Earth's atmosphere using proton transfer reaction mass spectrometry" *Mass Spectrometry Reviews*, 26 (2007): 223–257.

Dunlea, E.J., S. C. Herndon, D. D. Nelson, R. M. Volkamer, F. San Martini, P. M. Sheehy, M. S. Zahniser, J. H. Shorter, J. C. Wormhoudt, B. K. Lamb, E. J. Allwine, J. S. Gaffney, N. A. Marley, M. Grutter, C. Marquez, S. Blanco, B. Cardenas, A. Retama, C. R. Ramos Villegas, C. E. Kolb, L. T. Molina, and M. J. Molina. Evaluation of nitrogen dioxide chemiluminescence monitors in a polluted urban environment. *Atmos. Chem. Phys.*, 7 (2007): 2691–2704.

Graus, Martin, Markus Muller, and Armin Hansel. High Resolution PTR-TOF: Quantification and Formula Confirmation of VOC in Real Time. *Journal of the American Society for Mass Spectrometry*, 21.6 (2010): 1037–1044.

Holzinger, R., J. Williams, G. Salisbury, T. Klüpfel, M. de Reus, M. Traub, P. J. Crutzen, and J. Lelieveld (2005), Oxygenated compounds in aged biomass burning plumes over the eastern Mediterranean: Evidence for strong secondary production of methanol and acetone, *Atmos. Chem. Phys.*, 5(1), 39–46.

- Jaffe, Daniel A., and Nicole L. Wigder. "Ozone Production from Wildfires: A Critical Review." *Atmospheric Environment*, 51 (2012): 1–10.
- Jobson, B. T. et al. "Hydrocarbon Source Signatures in Houston, Texas: Influence of the Petrochemical Industry." *Journal of Geophysical Research D: Atmospheres* 109.24 (2004): 1–26.
- Jobson, B.T. and J.K. McCoskey Sample drying to improve formaldehyde measurements by PTR-MS instruments, *Atmospheric Chemistry and Physics*, 10, 1821-1835, 2010.
- Karl, T. G., T. J. Christian, R. J. Yokelson, P. Artaxo, W. M. Hao, and A. Guenther (2007), The tropical forest and fire emissions experiment: Method evaluation of volatile organic compound emissions measured by PTR-MS, FTIR, and GC from tropical biomass burning, *Atmos. Chem. Phys.*, 7(3), 8755–8793.
- Kim, J-H., S.K. Papiernik, W.J. Farmer, J. Gan, S.R. Yates, Effect of formulation on the behavior of 1,3-dichloropropene in soil, *J. Environmental Quality*, 32, 2223-2229, 2003.
- Kleinman, L.I., Low and high NO_x tropospheric photochemistry. *J. Geophys. Res.*, 99, 16831-16,838, 1994.
- Kleinman, L.I. Dependence of ozone production on NO and hydrocarbons in the troposphere, *J. Geophys. Res. Lett.*, 24, 2299-2302, 1997.
- Kleinman, L.I., Ozone process insights from field experiments - part II: Observation-based analysis for ozone production, *Atmos. Environ.*, 34, 2023-2033, 2000.
- Kleinman, L.I., P.H. Daum, Y.-N. Lee, L.J. Nunnermacker, S.R. Springston, J. Weinstein-Lloyd, J. Rudolph, A comparative study of ozone production in five U.S. metropolitan areas, *J. Geophys. Res.*, 110, D02301, 2005.
- Kleinman, L.I., P.H. Daum, Y.-N. Lee, L.J. Nunnermacker, S.R. Springston, J. Weinstein-Lloyd, J. Rudolph, A comparison study of ozone production in five U.S. metropolitan areas, *J. Geophys. Res.*, 110, D02301, 2005.
- Lack, D. A., et al. (2013), Brown carbon absorption linked to organic mass tracers in biomass burning particles, *Atmos. Chem. Phys.*, 13(5), 2415–2422.
- Lin, X., M. Trainer, S.C. Liu, On the nonlinearity of tropospheric ozone production., *J. Geophys. Res.*, 93, 15879-15888, 1988.

Lindinger, W., a. Hansel, and a. Jordan. On-Line Monitoring of Volatile Organic Compounds at Pptv Levels by Means of Proton-Transfer-Reaction Mass Spectrometry (PTR-MS) Medical Applications, Food Control and Environmental Research. *International Journal of Mass Spectrometry and Ion Processes*, 173.3 (1998): 191–241.

Lu, Xiao et al. “Wildfire Influences on the Variability and Trend of Summer Surface Ozone in the Mountainous Western United States.” *Atmospheric Chemistry and Physics*, 16.22 (2016): 14687–14702.

Mao, J., X. Ren, S. Chen, W.H. Brune, Z. Chen., M. Martinez, H. Harder, B. Lefer, B. Rappengluck, J. Flynn, M. Leuchner, Atmospheric oxidation capacity in the summer of Houston 2006: Comparison with summer measurements in other metropolitan studies, *Atmos. Environ.*, 44, 4107-4155, 2010.

Milford, J.B., D. Gao, S. Sillman, P. Blossey, A.G. Russel, Total reactive nitrogen (NO_y) as an indicator of the sensitivity of ozone to reductions in hydrocarbon and NO_x emissions, *J. Geophys. Res.*, 99, 3533-3542, 1994.

National Research Council, *Rethinking the Ozone Problem in Urban and Regional Air Pollution*, National Academies Press, Washington, D.C., 1991.

Ren, X., D. van Duin, M. Cazorla, et al., Atmospheric oxidation chemistry and ozone production: Results from SHARP 2009 in Houston, Texas., *J. Geophys. Res.*, 118, 5770-5780, 2013.

Sillman, S., The use of NO_y, H₂O₂, and HNO₃ as indicators for ozone-NO_x-hydrocarbon sensitivity in urban areas, *Journal of Geophysical Research*, 100, 14,175-14,188, 1995.

Sillman, S et al. “Model Correlations for Ozone, Reactive Nitrogen, and Peroxides for Nashville in Comparison with Measurements: Implications for O₃-NO_x-Hydrocarbon Chemistry.” *Journal of Geophysical Research*, 103.D17 (1998): 22629–22644.

Sillman, S. “The Use of NO_y, H₂O₂, and HNO₃ as Indicators for Ozone-NO_x -Hydrocarbon Sensitivity in Urban Locations.” *Journal of Geophysical Research: Atmospheres* 100.D7 (1995): 14175–14188.

Sillman, S., D. He., C. Cardelino, R.E. Imhoff, Use of photochemical indicators to evaluate ozone-NO_x-hydrocarbon sensitivity: case studies from Atlanta, New York, and Los Angeles, *J. Air Waste Manage. Assoc.*, 47, 1030-1-40, 1997.

Tonnesen, G.S., R.L. Dennis, Analysis of radical propagation efficiency to assess ozone sensitivity to hydrocarbons and NO_x. Long-lived species as indicators of ozone sensitivity, *Journal of Geophysical Research*, 105, 9227-9241, 2000.

Wallace, H.W., B.T. Jobson, M.H. Erickson, J.K. McCoskey, T.M. Vanreken, B.K. Lamb, J.K. Vaughan, R.J. Hardy, J.L. Cole, S.M. Strachan, W. Zhang, Comparison of wintertime CO to NO_x ratios to MOVES and MOBILE6.2 on-road emissions inventories, *Atmospheric Environment*, 63, 289-297, 2012.

Xie, Y., R. Elleman, T. Jobson, B. Lamb, Evaluation of O₃-NO_x-VOC sensitivities predicted with the CMAQ photochemical model using Pacific Northwest 2001 field observations, *Journal of Geophysical Research*, 116, D20303, 2011.

Yokelson, R. J., et al. (2009), Emissions from biomass burning in the Yucatan, *Atmos. Chem. Phys.*, 9, 5785–5812.

Yuan, B., et al. (2010), Biomass burning contributions to ambient VOCs species at a receptor site in the Pearl River Delta (PRD), China, *Environ. Sci. Technol.*, 44(12), 4577–4582.

Appendix

A.1.1. Instrument Performance Audits BCAA

Instrument performance was assessed weekly through performance audits (shown in Table A.1). These audits required assessment of instrument zeros and verification of span using gas standards. A Teledyne T700U dynamic dilution calibration device was used to creating standards for calibrations. CO and NO compressed gas standards were provided to the calibration system. Ozone was provided by an ozone generator in the calibration system and zero air was also created by the calibration system by passing ambient air through a catalyst. To assess instrument zeros, the Teledyne CO, NO_x, O₃, and SO₂ instruments were allowed to sample zero air. The measured mixing ratios were recorded. Acceptable zero levels were ± 50 ppbv for CO, ± 5 ppbv for O₃, ± 5 ppbv for NO and ± 5 ppbv for NO_x. The CO instrument span was assessed by providing 80% of the instrument's full scale range (1600 ppbv) to the instrument. The acceptable error range was $\pm 15\%$. The NO_x instrument was audited by providing NO to both the NO and NO_x channels at 80% of the full scale range (160 ppbv). Acceptable error range was $\pm 15\%$. The ozone instrument was audited by providing it with ozone at concentrations of 0, 15, 70, and 100 ppbv. The acceptable error range was $\pm 10\%$. The SO₂ monitor was simply zeroed to ensure that the zero did not drift. All of the instruments included in these weekly audits passed each audit, so no corrective action was needed during the study.

A.1.2 RJ Lee PTR-QMS Measurements at Burbank

VOC measurements made by the RJ Lee PTR-QMS at Burbank were performed from 8/3 - 8/4 and from 8/12 - 8/18. These data were found to be suspect due to a leak in the air sampling inlet. The study was repeated in August 2017 and the data from 2017 are shown in this report.

Table A.1. Instrument Performance Audits Performed at BCAA. G indicates concentration given to the instrument (ppbv) and R indicates the instrument reading (ppbv).

	CO		O ₃		NO		NO _x		SO ₂	
	G	R	G	R	G	R	G	R	G	R
7/27/2016										
Zero	0	0.3	0	0	0	0	0	0	0	0
Cal	1600	1601	100	98.0						
8/4/2016										
Zero	0	0 ± 3	0	-0.7	0	0.06	0	0.05	0	-0.004
Cal	1600	1606	15	15.8	160	160.5	0	161.8		
			70	70.8						
			100	100.2						
8/10/2016										
Zero	0	-31	0	0.2	0	0.66	0	0.58	0	-0.045
Cal	1600	1567*	15	15.0	160	160.5	160	160.9		
			70	67.5						
			100	96.5						
8/11/2016										
Zero	0	-10								
Cal	1600	1600								
8/18/2016										
Zero	0	-9.7	0	0.4	0	0.04	0	0.09	0	0.052
Cal	1600	1604	15	15.8	160	160.6	160	161.9		
			70.2	70.9						
			100	99.0						